MITNE-11

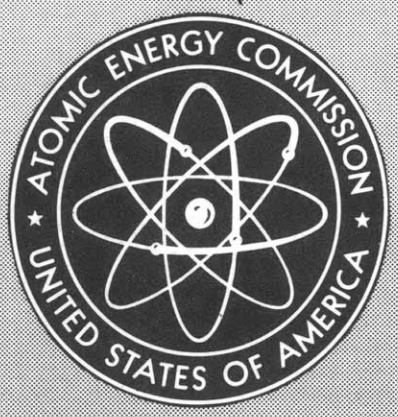

NYO-9659

MEASUREMENTS OF NEUTRON CAPTURE IN U^{238} IN LATTICES OF URANIUM RODS IN HEAVY WATER

By
A. Weitzberg
I. Kaplan
T. J. Thompson

January 8, 1962

Department of Nuclear Engineering
Massachusetts Institute of Technology
Cambridge, Massachusetts

UNITED STATES ATOMIC ENERGY COMMISSION • DIVISION OF TECHNICAL INFORMATION

LEGAL NOTICE

USAEC Division of Technical Information Extension, Oak Ridge, Tennessee

NYO-9659
PHYSICS

MASSACHUSETTS INSTITUTE OF TECHNOLOGY
DEPARTMENT OF NUCLEAR ENGINEERING
Cambridge 39, Massachusetts

MEASUREMENTS OF NEUTRON CAPTURE IN U^{238} IN LATTICES OF URANIUM RODS IN HEAVY WATER

by

A. Weitzberg, I. Kaplan, T. J. Thompson

January 8, 1962

Contract AT(30-1)2344
U.S. Atomic Energy Commission

The contents of this report have been submitted by Mr. Abraham Weitzberg to the Massachusetts Institute of Technology in partial fulfillment of the requirements for the degree of Doctor of Philosophy.

ABSTRACT

An experimental study of neutron capture in U^{238} in lattices of uranium rods in heavy water was undertaken as part of the Heavy Water Lattice Research Project, A.E.C. Contract AT(30-1)2344. An exponential facility was used for measurements on lattices of natural uranium rods one inch in diameter. The study included the following experiments:

(1) Measurement of the average U^{238} cadmium ratio of the fuel rods.

(2) Measurement of the average ratio of U^{238} capture to U^{235} fissions in the fuel rods (conversion ratio).

(3) Measurement of the distribution of the resonance neutrons in the moderator (both macroscopic and microscopic).

(4) Measurement of quantities directly related to the effective resonance integral of the rods.

The cadmium and conversion ratios were measured by using standard techniques and it was shown that, for the lattices considered, the two independent experimental methods gave equivalent results. The methods, therefore, seem reliable enough so that they can be applied to measurements in more complex systems such as clusters of rods or tight lattices of uranium oxide rods, where large discrepancies have been noted. By using both methods, together, it may be possible to determine the causes of these discrepancies.

The measurements of the resonance neutron distributions were made with cadmium covered dilute, natural uranium foils; together with the results of similar measurements made with bare and cadmium covered gold foils, they served to demonstrate the separability of the energy and spatial dependence of the flux over a considerable portion of the assembly. This result insured that the measurements of the microscopic parameters were made in a neutron energy spectrum representative of the lattice.

A new technique was developed to measure the effective resonance integral of the fuel rods, since standard single rod methods were found to be inadequate for measurements in the lattice. Instead of comparing the epicadmium activation of the fuel rod to that of a dilute U^{238} standard, the rod cadmium ratio was compared with the cadmium ratios of Na^{23}, a 1/v absorber, and Mn^{55} and Co^{59} whose principal resonances are at 332 and 137 ev, respectively. Thus, the standardization was rendered insensitive to perturbations in the asymptotic 1/E flux distribution which occur at energies corresponding to the large U^{238} resonances ($E \ll 137$ ev).

A γ-γ coincidence counting technique for measuring U^{238} activation in the presence of fission products was developed. Use of this technique reduces the fission product background in the 103kev region by roughly a factor of six over that obtained with the simple γ-ray counting method.

TABLE OF CONTENTS

		Page
1.	INTRODUCTION	1
2.	EXPERIMENTS	
	2.1 Experimental Facilities	9
	2.2 Cadmium Ratio Measurements.	12
	2.3 Conversion Ratio Measurements	17
	2.4 Measurements of the Distribution of Resonance Neutrons in the Moderator	26
	2.5 Measurements of the Effective Resonance Integral and Related Quantities	32
3.	DISCUSSION AND CONCLUSIONS	
	3.1 Relation of the U^{238} Cadmium Ratio to the Resonance Escape Probability.	45
	3.2 Comparison of Cadmium Ratio and Conversion Ratio Measurements.	52
	3.3 Evaluation of the Lattice Multiplication Factor	57
	3.4 Discussion of the Effective Resonance Integral Measurements.	64
	3.5 Summary	67
4.	APPENDICES	
	A. Gamma-Gamma Coincidence Technique for U^{238} Activation Measurements	69
	B. Effective Resonance Integrals for U^{238} in Thin Foils.	106
	C. Self-Attenuation of 103 kev Gamma Rays in Thin U^{238} Foils.	112
	D. Flux Depression in Composite Foils	116
	E. References	119
	F. Supplementary Literature Survey.	121

LIST OF TABLES

Table	Title	Page
2.2-1	Average U^{238} Cadmium Ratios.	15
2.2-2	Dilute Gold Cadmium Ratios in Fuel Rods.	16
2.3-1	Conversion Ratio Measurements.	25
2.4-1	Ratio of Resonance Flux in Moderator to that at Surface of Rod	31
2.5-1	Summary of the Measurements of the Effective Resonance Integral	.34
2.5-2	Summary of Cadmium Ratio Measurements with Na^{23}, Mn^{55}, Co^{59} and U^{238} in the MIT Reactor and in the Exponential Lattice.	36
2.5-3	Effective Resonance Integrals of Mn^{55} and Co^{59}, Calculated from Cadmium Ratio Measurements . . .	40
2.5-4	Summary of Calculations of β in the MIT Reactor and in the Exponential Lattice.	42
3.1-1	Parameters for the Calculation of the Resonance Escape Probability	48
3.1-2	Relation of the U^{238} Cadmium Ratio, R_{28}, to the Resonance Escape Probability, p.	50
3.2-1	Summary of the Calculation of the Initial Conversion Ratio, C	54
3.3-1	Lattice Multiplication Factors	61
3.4-1	Summary of Measurements of the Effective Resonance Integral of Lattice Fuel Rods.	65
A-1	Decay of Uranium Foil Depleted to 15 Parts Per Million U^{235}	78
A-2	Minimum Fission Product Correction Factors for Natural Uranium Foil	99
A-3	Minimum Fission Product Correction Factors as a Function of Window Width	101
B-1	Summary of Data and Results of the Measurements of the U^{238} Effective Resonance Integral for Thin Foils	109

LIST OF FIGURES

Figure	Title	Page
2.1-1	Vertical Section of the Subcritical Assembly .	10
2.1-2	Plan View of the Subcritical Assembly	11
2.2-1	Diagram of Central Cluster Arrangement.	13
2.3-1	Typical Data for Conversion Ratio Measurements .	20
2.3-2	Comparison Between R(t) STANDARD and Typical Data for Conversion Ratio Measurement	22
2.4-1	Epicadmium U^{238} Macroscopic Flux Traverses . .	28
2.4-2	Uranium Intracell Flux Traverse	30
A-1	Block Diagram of Counting Equipment	71
A-2	Np^{239} γ-ray Spectrum	74
A-3	Energy Dependence of Random to True Coincidence Ratio	76
A-4	Decay of Natural Uranium (0.005 inch) and U^{235} Foils	80
A-5	U^{235} Fission Product Spectra Below 200 kev. . .	82
A-6	Decay of 0.020 Inch Natural Uranium Foil and U^{235} Foils Shielded during Counting with U^{238}.	84
A-7	Comparison of Fission Product Correction Factor for 0.020 Inch Natural Uranium Foil	86
A-8	Fission Product Singles Correction Factors as Obtained by the Subtraction Method.	88
A-9	Fission Product Coincidence Correction Factors as Obtained by the Subtraction Method.	90
A-10	Fission Product Singles Correction Factors for Natural Uranium Foil 0.020 Inches Thick. . . .	92
A-11	Fission Product Coincidence Correction Factors for Natural Uranium Foil 0.020 Inches Thick. .	93
A-12	Final Fission Product Coincidence Correction Factors for Natural Uranium Foils	95
A-13	Decay of Dilute Natural Uranium and U^{235} Foils .	96

LIST OF FIGURES (Continued)

		Page
A-14	Fission Product Correction Factors for Infinitely Dilute Natural Uranium Foils . . .	97
B-1	U^{238} Effective Resonance Integrals for Thin Foils	110
C-1	Model Used to Calculate the Self-Attenuation of γ-rays in Thin Foils	114
C-2	Attenuation of 103 kev Np^{239} γ-rays in Thin U^{238} Foils.	114
D-1	Flux Depression in Composite Foils	117

1. INTRODUCTION

The general program of an experimental lattice study is the measurement of reactor physics parameters for the specific lattice in question and the use of the experimental results to test calculational techniques having wider applicability. An essential part of such a study is the determination of the neutron capture rates in U^{238}. For the design of reactor lattices containing appreciable amounts of U^{238}, knowledge of the capture rate in this material is most important, from both the standpoints of lattice reactivity and plutonium production. This report gives the results of a study of the experimental techniques used to determine the U^{238} capture rates in heavy water moderated lattices of uranium metal rods. The nuclear analysis for the development of power reactors is generally accomplished with multigroup computer codes, but these differ greatly from laboratory to laboratory. For this reason, the four-factor approach, which is useful conceptually, will be used to analyze the measurements to be described. The original data are included, however, to allow possible multigroup analysis.

The experimental determination of the U^{238} capture rates in heterogeneous systems has been approached in the past in several different ways. The three most important techniques are:

(1) The measurement of the effective resonance integral for a single fuel element.

(2) The measurement of the average U^{238} cadmium ratio for lattice fuel elements.

(3) The measurement of the initial conversion ratio for lattice fuel elements.

The first practical technique was the measurement of the effective resonance integral (ERI) for isolated (single) fuel elements, by comparing the activation of the fuel element to that of a sample with a known resonance integral, when both were immersed in the same resonance flux. Creutz, et al, (6) used iodine as the resonance flux monitor and dilute U^{238} as the standard of known resonance integral. Goldstein and Hughes (12), using cadmium ratio measurements, compared uranium to indium, and other investigators used still different techniques. The more recent work of Hellstrand (16) is based on the use of gold flux monitors and a dilute U^{238} standard. In addition to the measurements of the ERI for isolated fuel elements by activation techniques, there have been several pile oscillator and danger coefficient measurements. Among them are those by Davis (9), Muelhause (21), and Dayton and Pettus (10).

While the techniques of the ERI measurements vary greatly, their interpretation and the way in which they

are used for heterogeneous assemblies of fuel and moderator vary little. The ERI's measured for single fuel elements of different sizes can be correlated in terms of the ratio of surface area to mass, S/M. The first correlations were based on Wigner's (13) formulation of the volume and surface portions of the ERI, and were of the form:

$$ERI = a + b(S/M) \text{ barns}, \qquad (1\text{-}1)$$

where a and b are the mass and surface contributions respectively. Variations of this form have been used to include the effects of flux depression within the fuel element (23) and the probability of a neutron passing completely through the element without suffering a collision (11). In 1955, Gurevich and Pomeranchouck (14) proposed a theoretical model which indicated that the ERI varied linearly with $(S/M)^{1/2}$ rather than with (S/M). This form of the equation has also been found to correlate the ERI data well, and the equation generally used now for U^{238} metal elements is:

$$ERI = 2.81 + 24.7\ (S/M)^{1/2} \text{ barns}, \qquad (1\text{-}2)$$

as measured by Hellstrand.

To use the ERI's measured for single isolated fuel elements for actual lattices, it is necessary to consider

the interaction of many elements. Dancoff and Ginsburg (8) suggested that the surface portion of the ERI would be decreased in a lattice because of the shielding effect of surrounding elements, which can be considered black to those neutrons that contribute to the surface absorption. This correction, applied to the ERI as obtained from either equation 1-1 or 1-2, then gives the ERI for a lattice fuel element. The ERI is then used to calculate the resonance escape probability, p, according to some theoretical model. For example, an equation obtained from slowing down theory may be used, such as

$$p = \exp\left\{ - \frac{N_o V_o ERI}{V_1 \Sigma_{s1} \xi_1} \right\}, \qquad (1\text{-}3)$$

where N_o is the nuclide density in the fuel, V_o and V_1 are the volumes of fuel and moderator, respectively, in a unit cell, and Σ_{s1} and ξ_1 are the macroscopic scattering cross section and logarithmic energy decrement for the moderator. Modified forms of equation 1-3 have been used for various special cases, but the basic idea remains the same.

The second technique, used most often for actual lattice studies, is the measurement of the average U^{238} cadmium ratio R_{28}, for the fuel elements, which gives the

relative thermal and epithermal captures in U^{238}. These are then related to p through the neutron cycle. As with the measurements of the ERI, the techniques used by different investigators have varied considerably, two of the most important being the chemical separation, β-ray counting method used at Brookhaven (18), and the γ-ray counting method used at Bettis (19). The interpretation of these measurements has also showed considerable variation. The simplest equation used to relate R_{28} to p is that used at Bettis:

$$\rho_{28} = \frac{1}{R_{28}-1} = \frac{\text{epithermal } U^{238} \text{ capture}}{\text{thermal } U^{238} \text{ capture}} = \frac{1-p}{pfF} , \quad (1\text{-}4)$$

where f is the usual thermal utilization factor, F is the ratio of thermal captures in U^{238} to total thermal absorptions in the fuel and ρ_{28} is defined by the first equation. Solving for p yields:

$$p = \frac{1}{1 + \rho_{28} fF} . \quad (1\text{-}5)$$

Many corrections to equation 1-5 have been made to include the effects of fast U^{238} capture, 1/v capture above the cadmium cutoff, and leakage of neutrons in the fast, resonance, and thermal energy groups. The most

complicated expression for p is that used at Brookhaven which includes all of the above effects. A derivation of this equation is given in Reference (18). The choice of an equation to relate R_{28} to p is in part determined by the specific definitions used for the four factors, ϵ, p, f, η, as it is necessary to define these quantities consistently, i.e., to have each process in the neutron cycle counted once, and only once. Nevertheless, the method of deriving p from R_{28} measurements is somewhat arbitrary and considerable variation in the quantity (1-p) is possible.

The third approach to the problem of determining U^{238} capture rates in a lattice is the measurement of the initial conversion ratio C, usually defined as the ratio of the U^{238} capture rate to the U^{235} absorption rate. A basic description of the experimental method is given by Curtis, et al, (7), and slightly different techniques have been employed by Campbell and Carter (5) and by Baer, et al (3). For these measurements, it has been customary to redefine the measured conversion ratio C^*, in terms of the U^{235} fission rate, since this is the quantity that can be measured directly. The conversion ratio measurement is more directly suited to comparison with multigroup reactor calculations than it is to interpretation according to the four factor formula. It

can, however, be used in a calculation of the multiplication factor k, that is independent of the usual four factors. This calculation is based on the fundamental definition of the effective multiplication of neutrons (25):

$$k_{eff} = \frac{\text{production rate}}{\text{consumption rate + leakage rate}} , \qquad (1\text{-}6)$$

where the rates are summed over the components of the lattice cell. To obtain the infinite multiplication factor k_∞, the leakage is set equal to zero. The result should then be directly comparable to the quantity k_∞ as determined using the four factors.

With the three experimental techniques described above and the different methods of interpreting those results, there is considerable need for a critical evaluation of the various approaches to the problem of determining the U^{238} capture rates in lattices. To this end, a series of measurements was conducted on lattices of 1.010 inch diameter, natural uranium rods in heavy water and the results compared by using the different methods of interpretation. Included in the program were:

(1) Measurement of R^{28}, the average U^{238} cadmium ratio of the fuel rods.

(2) Measurement of C^*, the average ratio of U^{238} capture to U^{235} fissions in the fuel rods.

(3) Measurement of the distribution of the resonance neutrons in the moderator (both macroscopic and microscopic).

(4) Measurement of the quantities necessary to determine the effective resonance integral (ERI) of the rods.

It is believed that the measurements on this type of loosely spaced lattice with heavy water moderator will be more clear cut and without some of the problems inherent in close-packed water moderated lattices and in the use of uranium oxide fuel elements. If the problems can be resolved for the simpler heavy water lattices, the techniques will provide a starting point for the solution of the problems of the more complex systems.

2. EXPERIMENTS

2.1 Experimental Facilities

Lattice measurements were carried out in a subcritical assembly which uses the thermal column of the MIT Reactor as the neutron source. Cross section drawings of the assembly are given in Figure 2.1-1 and 2.1-2. The fuel elements were cylindrical rods of natural uranium, 1.010 $\pm$ 0.005 inches in diameter and 60 inches long; three triangular lattice spacings, 4.50, 5.00 and 5.75 inch were studied. The support beams for the fuel rods were fabricated so that three rods (the central rod and two adjacent rods of the inner hexagon) could be removed as a cluster. Measurements of the microscopic lattice parameters were made in this central cluster. The subcritical assembly is described in detail in Report NYO-9658 (15).

In addition to the subcritical assembly, the regular irradiation facilities of the MIT Reactor were used for foil irradiation and calibration.

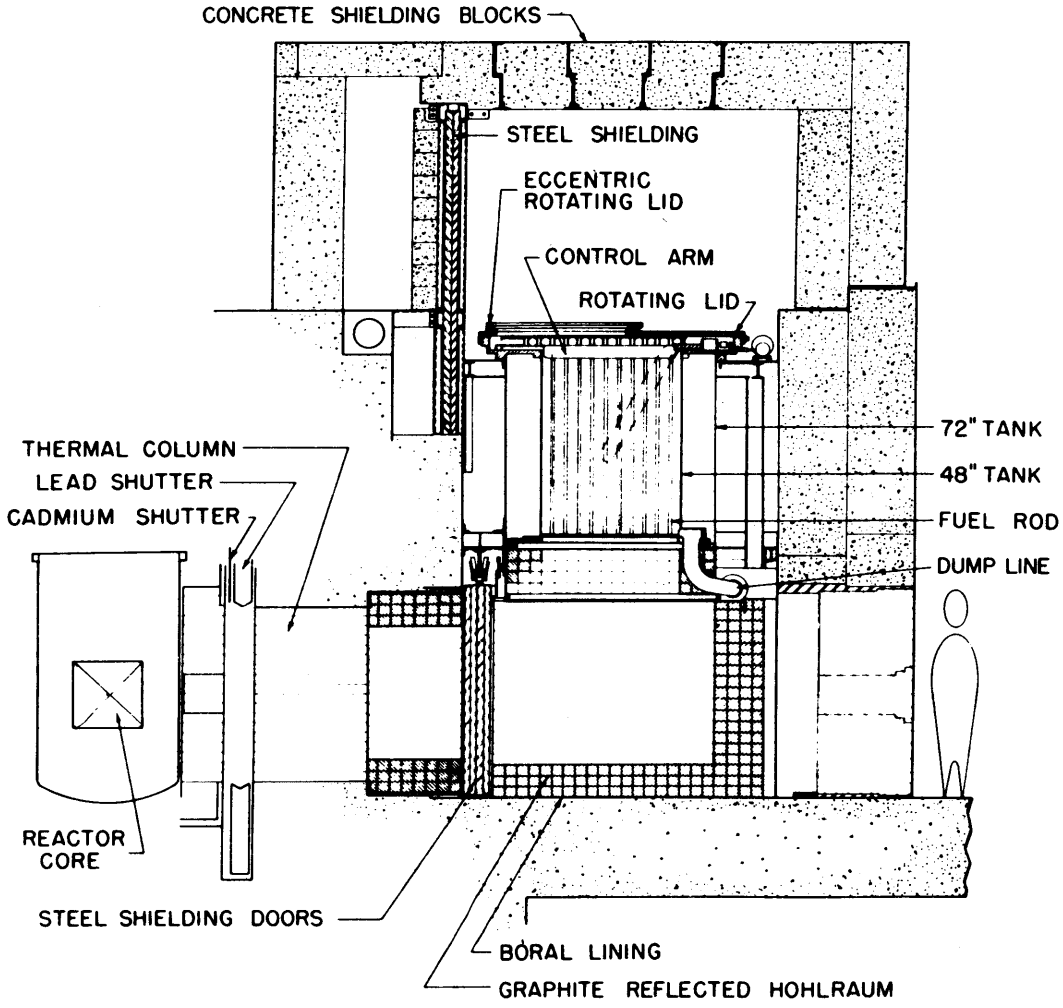

FIG. 2.1-1 VERTICAL SECTION OF THE SUBCRITICAL ASSEMBLY

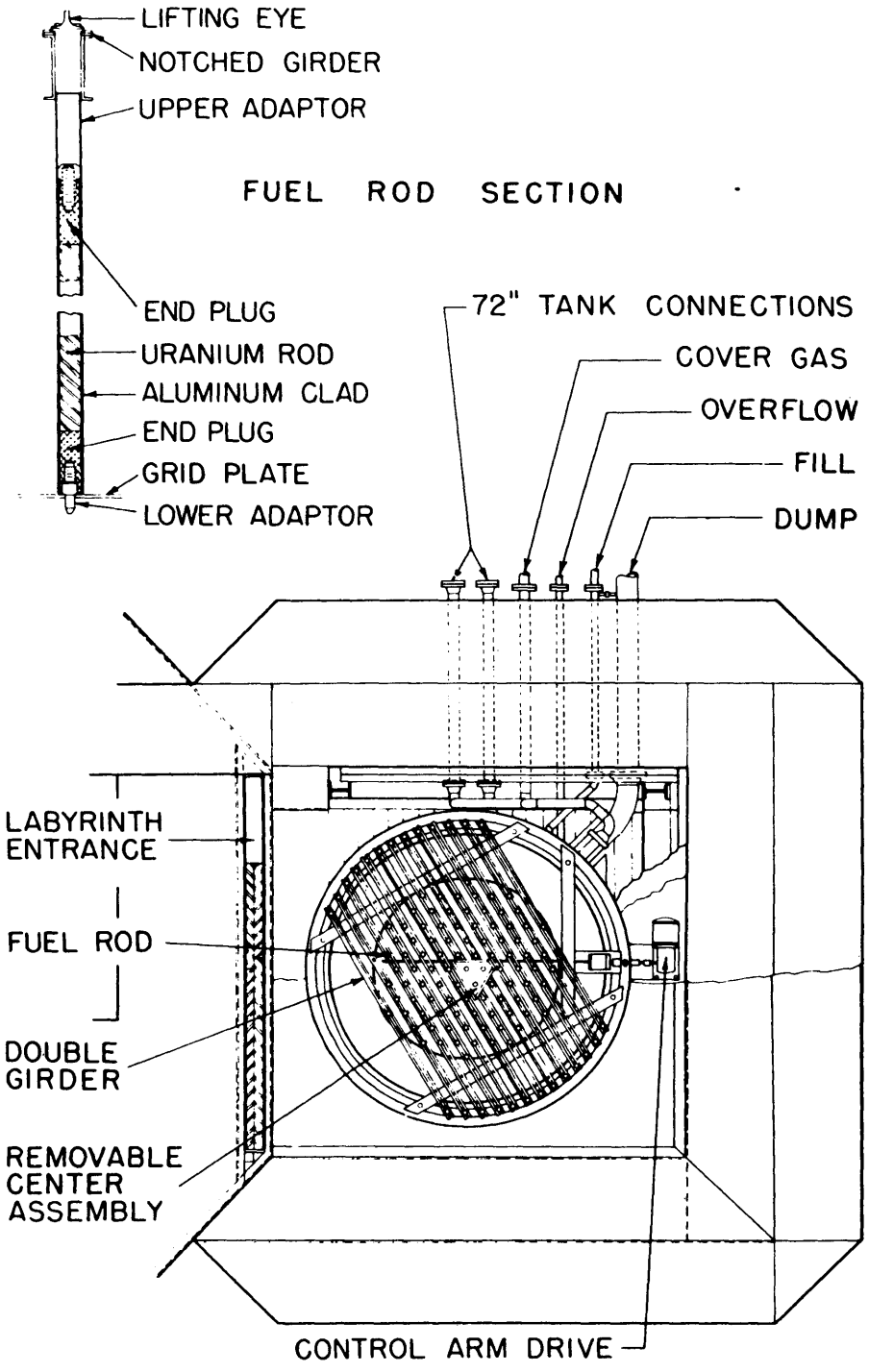

FIG. 2.1-2 PLAN VIEW OF THE SUBCRITICAL ASSEMBLY

2.2 Cadmium Ratio Measurements

The average U^{238} cadmium ratio, R_{28}, for 1.010 inch diameter rods of natural uranium was measured to determine the relative thermal and epithermal U^{238} capture rates. Two identical foils of uranium depleted to fifteen parts per million U^{235}, 1.010 inches in diameter and 0.005 inches thick, were irradiated in equivalent positions in the lattice at a height of two feet above the bottom of the fuel rods. One foil was placed between two fuel slugs with thin (0.001 inch thick) aluminum catcher foils on either side to prevent the pickup of fission products from the surrounding natural uranium. The other foil was placed in a pill box of 0.020 inch thick cadmium, composed of a sleeve 0.25 inches in length imbedded in the aluminum cladding and two 1.010 inch diameter discs which were placed on either side of the depleted foil. Two buttons of the natural uranium, 0.050 inches thick, were included within the cadmium covers to minimize the effect of streaming of resonance neutrons from the moderator through the cadmium. A schematic diagram of the irradiation setup is shown in Figure 2.2-1.

After a four-hour irradiation and a cooling period of from four to eight hours, the two foils were counted

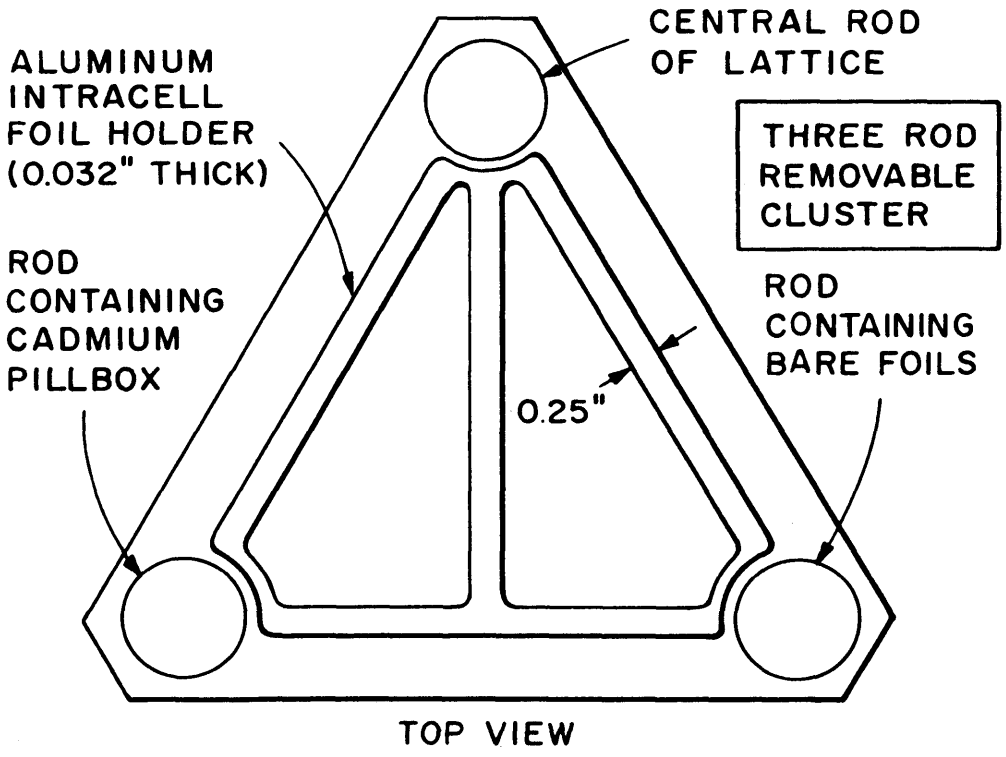

FIG. 2.2-1 DIAGRAM OF CENTRAL CLUSTER ARRANGEMENT

alternately in a gamma spectrometer. A detailed description of the spectrometer system is given in Section 2 of Appendix A. To increase the amount of data taken for these measurements, both single channels were used and the counts in each summed. The spectrometers were set to straddle the 103 kev peak of Np^{239} with window widths of 30 kev. The Np^{239} is produced from U^{238} by the reaction:

$$U^{238} \xrightarrow{(n,\gamma)} U^{239} \xrightarrow[23.3m]{(\beta,\gamma)} Np^{239}, \qquad (2.2\text{-}1)$$

and decays by β emission to Pu^{239} with a 2.33 day half-life. The foils were counted several times over a period of days to verify that the observed radiation decayed with the proper half-life. The ratio of the two activities was taken for each pair of counts and these were then averaged to yield the final results. Each pair of foils was matched in weight to within 0.5 per cent, to obviate the need to correct for the self-attenuation of the gamma rays, but a small weight correction was still required.

The results of the series of U^{238} cadmium ratio measurements for 1.010 inch natural uranium rods in hexagonal arrays of 4.50, 5.00, and 5.75 inch spacing are given in Table 2.2-1. Each number is an average

value obtained from at least two separate measurements; the error is the standard deviation of the mean value of these measurements.

Table 2.2-1

Average U^{238} Cadmium Ratios
1.010 Inch Natural Uranium Rods in Hexagonal Array.

Lattice Spacing (Inches)	R_{28}
4.50	2.972 ± 0.031
5.00	3.495 ± 0.010
5.75	4.223 ± 0.043

For the lattice of 4.50 inch pitch, the U^{238} cadmium ratio was also measured for fuel rods at a point halfway between the central cluster and the tank edge, and within experimental accuracy the results (3.007 ± 0.035) agreed with the value quoted in Table 2.2-1.

With the same experimental arrangement that was used for the U^{238} cadmium ratio measurements, the cadmium ratio for infinitely dilute gold foils, R^{o}_{Au}, was measured for the three lattices. The depleted uranium foils shown in Figure 2.2-1 were replaced by foils of an alloy of gold, one per cent by weight, in aluminum. After an irradiation of from 12 to 24 hours, the foils were

counted in the gamma spectrometer system with the pulse height analyzers set to straddle the 412 kev γ-ray peak of gold with a 60 kev window. To correct for weight differences and possible inhomogeneities in the alloy, each pair of foils was intercalibrated using a foil wheel technique. The results of these measurements are given in Table 2.2-2.

TABLE 2.2-2

Dilute Gold Cadmium Ratios in Fuel Rods

Lattice Spacing (Inches)	R^{o}_{Au}
4.50	1.69 ± 0.03
5.00	1.80 ± 0.05
5.75	2.27 ± 0.02

2.3 Conversion Ratio Measurements

The conversion ratio C^*, here defined as the ratio of the number of captures in U^{238} to that of fissions of U^{235}, was measured for several lattices of one inch diameter natural uranium rods at the same positions as were the cadmium ratios. It must be noted that this definition of conversion ratio is not the usual one, which is the ratio of U^{238} captures to U^{235} absorptions, but corresponds to those quantities that are directly measurable. Two foils, a 0.005-inch, depleted uranium foil and a 0.005-inch foil of uranium, 9.8 per cent by weight in aluminum and enriched to 93.17 atom per cent U^{235}, were exposed back to back in the position of the "bare" foils in Figure 2.2-1. Aluminum catcher foils (0.001 inches thick) were used to separate the foils from each other and from the surrounding rod. The composition of the U^{235}-Al foil is such that the fission rate is less than twice as great in the foil as in the surrounding rod. The effect of this on the test area is small because of the relatively small volume of the U^{235}-Al foil.

The foils were irradiated for four hours and, after a wait of from 4 to 8 hours, they were counted alternately several times a day for about a week in the gamma spectrometer system described previously. To increase

the amount of data taken, both singles channels were used and the counts in each summed. For the depleted uranium foil the 103 kev peak of Np^{239} was counted by using a 30 kev window width; for the U^{235} foil the 143 kev fission product peak was counted, also by using a 30 kev window. The spectrometer energies were calibrated by using three peaks: the 103 kev peak of Np^{239}, and the 70 kev and 280 kev peaks of Hg^{203}. Figure A-5, in Appendix A, shows the fission product gamma spectrum in this energy range, with the upper curve illustrating the spectrum obtained from a U^{235}-Al foil 10 days after irradiation. When the foils were counted several days after irradiation, the only differences found in the spectra were changes in the relative peak heights due to differing half lives.

The decaying 143 kev activity was followed for a period of about three weeks and it had not assumed a simple exponential form at the end of this period. Analysis of the decay curve by use of the "peeling" technique indicated the presence of at least three contributing γ-rays of this energy. The 143 kev peak was chosen because of the good resolution of the 1/2 inch crystals for low energies, and because this peak gives the lowest relative foil background of any of the fission product peaks below 200 kev.

The ratio of the 143 kev fission product activity to the 103 kev Np^{239} activity, $R_{LATTICE}$, was calculated for each pair of counts. Typical results are shown in Figure 2.3-1 as a function of time after irradiation. To facilitate computation, the count rates were always normalized to foils of standard weight (1.1500 grams for the depleted uranium, and 0.2000 grams for the U^{235}-Al). The actual foil weights varied near these values. For the U^{235}-Al foil only a weight correction was necessary, but for the depleted uranium a self-attenuation correction also had to be applied. For a difference in foil thickness of 6%, the attenuation correction amounts to about 1%, with a linear variation with thickness in this range. The simple technique used to obtain this correction factor is described in Appendix C.

To normalize the relative fission product and Np^{239} activities of the test foils to a known standard, similar foils were irradiated back to back in a well-thermalized flux. This method was used by Baer, et al (3). The D_2O-filled lattice tank was used without the uranium fuel rods and the measured gold cadmium ratio was 2000 ± 100. This method of normalization is enhanced by the fact that the flux depression in the foils during the standardization run may be neglected. The absorption mean free path λ

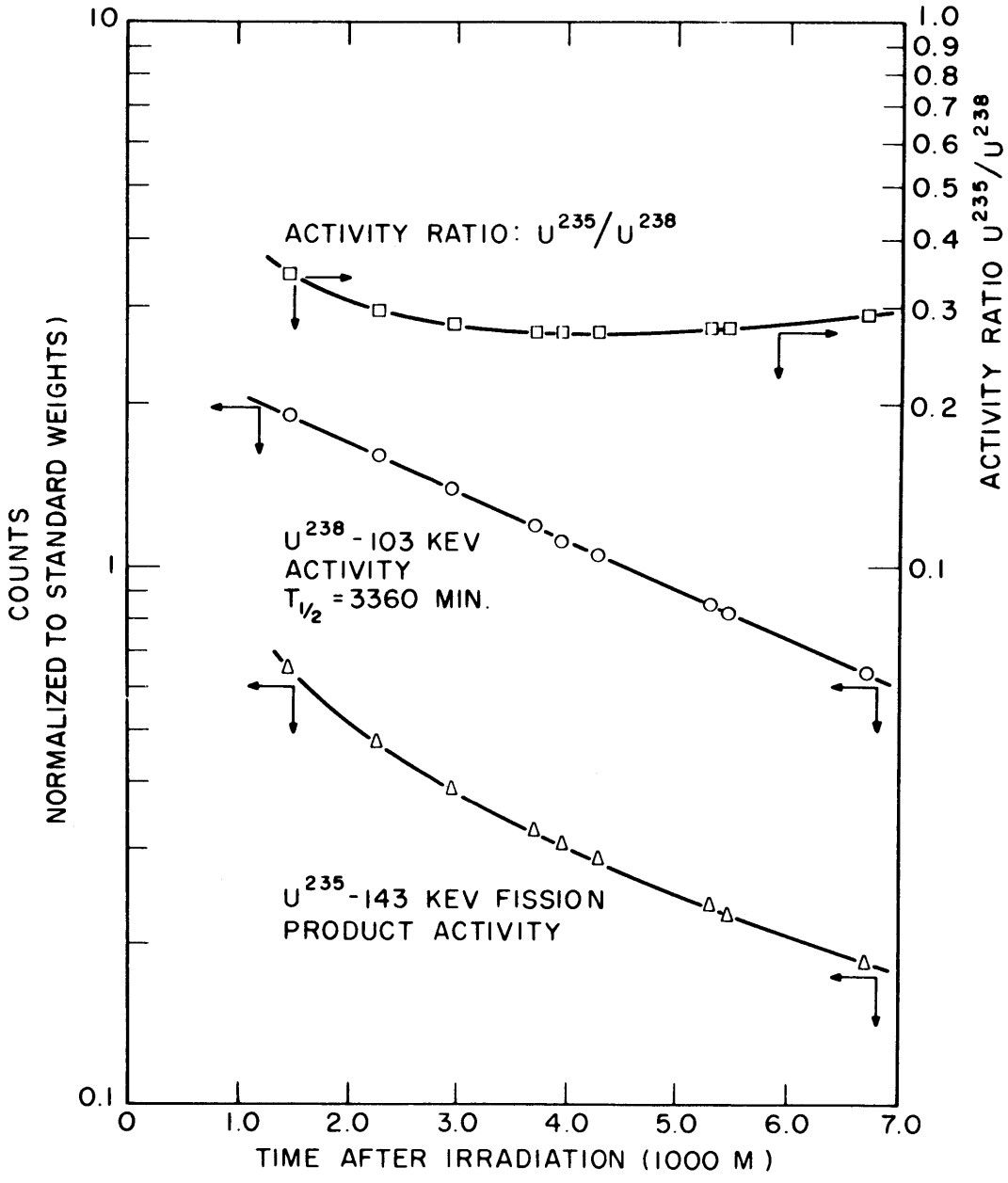

FIG. 2.3-1 TYPICAL DATA FOR CONVERSION RATIO MEASUREMENT

is 3.0 inches in the depleted uranium and 0.68 inches in the U^{235}-Al alloy. Wilkins (27) gives the following equation for the fractional activation f of a foil of thickness t when irradiated in a purely thermal flux:

$$f = 1 + \pi^{-1/2} y \ln y\left(1 + \frac{y^2}{12}\right) + 0.131y - y^{2/3} - 0.007y^3, \quad (2.3\text{-}1)$$

where $y = t/\lambda$. For single 0.005 inch depleted uranium foils and U^{235}-Al foils, f is 0.994 and 0.981 respectively. However, the foils are irradiated back to back and there is an interaction effect to be considered. As is demonstrated in Appendix D, two foils whose fractional activations are f_1 and f_2 $(1-f \ll 1)$ each have a fractional activation of $f_1 f_2$ when irradiated back to back. Thus, for the standardization runs the depression is the same in both foils, and its effect is cancelled out of the activity ratio.

The 103 kev Np^{238} and 143 kev fission product activities were again measured and the ratio of fission product to Np^{239} activity determined as a function of time. A least squares fitting code, written by J. Wolberg (28) for the IBM 709 computer, was used to fit a fifth order power series to the data, the results were normalized to the standard weight foils, and the self-attenuation factor was applied to the U^{238} foil.

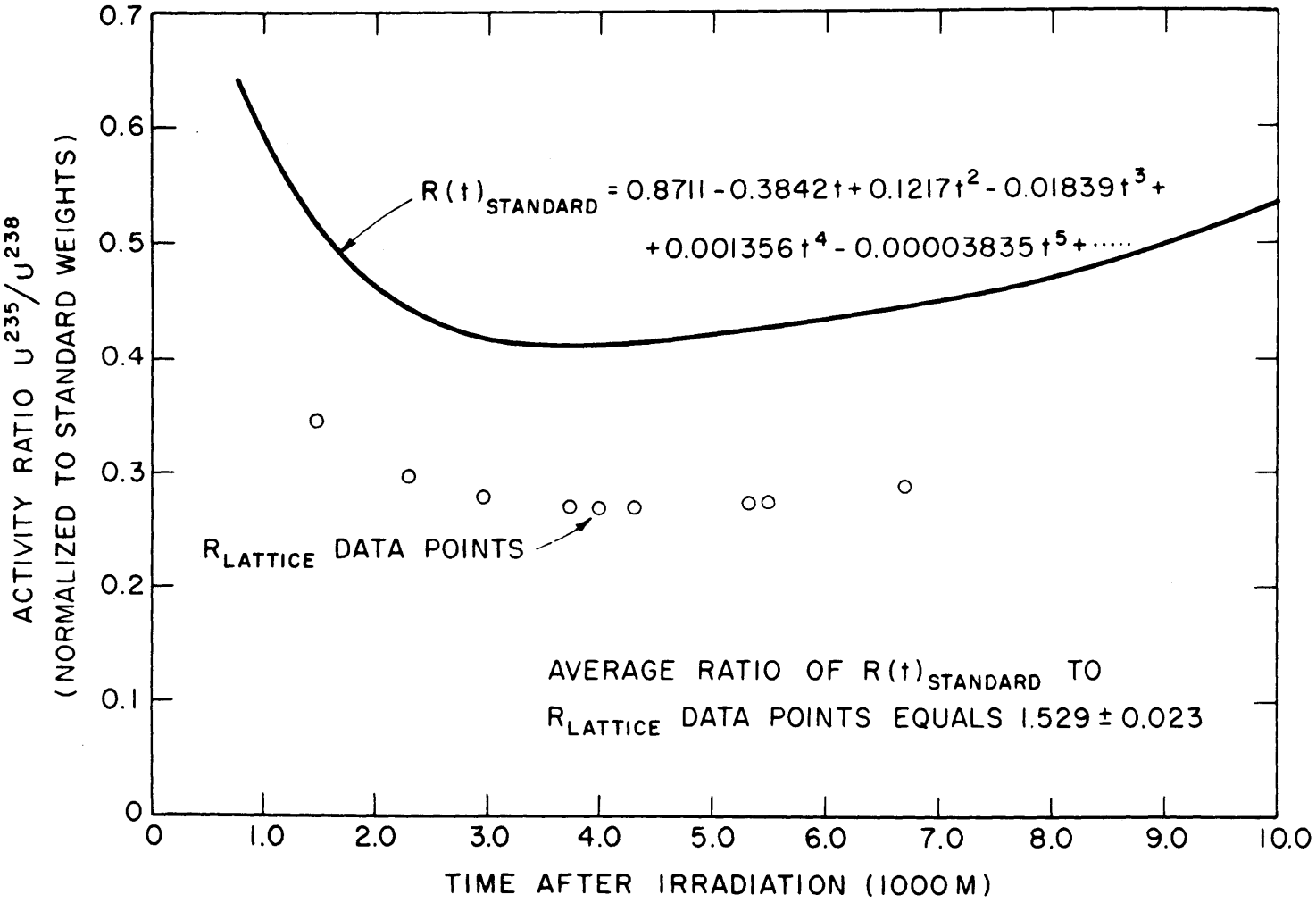

FIG. 2.3-2 COMPARISON BETWEEN $R(t)_{STANDARD}$ AND TYPICAL DATA FOR CONVERSION RATIO MEASUREMENT

Several measurements of this ratio of fission product activity to Np^{239} activity were made, and the average of these is:

$$R_{STANDARD}(t) = 0.8711 - 0.3842t + 0.1217t^2 - 0.01839t^3 + 0.001356t^4 - 0.00003835t^5, \qquad (2.3\text{-}2)$$

where t is the time after irradiation in units of 1000 minutes. This equation is valid in the range of t between 800 and 10,000 minutes after irradiation, and fits the data of several standarization runs to better than 0.1 per cent. In Figure 2.3-2, the standard curve $R_{STANDARD}(t)$ is compared with typical data from a lattice measurement. From equation 2.3-2, the value of $R_{STANDARD}$ for the time after irradiation corresponding to each $R_{LATTICE}$ data point was calculated and the ratio $\frac{R_{STANDARD}}{R_{LATTICE}}$ taken. These were then averaged to yield the final result for the experiment, $(\frac{R_{STANDARD}}{R_{LATTICE}})_{avg}$

Using this technique, the actual composition of the test foils is cancelled out of the ratio, leaving just the effective flux and cross-section ratios for U^{235} and U^{238}. The U^{235} and U^{238} reaction rates corresponding to an irradiation of natural uranium in the standard flux were then calculated from the nuclide concentrations and

thermal cross sections. For the highly thermalized flux, it was assumed that the neutron temperature was equal to that of the D_2O, 25°C. The reaction rates were calculated by using Westcott's (26) formulation for effective thermal cross sections, $\hat{\sigma}$:

$$\hat{\sigma} = \sigma^{2200}(g + rs), \qquad (2.3\text{-}3)$$

where r is the epithermal flux index and is equal to zero for this measurement. The g-factor indicates deviation of the cross section from the 1/v law. For U^{238} (a 1/v- absorber) it is equal to unity and for the non-1/v U^{235} fission cross section at 25°C it is equal to 0.9737. The currently used values for the 2200 m/sec fission cross section of U^{235} and activation cross section of U^{238} are 582 ± 4 and 2.71 ± 0.02 barns respectively, and the conversion ratio for natural uranium in the standard flux is, therefore:

$$C^*_{STANDARD} = \left(\frac{0.99274}{0.00720}\right) \frac{2.71}{582 \times 0.9737} = 0.6596 \pm 0.0066. \qquad (2.3\text{-}4)$$

Multiplying (2.3-4) by the average value $\left(\frac{R_{STANDARD}}{R_{LATTICE}}\right)_{avg}$ for the test foils yields $C^*_{LATTICE}$. The results of the conversion ratio measurements $C^*_{LATTICE}$, as well as the

intermediate values of $\left(\frac{R_{STANDARD}}{R_{LATTICE}}\right)_{avg}$ for the three lattice spacings, are summarized in Table 2.3-1. Each value is the average of several independent runs; the error is the standard deviation of the mean value of these measurements.

For the lattice of 4.50 inch spacing, C^* was also measured in a fuel rod at a point halfway between the central cluster and the tank edge, and within the experimental accuracy the results for C^* (1.022 $\pm$ 0.020) agreed with the value quoted in Table 2.3-1.

TABLE 2.3-1

Conversion Ratio Measurements[a]

1.010 Inch Natural Uranium Rods in Hexagonal Array

Lattice Spacing (Inches)	$\left(\frac{R_{STANDARD}}{R_{LATTICE}}\right)_{avg}$	$C^*_{LATTICE}$
4.50	1.542 $\pm$ 0.031	1.017 $\pm$ 0.023
5.00	1.437 $\pm$ 0.026	0.948 $\pm$ 0.020
5.75	1.303 $\pm$ 0.021	0.859 $\pm$ 0.016

(a) Measured conversion ratio defined as ratio of U^{238} capture rate to U-235 fission rate.

2.4 Measurements of the Distribution of Resonance Neutrons in the Moderator

Two types of measurements were made to determine the source distribution of neutrons with energies corresponding to the principal U^{238} resonances: macroscopic axial and radial flux traverses and microscopic intracell traverses. For these measurements cadmium covered foils 0.003 inches thick of an alloy of one per cent by weight natural uranium in aluminum were used. The effective U^{238} thickness was 0.2 mg/cm^2, small enough so that self-shielding of the U^{238} was negligible, as was verified by measuring the same specific epicadmium activity for different foil thicknesses up to 0.015 inches.

The macroscopic measurements were made and analyzed by using the techniques developed by P. F. Palmedo (22) for buckling measurements. One-half inch diameter foils were used and, because of the small concentration of U^{238}, they were irradiated for about 24 hours. After a suitable cooling period, the foils were counted in a gamma spectrometer similar to the ones described previously, except that the NaI detector was placed in a Nuclear Chicago automatic sample changer consisting of a N/C C110B changer, N/C 186 scaler and a N/C C11B printer, and the output of the Baird Atomic pulse height

analyzer of the spectrometer system was fed into the Nuclear Chicago scaler. Thus, both the benefits of differential energy discrimination and automatic sample changing were obtained. For the uranium-aluminum foils the spectrometer was set to straddle the 103 kev Np^{239} peak with a window width of 30 kev. The foils were counted consecutively and their measured activities corrected back to some arbitrary time by using the known half life of 2.33 days. For each run the foil weights were matched to within $\pm$ 0.3% so that no weight correction was needed and, since the foils were cadmium covered during irradiation, no correction for U^{235} fission products was necessary.

Macroscopic traverses were made on the lattice of 1.010 inch natural uranium rods in a hexagonal array of 4.50 inch pitch. They yielded results in agreement with both the bare and cadmium covered gold traverses of Palmedo, but the spread of the data was much greater than could be expected using the foils of matched weights. This result suggested that the natural uranium-aluminum alloy was not homogeneous. To check this possibility, the same foils were intercalibrated in the same flux using a wheel technique and differences in activation up to 10 per cent were measured. Consequently, all foils of this alloy were first intercalibrated before use.

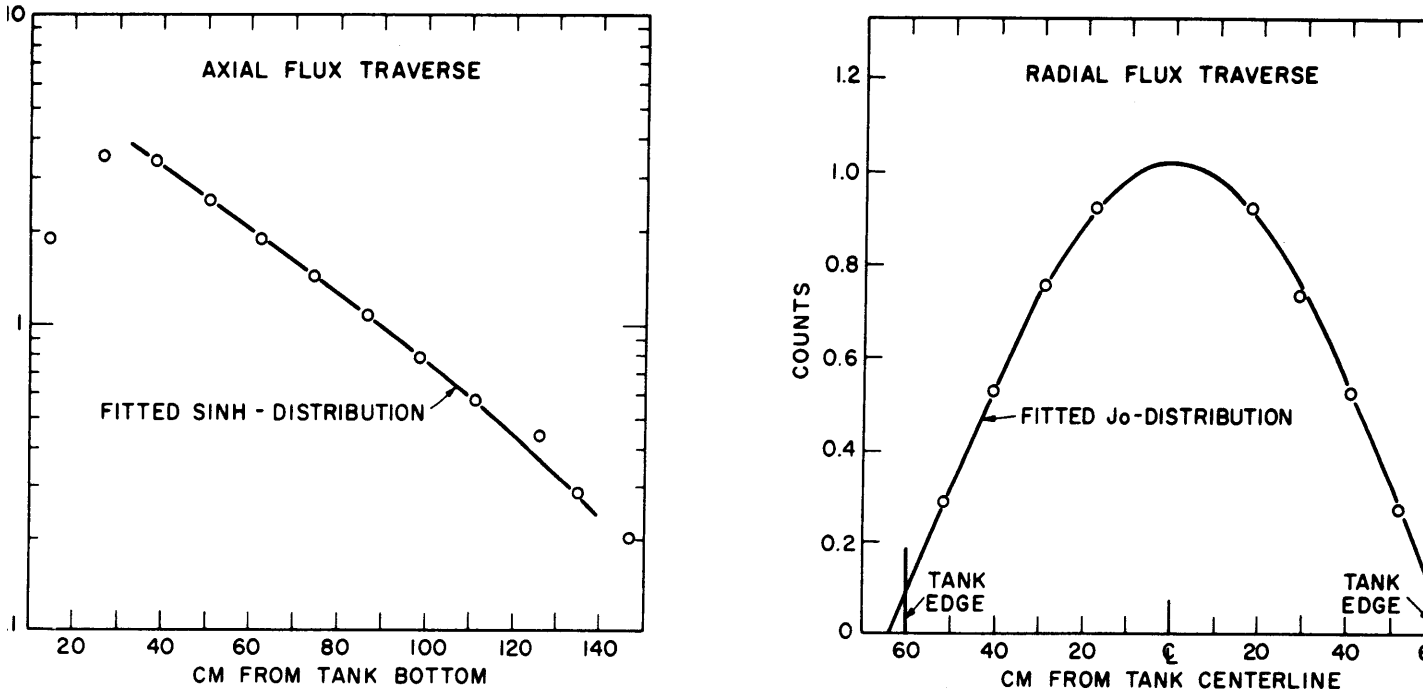

FIG. 2.4-1 EPICADMIUM U^{238} MACROSCOPIC FLUX TRAVERSES

LATTICE OF 1.010 INCH NATURAL URANIUM RODS IN HEAVY WATER – 4.50 INCH PITCH. DATA POINTS OBTAINED WITH CADMIUM COVERED FOILS OF ALLOY OF NATURAL URANIUM IN ALUMINUM, ONE PERCENT BY WEIGHT. CURVES FITTED TO FLUX TRAVERSE DATA OF P.F. PALMEDO (22) FOR BARE AND CADMIUM COVERED GOLD FOILS.

The corrected results of the axial and radial traverses on the lattice of 4.50 inch spacing are shown in Figure 2.4-1. The experimental data points are compared with the fitted curves as determined by Palmedo from gold traverses, and the agreement is very good except for the extremes of the axial traverse. The fitted J_o distribution yields a radial buckling of $14.2 \pm 0.1\ m^{-2}$ and an extrapolated radius of 63.9cm. The axial traverse yields an axial buckling of $5.7 \pm 0.2\ m^{-2}$ and a relaxation length of 41.8 cm, and also shows that at the height of 2 feet above the bottom of the fuel rods the resonance flux has already assumed its exponential mode of decay. This result ensures that the cadmium ratio and conversion ratio measurements were made in a flux representative of this exponential lattice.

The intracell measurements were made with 0.25 inch diameter cadmium covered foils placed on a thin aluminum foil holder that fit between the rods of the removable center cluster at a point level with the foil positions of the cadmium ratio and conversion ratio measurements. A diagram of this arrangement is also shown in Figure 2.2-1. The irradiation and counting procedure were the same as those for the macroscopic traverses and, in addition, the intracell data were corrected for the J_o shape of the macroscopic flux distribution as determined

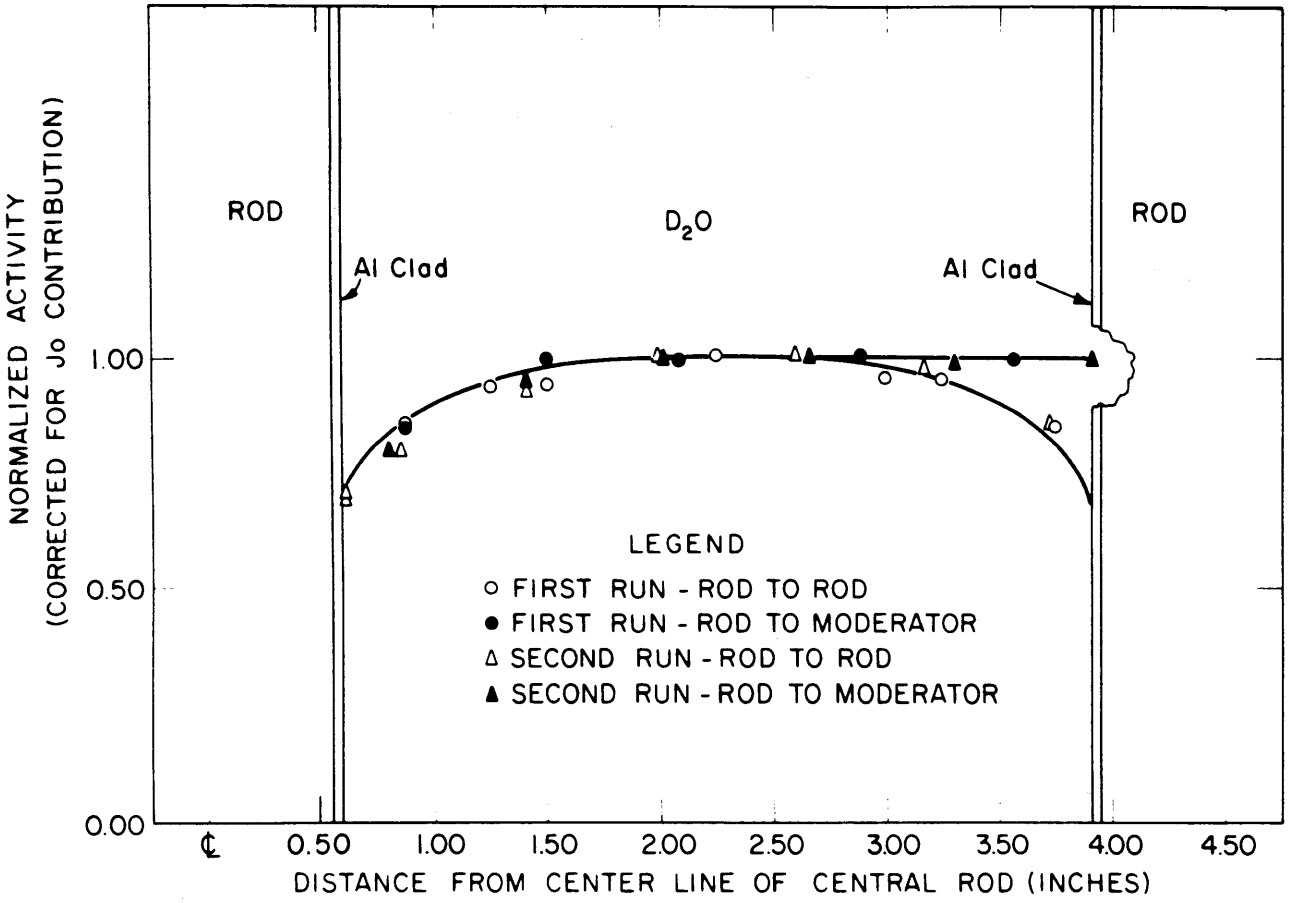

FIG. 2.4-2 URANIUM INTRACELL FLUX TRAVERSE. INTRACELL TRAVERSE WITH CADMIUM COVERED DILUTE NATURAL URANIUM FOILS - 1.010 INCH NATURAL URANIUM RODS - 4.50 INCH TRIANGULAR PITCH

above. The results for the lattice with 4.50 inch spacing are shown in Figure 2.4-2. The rod-to-rod traverse shows the characteristic dip near the rods, and the rod-to-moderator traverse shows the same dip at the rod but flattens out in the region away from the rods.

Similar results were obtained on the lattices of 5.00 and 5.75 inch pitch. To characterize the shape of the flux distributions for the three lattices, the ratio of the flux at the point midway between the rods to the flux at the surface of the rods was measured separately with the same detector foils. The resonance flux in the moderator away from the fuel rods is flat and it is a convenient point of reference. These results are presented in Table 2.4-1.

TABLE 2.4-1

Ratio of Resonance Flux in Moderator[a] to That at Surface of Rod.

Measured with Cadmium Covered Foils of One Weight Per Cent Natural Uranium in Aluminum for Lattices of 1.010 Inch Natural Uranium Rods in Hexagonal Array.

Lattice Spacing (Inches)	Flux Ratio ($\frac{\text{Moderator}}{\text{Surface}}$)
4.50	1.407 ± 0.024[b]
5.00	1.410 ± 0.015
5.75	1.359 ± 0.005

(a) Moderator flux measured at the point midway between two adjacent rods.

(b) Errors are the standard deviations of the mean value of at least two separate measurements.

2.5 Measurements of the Effective Resonance Integral and Related Quantities

A careful study of the measurement of the effective resonance integral (ERI) was made in the lattices of 1.010 inch diameter natural uranium rods. First, a technique similar to that used by Hellstrand (16) was tried. Two 1.010 inch, cadmium covered, infinitely dilute natural uranium foils were irradiated, one in a rod and the other at the surface of the rod. The foils, 0.003 inches thick, were made of an alloy of natural uranium, one per cent by weight, in aluminum and were proven to be infinitely dilute by measuring the same specific epicadmium activity for different thicknesses up to 0.015 inches.

The foil in the rod was placed in the same position as were the cadmium covered foils for the cadmium ratio measurements (see Figure 2.2-1), and the other foil was placed at the same height on the outside of the central rod of the removable cluster. A J_o correction was made to normalize the activities to the same position. The ratio of the foil activities was measured in the gamma spectrometer system previously described. The ratio was then used to obtain the ERI of the rod from the known resonance integral for a dilute sample:

$$\text{ERI (rod)} = \left[\text{ERI (dilute)} + 1.4 \text{ barns}\right] \times \frac{\text{activity of rod}}{\text{dilute sample activity}} - 1.4 \text{ barns}, \qquad (2.5\text{-}1)$$

where the resonance integrals are expressed in barns, and 1.4 barns is the epicadmium 1/v contribution to the U^{238} activation, with the cadmium cutoff energy taken to be 0.40 ev for 0.020 inch thick cadmium. For U^{238} the dilute resonance integral in a 1/E flux is 282 barns. First measurements gave results that indicated the ERI of the rod was about three times the accepted value, taken to be 9.9 barns. This is the average of the value 10.0 barns obtained from Hellstrand's measurements (Equation 1-2), and the value 9.8 barns calculated by means of the method of Adler, Hinman, and Nordheim (1).

Three possible reasons for the large discrepancy are:

(1) The dilute uranium foils used for the standardization were not infinitely dilute.

(2) The resonance neutron flux in the lattice was depressed from the asymptotic 1/E distribution at the energies of the U^{238} resonances.

(3) There was streaming of resonance neutrons through the aluminum of the foil in the rod.

The first two possibilities would cause the activity of the foil at the surface of the rod to be low; the third would cause the activity of the foil in the rod to be high. Either of these effects would result in a measured ERI of the fuel rod that is too high.

The possibility of streaming of resonance neutrons through the aluminum of the foil in the rod was investigate by irradiating a depleted uranium foil in its place, and then intercalibrating the two foils in a highly thermal flux. For the intercalibration, small corrections were made for the thermal flux depression and γ-ray self-attenuation in the depleted uranium foils. This method of measuring the ERI gave results that were closer to the accepted value than those obtained with the first method. The results of these measurements for the three lattices are given in Table 2-5.1 with each value the average of at least two separate measurements.

TABLE 2.5-1

Summary of the Measurements of
the Effective Resonance Integral

Lattice Spacing (Inches)	$\frac{\text{Activity of Rod}}{\text{Dilute Sample Activity}}$
4.50	0.0742 ± 0.0022
5.00	0.0725 ± 0.0036
5.75	0.0729 ± 0.0013

Average activity ratio: 0.0730 ± 0.0006

Value of ERI calculated with equation (2.5-1):

19.3 ± 0.3 barns

It is seen that the measured values of the activity ratio are independent of the lattice spacing, as is to be expected for the lattice spacings of the experiment, i.e., the Dancoff effect is negligible. However, the value of the ERI as calculated with equation 2.5-1 is still twice the accepted value. To reconcile this large discrepancy a detailed study of the resonance integral measurement was undertaken in the lattice with 5.75 inch spacing.

First, the activation of the cadmium covered dilute foil at the surface of the rod was compared to that of a similar foil placed in the moderator midway between two adjacent rods; the same method of monitoring the resonance flux was used as was used by Hellstrand. The flux monitors were cadmium covered thin gold foils (an alloy of one per cent by weight in aluminum) backed on one side with thick (0.010 inch) gold foils. The thick foil, which was placed between the fuel rod and the thin foil, was used to shield the thin foil from those resonance neutrons transmitted through the rod. Thus, the thin foil monitored only the incoming flux. The ratio of the dilute uranium foil activity in the moderator to that at the surface of the rod, obtained from Table 2.4-1, was 1.359 ± 0.005 and the corresponding activity ratio for the flux monitors was 1.06 ± 0.03,

TABLE 2.5-2

Summary of Cadmium Ratio Measurements
with Na^{23}, Mn^{55}, Co^{59} and U^{238} in
the MIT Reactor and in the Exponential Lattice

Location	Na^{23}	Mn^{55}	Co^{59}	U^{238}
MIT Reactor	61.8 ± 1.1	36.8 ± 0.4	30.2 ± 0.6	1.33 ± 0.04[c]
Lattice-Moderator[a]	42.2 ± 1.7	24.6 ± 0.5	22.6 ± 0.5	1.31 ± 0.01
Lattice-Rod[b]	33.6 ± 1.8	19.1 ± 0.4	18.3 ± 0.6	1.28 ± 0.03

(a) Measured at a point midway between two adjacent rods.

(b) Measured at rod surface.

(c) Errors are the standard deviations of the mean values of at least two measurements.

which means that the activity of the uranium foil in the moderator and hence its ERI, is greater by a factor of 1.28 ± 0.04. This accounts for part of the discrepancy in the original measurement of the ERI for the fuel rods, since a low activation of the dilute standard will result in a high value of the ERI. The most probable cause of the low activation of the dilute uranium foils is the deviation of the resonance neutron flux from the asymptotic 1/E distribution, particularly at the energies of the lowest U^{238} resonances. These resonances contribute about 75 per cent of the dilute resonance integral. The magnitude of this deviation was next investigated by comparison with the resonance neutron spectrum in the MIT Reactor, which was shown to vary as 1/E by C. Anderson (2).

Cadmium ratio measurements were made for foils of Mn^{55}, Co^{59} and Na^{23} as well as for the dilute uranium foils, in the MIT Reactor and in the lattice with 5.75 inch spacing, at the rod surface and at a point midway between two adjacent rods. Mn^{55} has its principle resonance at 332 ev and Co^{59} has its principle resonance at 137 ev, while Na^{23} is a 1/v detector. The Na^{23} and Mn^{55} foils were made of Na_2CO_3 and MnO_2 powders, respectively, on mylar tape and were infinitely dilute. The Co^{59} foil was of metal, 0.005 inches thick. The results of these measurements are given in Table 2.5-2.

The values quoted are averages of two separate measurements.

The equations used to analyze these measurements are derived as follows. The resonance activation is divided into a portion due to the true resonance integral and a portion due to the epicadmium 1/v activation. Similarly, the thermal activation is divided into two portions, one due to a Maxwellian flux M(E), and the other due to a $\frac{1}{E}$ flux which is joined to the Maxwellian flux at 0.12 ev. This corresponds to the 5kT joining point commonly used but, for the well-thermalized spectra under consideration, the analysis is not very sensitive to this choice. We can then write:

$$R - 1 = \frac{\text{thermal activation}}{\text{resonance activation}}$$

$$= \frac{\int_0^{0.12} M(E)\sigma_{1/v}(E)dE + \int_{0.12}^{0.40} \frac{\beta}{E}\sigma_{1/v}(E)dE}{\int_{0.40}^{\infty} \frac{\beta}{E}\sigma_{RES}(E)dE + \int_{0.40}^{\infty} \frac{\beta}{E}\sigma_{1/v}(E)dE}, \quad (2.5\text{-}2)$$

where R is the measured cadmium ratio, and β is the normalization constant between the Maxwellian and 1/E fluxes. The cadmium cutoff energy is taken as 0.40 ev

for a cadmium thickness of 0.020 inches. Performing the integrations gives:

$$R - 1 = \frac{0.886\ \sigma_o + 0.414\ \beta\ \sigma_o}{\beta\ ERI + 0.500\ \beta\ \sigma_o}, \qquad (2.5\text{-}3)$$

where σ_o is the thermal cross section at 2200 m/sec and ERI is the effective resonance integral. A simpler form of this equation is:

$$\frac{ERI}{\sigma_o} = \frac{1}{R-1}\left(\frac{0.886}{\beta} + 0.414\right) - 0.500. \qquad (2.5\text{-}4)$$

When equation (2.5-4) is written for two nuclides, a and b, β can be eliminated from the relationship, yielding the equation:

$$\left(\frac{ERI}{\sigma_o}\right)_a = \frac{(R-1)_b}{(R-1)_a}\left[\left(\frac{ERI}{\sigma_o}\right)_b + 0.500\right] - 0.500. \qquad (2.5\text{-}5)$$

The first step in the analysis was the comparison of the Mn and Co cadmium ratios with the Na cadmium ratios. The ERI's of Mn and Co were calculated with the use of equation (2.5-5) with Na as the standard and assuming:

$$\left(\frac{ERI}{\sigma_o}\right)_{Na} = 0.$$

The calculated ERI's are summarized in Table 2.5-3 and

TABLE 2.5-3

Effective Resonance Integrals of Mn^{55} and Co^{59}, Calculated from Cadmium Ration Measurements

Location	Mn^{55} (Infinitely Dilute)	Co^{59} (0.005 inches thick)
MIT Reactor	4.62 ± 0.24	20.0 ± 1.4
Lattice-Moderator	4.90 ± 0.55	16.8 ± 1.9
Lattice-Rod	5.29 ± 0.71	16.4 ± 2.4
Average Value	4.94 ± 0.19	17.7 ± 0.7

are based on the values of σ_o for Mn and Co of 13.2 $\pm$ 0.4 and 37.0 $\pm$ 1.5, respectively. The depression of the thermal flux in the foils is negligible.

These results indicate that there is no depression of the 1/E flux in the lattice for energies of 137 ev and 332 ev. Since most of the absorptions in U^{238} occur below these energies, these results are to be expected. The ERI for Mn^{55} quoted in Table 2.5-3 is in close agreement with that measured by Macklin and Pomerance (20): the ERI of 4.94 barns plus the epicadmium 1/v contribution of 6.6 barns results in a total resonance cross section of 11.5 barns which is comparable to the published value of $\sim$ 11.8 barns. The Co^{59} measurement cannot be directly compared with published values because the foil is not infinitely dilute, but its magnitude is approximately 3/4 of the dilute value.

Next, the values of β for the three locations were calculated from equation 2.5-4 and the values of the Na, Mn and Co cadmium ratios. The values of the ERI for Mn and Co used were the average values listed in Table 2.5-3, and the thermal cross section values were those quoted previously; the ERI of Na was again taken to be zero. The results of these calculations are summarized in Table 2.5-4.

TABLE 2.5-4

Summary of Calculations of β, the Normalization Constant Between the Thermal and Resonance Fluxes, in the MIT Reactor and in the Exponential Lattice

Position	Na	Mn	Co	Average
MIT Reactor	0.0295	0.0287	0.0314	0.0299 ± 0.0008
Lattice-Moderator	0.0352	0.0439	0.0428	0.0406 ± 0.0023
Lattice-Rod	0.0557	0.0575	0.0537	0.0556 ± 0.0011

These values of β, together with the measured U^{238} cadmium ratios were then used in equation (2.5-4) to calculate the ERI for U^{238} in the three positions. The results for the Reactor, Lattice-Moderator and Lattice-Rod positions are 243 ± 24, 195 ± 6, and 160 ± 18 barns, respectively. The value in the Reactor is lower than the accepted value of 282 barns, indicating the possibility that the foil is not infinitely dilute. The experimental uncertainty is large, however, mainly because the cadmium ratios are close to unity, so that the uncertainties in the cadmium ratio minus one are very large. Even with the large errors associated with the measured value of the resonance integrals, the relative depression of the ERI in the lattice is evident, particularly near the rods. This result explains the large discrepancies in the original measurements of the ERI of the fuel rods in the

lattice. If the measured values of the resonance integral for the dilute U^{238} foils in the lattice are used to evaluate equation (2.5-1) with the activity ratio of Table 2.5-1, the resulting ERI of the fuel rod is 10.4 $\pm$ 1.3 barns if the comparison is made at the rod surface and 9.8 $\pm$ 0.4 barns if it is made in the moderator. Both of these values are in agreement with the accepted value.

An additional independent determination of the ERI of the lattice rods can be made by using the value of β at the rod surface together with the average cadmium ratio of the rod, R_{28}, as previously measured for the lattice of 5.75 inch spacing. Substituting β = 0.0556 $\pm$ 0.0011 and R_{28} = 4.223 $\pm$ 0.043 into equation (2.5-4) gives: $\frac{ERI}{\sigma_o}$ = 4.57 $\pm$ 0.12. At this point, a correction to the value of σ_o is needed to account for the effect of flux depression in the fuel rod, since equation (2.5-4)is defined in terms of the reaction rates at a given position, in this case, the rod's surface. The ERI for the fuel rod is defined in terms of the flux at the rod's surface, so that the effect of resonance flux depression is included in the definition. However, the average thermal activation rate of the rod, which is measured for R_{28}, is less than $\phi_s\sigma_o$, where ϕ_s is the thermal flux at the rod surface. The average cross

section, $\bar{\sigma}$, is equal to $\bar{\phi}/\phi_s\sigma_o$, where $\bar{\phi}/\phi_s$ is the ratio of the average flux to the flux at the surface. Since $\bar{\sigma}$ is the cross section corresponding to the measured values of R_{28}, it is used in place of σ_o in equation (2.5-4). The value of $\bar{\phi}/\phi_o$ for the 1.010 inch diameter natural uranium rods, calculated with the THERMOS code (17), was 0.784, independent of the lattice spacing. Thus $\bar{\sigma}$ = 0.784 x (2.71 $\pm$ 0.02 barns), and the final value for the ERI of the fuel rods is found to be 9.71 $\pm$ 0.27 barns. This result is in excellent agreement with the accepted value of 9.9 barns.

3. DISCUSSION AND CONCLUSIONS

3.1 Relation of the U^{238} Cadmium Ratio to the Resonance Escape Probability

According to the usual four-factor formula, the infinite multiplication factor k_∞, of a reactor assembly, is the ratio of neutron populations in successive generations in a system in which there is no leakage of neutrons. By following one neutron through its life cycle, the well known relationship is obtained:

$$k_\infty = \eta \epsilon p f, \qquad (3.1\text{-}1)$$

where η is the number of neutrons produced per absorption of one thermal neutron in the fuel, ϵ is the total number of neutrons produced per neutron produced by thermal fission, p is the probability that a fission neutron escapes capture while slowing down to thermal energies, and f is the probability that a thermal neutron is absorbed in the fuel.

In order to use the measured U^{238} cadmium ratios in this formula for the infinite multiplication factor of a lattice, it is first necessary to obtain consistent definitions of the four factors. The resonance escape probability, p, is basically defined as the probability that a neutron escapes resonance capture while slowing

down to thermal energies. Since the cadmium cutoff energy is the most common measurable dividing point between thermal and epithermal captures, it is chosen as the lower limit for p. Above this energy, however, several processes take place in addition to the resonance capture, namely: fast capture, 1/v-capture, and leakage. Usually, the fast capture is included in ϵ, the fast fission factor, and the epicadmium 1/v-capture is included in f, the thermal utilization factor and it is necessary to separate these effects from the measured epicadmium captures. The magnitude of these corrections is sometimes small and they are often neglected.

The simplest equation used to relate the measured U^{238} cadmium ratio, R_{28}, to p was derived in Section 1:

$$p = \frac{1}{1 + \rho_{28} fF} , \qquad (1\text{-}5)$$

where $\rho_{28} = (R_{28} - 1)^{-1}$, f is the thermal utilization factor, and F is the ratio of thermal captures in U^{238} to total thermal absorptions in the fuel. At the other extreme is the following equation derived by Kouts and Sher (18) which includes all the effects previously mentioned:

$$p = \frac{1 + (\epsilon - 1)\alpha_{28}/\epsilon \ (\nu_{28} - 1 - \alpha_{28})L_1}{1 + f\Sigma L_2 L_3 S(1 - \frac{\delta}{S})/(1 + \delta)}, \qquad (3.1\text{-}2)$$

where S is equivalent to ρ_{28} and Σ is equivalent to F, defined for equation 1-5. By substituting the usual definition for ϵ :

$$\epsilon = 1 + \frac{\delta^{28}}{\nu 25}(\nu^{28} - 1 - \alpha^{28}), \qquad (3.1\text{-}3)$$

and using the nomenclature of this report this formula can be rewritten as:

$$p = \frac{1 + (\frac{1}{\alpha_{28} L_1})(\frac{1}{\frac{\nu_{25}}{\delta_{28}} + (\nu_{28} - 1 - \alpha_{28})})}{1 + \rho_{28} f F L_2 L_3 (1 - \frac{\delta}{\rho_{28}})/(1 + \delta)}, \qquad (3.1\text{-}4)$$

where L_1, L_2 and L_3 are the non-leakage probabilities in the fast, resonance and thermal energy groups; δ_{28} is the ratio of fissions in U^{238} to fissions in U^{235}; and δ is defined so that δ/ρ_{28} is the fraction of the epicadmium captures in U^{238}, due to the 1/v capture cross section; δ_{28}, ν_{28} and ν_{25} have their usual meanings.

To determine the possible variation in p resulting from differences in definition, equations 1-5 and 3.1-4

TABLE 3.1-1

Parameters for the Calculation of the Resonance Escape Probability

Lattice Pitch (Inches)	F (a)	f (b)	δ_{28} (c)	δ (d)	δ (e)	avg. δ	L_1 (f)	L_2 (f)	L_3 (f)	B^2 (f) (m^{-2})
4.50	0.365	0.980	0.061	0.047	0.048	0.047	0.932	0.964	0.856	8.5±0.2
5.00	0.365	0.977	0.061	0.041	0.035	0.038	0.932	0.964	0.831	8.5±0.2
5.75	0.364	0.971	0.061	0.026	0.026	0.026	0.934	0.965	0.811	8.2±0.2

Constants: α_{28} = 0.107, average U^{238} capture to fission ratio above 0.1 Mev.

ν_{28} = 2.76 ± 0.09, average number of neutrons per U^{238} fission.

ν_{25} = 2.43 ± 0.03, average number of neutrons per U^{235} fission.

(a) Calculated by means of the THERMOS code (17).

(b) Measured by P. S. Brown (4).

(c) Measured by J. R. Wolberg (28).

(d) $\delta = 0.0327\ (R^{o}_{Au} - 1)^{-1}$, where R^{o}_{Au} measurement is described in Section 2.2. See also Ref. (18).

(e) $\delta = \delta^{25}$, measured by J. R. Wolberg (28). See also Ref. (18).

(f) $L_1 = \exp(-B^2 \tau_1)$; τ_1 is the age in D_2O from 2 Mev to 30 ev, estimated to be 78 cm^2,

$L_2 = \exp(-B^2 \tau_2)$; τ_2 is the age from 30 ev to thermal, estimated to be 42 cm^2,

$L_3 = (1 + L^2B^2)^{-1}$; $L^2 = L_o^2\ (1 - f)$ where L_o is the thermal diffusion length in D_2O, estimated to be 99 cm for D_2O purity of 0.9975 atom fraction; f is the thermal utilization factor;

B^2 is the critical buckling measured by P. F. Palmedo (22).

were evaluated numerically for the lattices of 1.010 inch natural uranium rods. The values of f were measured by Mr. P. S. Brown (4) and the values of F were obtained by using the THERMOS code developed by Dr. H. Honeck (17) for the IBM 704 and modified by Brown. Use of the THERMOS code gives better values for the thermal cross sections since it takes into account the hardening of the neutron energy spectrum in the fuel rods. However, the U^{238} cross section follows the 1/v law in the thermal region and the U^{235} cross section deviates from it only by a few per cent, so that this correction is small. The leakage factors were estimated by using age-diffusion theory with values of the bucklings measured by Mr. P. F. Palmedo (22), and the values of δ were calculated using the method of Kouts and Sher, both from measured cadmium ratios of thin gold foils and from the values of δ^{25} measured by Mr. J. R. Wolberg (28). The parameters used in the calculations are summarized in Table 3.1-1, and the calculated values of p together with the measured values of R_{28} and ρ_{28} are summarized in Table 3.1-2. For comparison, the results calculated with equation 3.1-4 without leakage corrections are also included in Table 3.1-2.

Comparison of the results summarized in Table 3.1-2 shows that large variations in the calculated values of

TABLE 3.1-2

Relation of the U^{238} Cadmium Ratio, R_{28}, to
the Resonance Escape Probability, p.
1.010 Inch Diameter Natural Uranium Rods in Heavy Water

Lattice Pitch (Inches)	R_{28} (a)	ρ_{28} (b)	p (Eq. 1-5)	p (Eq. 3.1-4)	
				$L_1=L_2=L_3=1$	Complete
4.50	2.972 ± 0.031	0.507 ± 0.008	0.846 ± 0.002(c)	0.866 ± 0.003	0.887 ± 0.003
5.00	3.495 ± 0.010	0.401 ± 0.002	0.875 ± 0.001	0.891 ± 0.002	0.912 ± 0.002
5.75	4.223 ± 0.043	0.310 ± 0.004	0.902 ± 0.002	0.913 ± 0.003	0.931 ± 0.003

(a) Values obtained from Table 2.2-1.

(b) $\rho_{28} = (R_{28}-1)^{-1}$.

(c) The uncertainty in p is obtained from the experimental uncertainty in R_{28} and from an estimated one per cent uncertainty in all thermal cross section values used.

the resonance escape probability are possible if different definitions are used to relate R_{28} to p. This result serves to emphasize the necessity of using consistent definitions for each of the four factors. If equation 1-5 is used for p, it is necessary to exclude the effect of epicadmium 1/v-captures from f and to exclude the effect of fast capture from ϵ. If this is done properly, the resulting product pfϵ should be the same as that obtained by using Equation 3.1-4 for p, Equation 3.1-3 for ϵ and the values of f which include all 1/v processes (Table 3.1-1). In addition to these considerations, there is the additional problem of the effect of leakage on the measured quantities, since k_∞ is for a system with no leakage and R_{28} is measured in a finite system. The ratio of resonance to thermal captures, ρ_{28}, will be higher in the finite system since the number of thermal captures is decreased by the thermal leakage. The derivation of Eq. 3.1-4 takes this into account and for this reason it will be used for further analysis of these lattices. The last column of Table 3.1-2 gives the values of the resonance escape probabilities for these lattices, based on this model.

3.2 Comparison of Cadmium Ratio and Conversion Ratio Measurements

The initial conversion ratio C, for a lattice is defined as the ratio of the capture rate in U^{238} to the absorption (capture + fission) rate in U^{235}, and can be calculated from C^*, the measured conversion ratio (Section 2.3) or independently, from R_{28}, the measured U^{238} cadmium ratio (Section 2.2). C^* was defined as the ratio of the U^{238} capture rate to the U^{235} fission rate, because these are the quantities that are actually measured. C is related to C^* by the simple equation:

$$C = C^*(1 + \bar{\alpha})^{-1}, \qquad (3.2\text{-}1)$$

where $\bar{\alpha}$ is the average value of the ratio of capture to fission in the U^{235} in the fuel. C is also related to R_{28} by the equation:

$$C = \frac{1 + \rho_{28}}{1 + \rho_{25}} \left(\frac{\Sigma_a^{28}}{\Sigma_a^{25}}\right), \qquad (3.2\text{-}2)$$

where $\rho_{28} = (R_{28} - 1)^{-1}$, the ratio of epicadmium to subcadmium absorption in U^{238}; $\left(\frac{\Sigma_a^{28}}{\Sigma_a^{25}}\right)$ is the ratio of the U^{238} absorption rate to the U^{235} absorption rate below the cadmium cutoff; and ρ_{25} is the ratio of epicadmium to subcadmium absorption in U^{235}.

To evaluate these equations numerically it is first necessary to obtain values for $\bar{\alpha}$, $(\frac{\Sigma_a^{28}}{\Sigma_a^{25}})$, and ρ_{25}. For the well thermalized heavy water lattices under consideration $\bar{\alpha}$ and $(\frac{\Sigma_a^{28}}{\Sigma_a^{25}})$ may be taken from thermal cross section data. This approximation was checked by comparison with results of the THERMOS code, which takes into account the hardening of the spectrum within the fuel elements. To the same order of approximation ρ_{25} may be taken equal to the ratio of epicadmium to subcadmium fissions in U^{235}. This quantity, δ^{25}, is equivalent to δ, the calculation of which was described in the previous section. The evaluation of equations 3.2-1 and 3.2-2 is summarized in Table 3.2-1. The uncertainties in the calculated parameters are estimated from thermal cross section data, and the uncertainties in the measured parameters represent the standard deviation of the mean value of several measurements.

Comparison of the results for C, summarized in Table 3.2-1, shows that the initial conversion ratios calculated from the cadmium ratio measurements are in reasonably good agreement with those calculated from the measured conversion ratios, although the latter are slightly higher. It also appears as though there is a small systematic effect present, which causes the difference in the two methods to be greater for the tighter lattices, but this error is only slightly greater than the

TABLE 3.2-1

Summary of the Calculation of the Initial Conversion Ratio, C
Lattices of 1.010 Inch Diameter Natural Uranium Rods in Heavy Water

Lattice Pitch (Inches)	(a) $\rho_{28}=(R_{28}-1)^{-1}$	C^* (b)	δ_{25} (c)	C (Eq. 3.2-1)	C (Eq. 3.2-2)
4.50	0.507 ± 0.008	1.017 ± 0.023	0.047 ± 0.001	0.866 ± 0.021	0.826 ± 0.010
5.00	0.401 ± 0.002	0.948 ± 0.020	0.038 ± 0.003	0.808 ± 0.018	0.775 ± 0.009
5.75	0.310 ± 0.004	0.859 ± 0.016	0.026 ± 0.001	0.732 ± 0.018	0.733 ± 0.008

Constants independent of lattice pitch

$1 + \bar{\alpha} = 1.174 \pm 0.010$, calculated by means of the THERMOS code (17);

$\left(\frac{a^{28}}{25}\right) = 0.574 \pm 0.006$, calculated by means of the THERMOS code.

(a) From Table 2.2-1.

(b) From Table 2.3-1.

(c) From Table 3.1-1 (average value of δ).

experimental uncertainty. Since the overall agreement is good for values of the conversion ratio that vary considerably from lattice to lattice, it may be premature to infer a systematic effect from the small discrepancies noted. If this effect does exist, however, further study of these two experimental methods in tighter lattices (using 0.25 inch diameter rods) should permit the determination of the contributing factors.

There are three obvious possible sources of such a systematic effect in the experimental techniques used.

(1) The cadmium pillbox, which depresses the thermal flux in the "cadmium" rod, may also depress the thermal flux in the "bare" rod and the resonance flux in the "cadmium" rod.

(2) There may be leakage of thermal neutrons through the cadmium pillbox.

(3) The aluminum of the U^{238}-Al foil may permit streaming of resonance neutrons into the adjacent U^{238} foil.

Both the effect of the cadmium on the resonance flux and the streaming of neutrons through the aluminum should not vary with lattice spacing, while the effect of the cadmium on the thermal flux should vary in the direction opposite to that of the apparent trend in the data. Leakage of thermal neutrons into the cadmium covered foil

would cause the conversion ratios calculated from the cadmium ratios to be high, which is also not the case. Thus it would seem as though an explanation of the discrepancy is not readily forthcoming from possible errors in the experimental techniques. One additional possibility is that the effective cross section for the rods, calculated with the THERMOS code, may be in error. This, however, seems unlikely, since the code has accurately predicted the flux distribution in the rods and, at most, it could account for a discrepancy of only one or two per cent.

In summary, the general agreement of the conversion ratios, calculated from the two independent experimental techniques, verifies each of these measurements for the lattices studied. These measurements will then serve as a starting point for analysis of more complex systems where much larger discrepancies have been noted. The possible systematic effect observed in the data may be an indication of future trends as tighter lattices are studied. In these lattices the interaction between the fuel rods will be greater and the effect of the cadmium on adjacent rods should become more important.

3.3 Evaluation of the Lattice Multiplication Factor

The infinite multiplication factor k_∞, of a reactive assembly has been defined in two equivalent ways. The first is by means of the four-factor formulation:

$$k_\infty = \eta \epsilon p f, \qquad (3.1\text{-}1)$$

which was discussed in Section 3.1. Numerical evaluation of equation 3.1-1 was carried out for the three lattices of 1.010 inch natural uranium rods; the following values were used for the four factors:

η = 1.313 $\pm$ 0.016, calculated by means of the THERMOS Code (17),

ϵ, from eq. 3.1-3,

p, as obtained from the last column of Table 3.1-2, and

f, as obtained from Table 3.1-1.

This choice of parameters gives a consistent set of definitions and also includes the effect of leakage on the parameters measured in the finite system. The results of these calculations are summarized in Table 3.3-1.

The second definition for k_∞ is:

$$k_\infty = \frac{\text{average number of neutrons produced per unit time}}{\text{average number of neutrons absorbed per unit time}}, \qquad (3.3\text{-}1)$$

which is obtained from the definition of k_{eff} (Eq. 1-6)

by setting the leakage term in the denominator equal to zero. This definition of k_∞ should be equivalent to the four-factor definition if the interpretations of the various contributing factors are consistent. Equation 3.3-1 is evaluated simply by enumerating all separate production and absorption rates in the system, and then combining them in terms of measurable parameters. The net rate of production is:

$$\text{Production rate} = \nu^{25}\Sigma_f(25) + (\nu^{28}-1)\Sigma_f(28), \quad (3.3\text{-}2)$$

where the Σ's are flux-weighted effective macroscopic cross sections. The second term takes into account the fact that one neutron from thermal fission is lost for each fast fission taking place. The absorption rate is:

$$\text{Absorption rate} = \Sigma_a(28) + \Sigma_a(25) + \Sigma_a(x), \quad (3.3\text{-}3)$$

where $\Sigma_a(28)$ and $\Sigma_a(25)$ are flux-weighted effective cross sections for U^{238} and U^{235}, respectively, and $\Sigma_a(x)$ is the corresponding absorption rate in the moderator and cladding. Taking the ratio of production to consumption rate and dividing both numerator and denomenator by $\Sigma_f(25)$ yields:

$$k_\infty = \frac{\nu^{25} + (\nu^{28} - 1)\dfrac{\Sigma_f(28)}{\Sigma_f(25)}}{\dfrac{\Sigma_a(28)}{\Sigma_f(25)} + \dfrac{\Sigma_a(25)}{\Sigma_f(25)} + \dfrac{\Sigma_a(x)}{\Sigma_f(25)}} \cdot \qquad (3.3\text{-}4)$$

Equation 3.3-4 may now be expressed in terms of the measured parameters; $\frac{\Sigma_f(28)}{\Sigma_f(25)}$ is equivalent to δ^{28}, and $\frac{\Sigma_a(28)}{\Sigma_f(25)}$ to C^*, both of which are directly measurable, and $\frac{\Sigma_a(25)}{\Sigma_f(25)}$ is just $1 + \bar{\alpha}$. The remaining term $\frac{\Sigma_a(x)}{\Sigma_f(25)}$, can be calculated from the lattice parameters f and F, as defined in Section 3.1, with the reasonable assumption that $\Sigma_a(x)$ is due only to thermal absorptions. The derivation is as follows:

$$f = \frac{\Sigma_a(\text{fuel})}{\Sigma_a(\text{fuel}) + \Sigma_a(x)} = \frac{\Sigma_a(25) + \Sigma_a(28)}{\Sigma_a(25) + \Sigma_a(28) + \Sigma_a(x)} \qquad (3.3\text{-}5)$$

$$\frac{\Sigma_a(x)}{\Sigma_f(25)} = \left(\frac{1}{f} - 1\right)\frac{\Sigma_a(25)}{\Sigma_f(25)}\,\frac{\Sigma_a(28) + \Sigma_a(25)}{\Sigma_a(25)}$$

$$= \left(\frac{1}{f} - 1\right)(1 + \bar{\alpha})\left(\frac{1}{1 - F}\right) \cdot$$

Substituting the above relationships into equation 3.3-4 yields the final result:

$$k_{\infty} = \frac{\nu^{25}_{+} (\nu^{28} - 1)\delta^{28}}{C^{*} + (1 + \bar{\alpha}) + (\frac{1}{\bar{f}} - 1)(1 + \bar{\alpha})(\frac{1}{1-F})} \quad , \qquad (3.3\text{-}6)$$

which is essentially independent of the formulation of equation 3.3-1. In accord with the conclusions reached in Section 3.1, it is necessary to correct the measured quantities of equation 3.3-6 for the effects of leakage before the comparison can be made with the four factor formulation which has the leakage effects included in p. To a first order approximation, the only quantity affected by leakage is C^{*} since the processes involved include both resonance and thermal neutrons. The other parameters involve reactions which take place primarily in only one energy group so that their ratios are not affected by leakage. To estimate the effect of leakage on C^{*}, the equivalence of the two definitions of C (Section 3.2) is used and, neglecting the effect of leakage on ρ_{25}, C^{*} is taken to vary as $(1 + \rho_{28})$. The measured value of ρ_{28} is greater than the corresponding value of $(\rho_{28})_{\infty}$, for an infinite system, because of the leakage of neutrons between the resonance region and the absorption in the thermal region. Attributing this effect to both leakage while slowing down from resonance to thermal energies, and to thermal leakage, leads to the approximation:

$$\rho_{28} = \frac{1}{L_2 L_3} (\rho_{28})_{\infty} \, , \qquad (3.3\text{-}7)$$

where L_2 and L_3 are the non-leakage probabilities calculated in Section 3.1. Consequently, the quantity $(C^*)_\infty$ may be substituted in equation 3.3-6 for C^*, where:

$$(C^*)_\infty = \left(\frac{1 + L_2 L_3 \rho_{28}}{1 + \rho_{28}}\right) C^*. \quad (3.3\text{-}8)$$

Equation 3.3-6 may now be evaluated numerically using the appropriate parameters which have been summarized previously in Tables 3.1-1 and 3.2-1. The results of these calculations are summarized in Table 3.3-1.

TABLE 3.3-1

Lattice Multiplication Factors

Lattice Pitch Inches	k_∞	
	Eq. 3.1-1 (a)	Eq. 3.3-6 (b)
4.50	1.189 ± 0.013	1.171 ± 0.017
5.00	1.219 ± 0.014	1.203 ± 0.017
5.75	1.239 ± 0.014	1.243 ± 0.018

(a) Uses values of p calculated with complete form of Eq. 3.1-4.

(b) Includes leakage correction to C^* (Eq. 3.3-8).

Comparison of the results summarized in Table 3.3-1 shows that the two methods of calculation of k_∞ give results, which are quite close, but it appears that there is a small systematic difference present. This difference may be traced back directly to the analogous discrepancy in the conversion ratios calculated in Section 3.2 from C^* and from R_{28}. In Table 3.2-1 it is seen that for the tighter lattices the C^* measurements lead to higher conversion ratios and this is equivalent to the lower calculated value of k_∞ of Table 3.3-1. If the same values of the conversion ratio were used to evaluate equations 3.1-1 and 3.3-6, the small discrepancies in Table 4.3-1 would be eliminated. Thus, for the lattices under consideration the two methods for obtaining the multiplication factor do give results that are in agreement -- well within the experimental uncertainty. The parameters that contribute most to the uncertainties in the values of k_∞ are η, for the four-factor method, and ν^{25}, for the second method. If the uncertainties in these parameters are reduced, a further comparison between the two methods can be made. Also, it is to be expected that as tighter lattices are examined the discrepancies in the two methods will become greater which, in turn, may lead to the sources of the errors in the calculational models as well as to the sources of

systematic errors in the measurements. The differences seen with the present lattices are too small to warrant further analysis of these problems.

3.4 Discussion of the Effective Resonance Integral Measurements.

The series of measurements described in Section 2.5 and summarized in Table 3.4-1 serves to illustrate an important point, namely, that there is considerable depression of the 1/E flux in these lattices at the energies corresponding to the lower U^{238} resonances. This effect manifests itself by the low values obtained for the dilute U^{238} resonance integral in the lattice, particularly near the surface of the fuel rods and is further verified by the subsequent agreement of the ERI of the fuel rod with the accepted value when the measured dilute resonance integrals are used for standardization purposes.

The question is raised, however, as to the effect of this flux depression on the ERI of lattice fuel rods as compared to the resonance integral for a single rod. This effect would be in addition to the Dancoff effect which is negligible for these lattices. From the measured values of the ERI for the 1.010 inch diameter rods, which are in agreement with the accepted single rod value it appears that the flux depression effect is negligible. However, the ERI of these rods is low and the relative importance of the lower U^{238} resonance is smaller than would be the case for rods of smaller diameter having a

TABLE 3.4-1

Summary of Measurements of the Effective Resonance Integral of Lattice Fuel Rods

1.010 Inch Natural Uranium Rods - 5.75 Inch Triangular Pitch

	Effective Resonance Integral (barns)	
	Comparison at rod surface	Comparison in moderator
Comparison with Dilute U^{238} foil, based on assumed value of dilute ERI of 282 barns	19.3 ± 0.3	15.1 ± 0.5
Comparison with Dilute U^{238} foil, based on measured values of dilute ERI	10.4 ± 0.4	9.8 ± 0.4
Comparison of rod cadmium ratio with cadmium ratios of Na, Mn, and Co	9.71 ±0.27	-----

Accepted value of Effective Resonance Integral: 9.9 barns

Measured dilute resonance integrals:

At surface of fuel rod: 160 ± 18 barns

In moderator: 195 ± 6 barns

larger ERI. The possible implications of this effect are sufficiently important to warrant further investigation. It is suggested that measurements and comparisons similar to those of Section 2.5 be made for lattices of 0.25 inch diameter rods over a wide range of spacings, making, if possible, the transition between separate single rods and strongly interacting clusters. Since the depression of the resonance flux from the asymptotic 1/E distribution near strong resonances would be strongly a function of moderator, it is further suggested that these experiments be carried out both with ordinary and heavy water moderators.

For future measurements of resonance integrals for lattice rods the method of comparing the cadmium ratio of the rod with those of Na, Mn, Co and other possible resonance absorbers is recommended. This technique of measurement is to be preferred over the standard method of comparison of epicadmium rod and dilute foil activities, since the standardization is no longer made in an energy region sensitive to the U^{238} resonance absorption. Use of the ERI for calculations and for comparison with theory is usually based on the assumption of a 1/E flux and if the ERI standardization is made at energies above the strong U^{238} absorption the measured resonance integral is truly defined in terms of a 1/E flux.

3.5 Summary

Measurements of the fuel rod cadmium ratio, R_{28}, and the conversion ratio, C^*, were made on lattices of 1.010 inch diameter natural uranium rods with spacings of 4.50, 5.00, and 5.75 inches. Comparison of the two parameters through the conventional conversion ratio, C, showed that the results of the measurements were in reasonably good agreement. A small discrepancy, slightly greater than the experimental uncertainty, was noted for the tighter lattices, but its magnitude was too small to warrant additional investigation in these lattices. The measured parameters, R_{28}, and C^*, were also used to evaluate the infinite multiplication factor, k_∞, of the lattices in two ways, by means the usual four factor formula and from a formula based on net neutron production and consumption rates in the lattice. For these lattices it was found that the two methods of calculation gave results that were in good agreement.

Measurements of the effective resonance integral of the fuel rods in the lattices showed that there was considerable depression of the asymptotic 1/E flux energies corresponding to the lower U^{238} resonances

but the measured resonance integral agreed well with the accepted single rod value.

It is strongly recommended that the experimental program described in this report be extended to tighter lattices of 0.25 inch diameter rods. The slight discrepancies noted in the R_{28} and C^* measurements, if actually present, should increase in magnitude in the tighter lattices and would permit the determination of the sources of systematic error. Also, the 1/E flux depression noted in the resonance integral measurements, should increase in these lattices permitting further a analysis of this effect. The present measurements made on loose lattices of one inch diameter rods will serve as a point of reference, illustrating the validity of the experimental and analytical techniques for at least one type of system.

4. APPENDICES

Appendix A

Gamma-Gamma Coincidence Technique for U^{238} Activation Measurements

1. Introduction

Measurements, by means of activation techniques, of quantities used for the calculation of the effective resonance integral and the resonance escape probability require a method of determining the ratio of the amounts of plutonium produced in different foils. The two methods most often used are: counting of either the U^{239} or Np^{239} β-particles following chemical removal of the fission products (18), and counting the 103 kev peak in the γ-ray spectrum of Np^{239} (19). The γ-counting method requires the use of foils depleted in U^{235} for accurate results, while the chemical separation for the β-counting method is sometimes difficult to achieve and destroys the foil material. To avoid these drawbacks, a counting method based on the use of coincident γ-rays in the Np^{239} decay was suggested by R. Sher (24). Using depleted foils, he was able to duplicate the cadmium ratios obtained by the β-counting method for U-H_2O lattices of 0.25 inch diameter rods.

This report presents the results of a further development of the coincidence technique, including a detailed study of the effects due to fission products arising when non-depleted uranium foils are irradiated. The method described can be used with any low-enrichment uranium foil and appears to offer increased reliability over other methods currently in use with non-depleted foils.

2. Equipment

To test the feasibility of the coincidence method for determining Np^{239} content, two identical gamma spectrometer channels were employed (see Figure A-1). Each consisted of the following components: an integral package of 1/2" thick 1 1/2" diameter NaI(Tl) crystal and RCA 6342A photomultiplier as detector, a cathode follower preamplifier, together with Baird-Atomic Model 312A high voltage supply, Model 215 linear amplifier, Model 510 single channel pulse height analyzer, and Model 132 scaler. The pulse height selector (PHS) outputs of the amplifiers were fed to a fast coincidence circuit, whose measured resolving time was about 0.5 microsecond. The output of this circuit was then fed to a triple coincidence circuit (resolving time about 10 microseconds) together with the outputs of the single channel analyzers. This output in turn was fed to a

FIGURE A-1

BLOCK DIAGRAM OF COUNTING EQUIPMENT

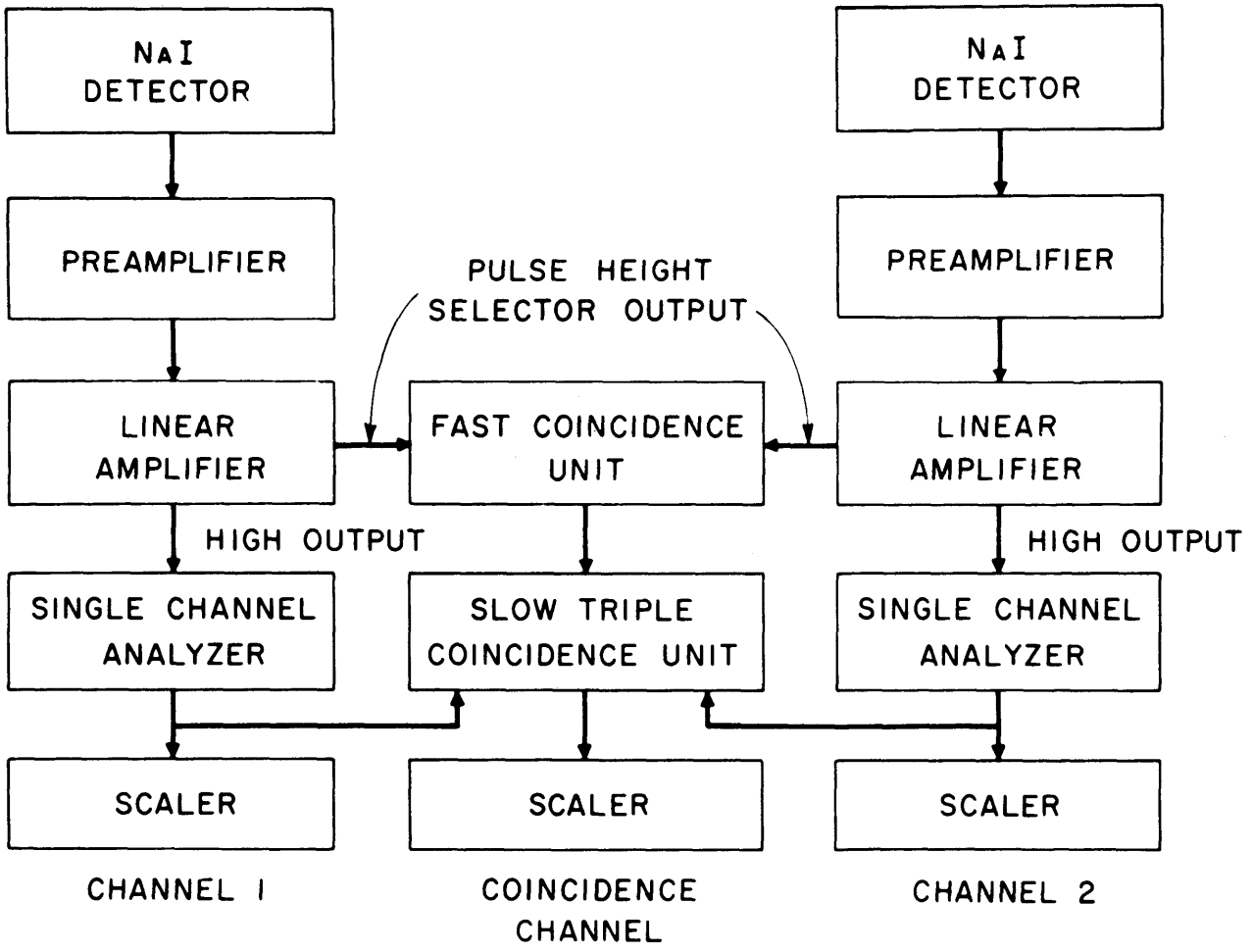

Baird-Atomic Model 131A scaler, which was biased so as to accept only triple coincidence pulses. The purpose of this arrangement of coincidence circuitry was to compensate for the different transit times through each channel, amounting sometimes to several microseconds, while permitting the use of a short resolving time to reduce the random coincidences. The only restriction on operation is that the PHS settings of the amplifiers be below the baselines of the single channel analyzer. This limitation insures that the single channel analyzer sees all the pulses that enter the fast coincidence circuit.

The complete spectrometer systems were checked for drift, which was determined to be normally less than 0.5% per day in both energy and count rate.

3. Experiment and Results

Foils of uranium depleted to fifteen parts per million of U^{235} and of natural uranium, both bare and cadmium covered, were irradiated in the MITR and the decaying activities were followed for several weeks. At the high fluxes used, the natural background of the uranium foils, as well as the counter background, was negligible, except after very long times--of the order of six weeks. For each counting period the single counts

in channels 1 and 2 and the coincidence counts (N_C) were recorded. The two-source method was used periodically to measure the coincidence resolving time (ρ) of the apparatus, which was then used to correct the measured coincidence count rates for random counts, $N_R = N_1 N_2 \rho$. The resolving time was found to decrease slightly at high counting rates.

The first measurements made accepted coincidences of gamma rays of all energies above the baselines. However, the decay of the natural foil coincidences did not closely follow the Np^{239} half life and, in addition, the coincidence activity of the natural foil greatly exceeded that of a similarly irradiated depleted foil. This effect was apparently due to true coincidences among the many U^{235} fission products. It seemed essential to reduce the background due to these true, but undesirable, fission produce coincidences and also to reduce random coincidences by resorting to energy discrimination as well as coincidence techniques.

Examination of a typical gamma ray spectrum of Np^{239} measured with this equipment (see Figure A-2) shows three principal energy groups. These are: the 103 kev peak, the combined 210-228 kev peak, and the 278 kev peak. The resolution of these peaks is from 15 to 25%. The

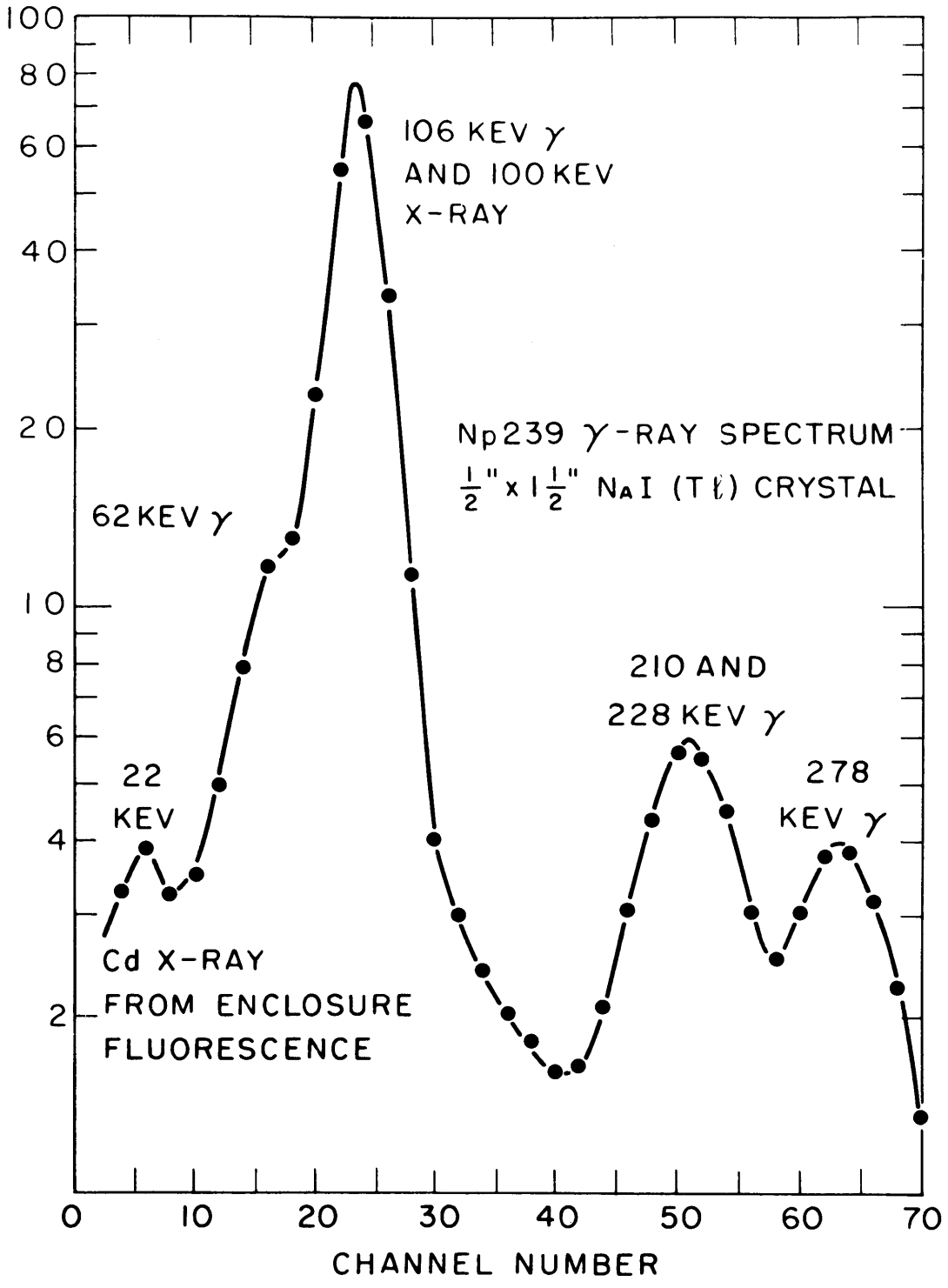

FIG. A-2 Np^{239} γ-RAY SPECTRUM

103 kev peak is a composite of a 106 kev γ-ray and the 99 and 100 kev K X-rays of plutonium which result from the internal conversion of the higher energy γ-rays. By using a depleted foil which had been cadmium covered during the irradiation, a measurement was made to determine the optimum differential energy settings to reduce the fission product coincidences and the random coincidences to an acceptably low level and still retain a reasonable rate of counting. Since Figure A-2 shows that about 90% of the Np γ-activity appears in the 103 kev peak, one channel was set to straddle this energy. The window width was set at 60 kev to maximize count rate and to minimize the effect of drift. The second channel, with a 25 kev window, was used to scan the entire Np^{239} spectrum in steps of 25 kev. The results, plotted as a normalized ratio of random (N_R) to true coincidence counts (N_C-N_R), are shown in Figure A-3. For energies below 280 kev, the ratio only varies between 1.0 and 1.5 with relative minima occuring clearly in the vicinity of the 103 and 278 kev peaks and less markedly at the 210-228 kev peak. Since both the highest coincidence counting rate and the lowest ratio of random to true counts occurs near 103 kev, this was taken to be the optimum energy setting of the second channel. Examination of the energy

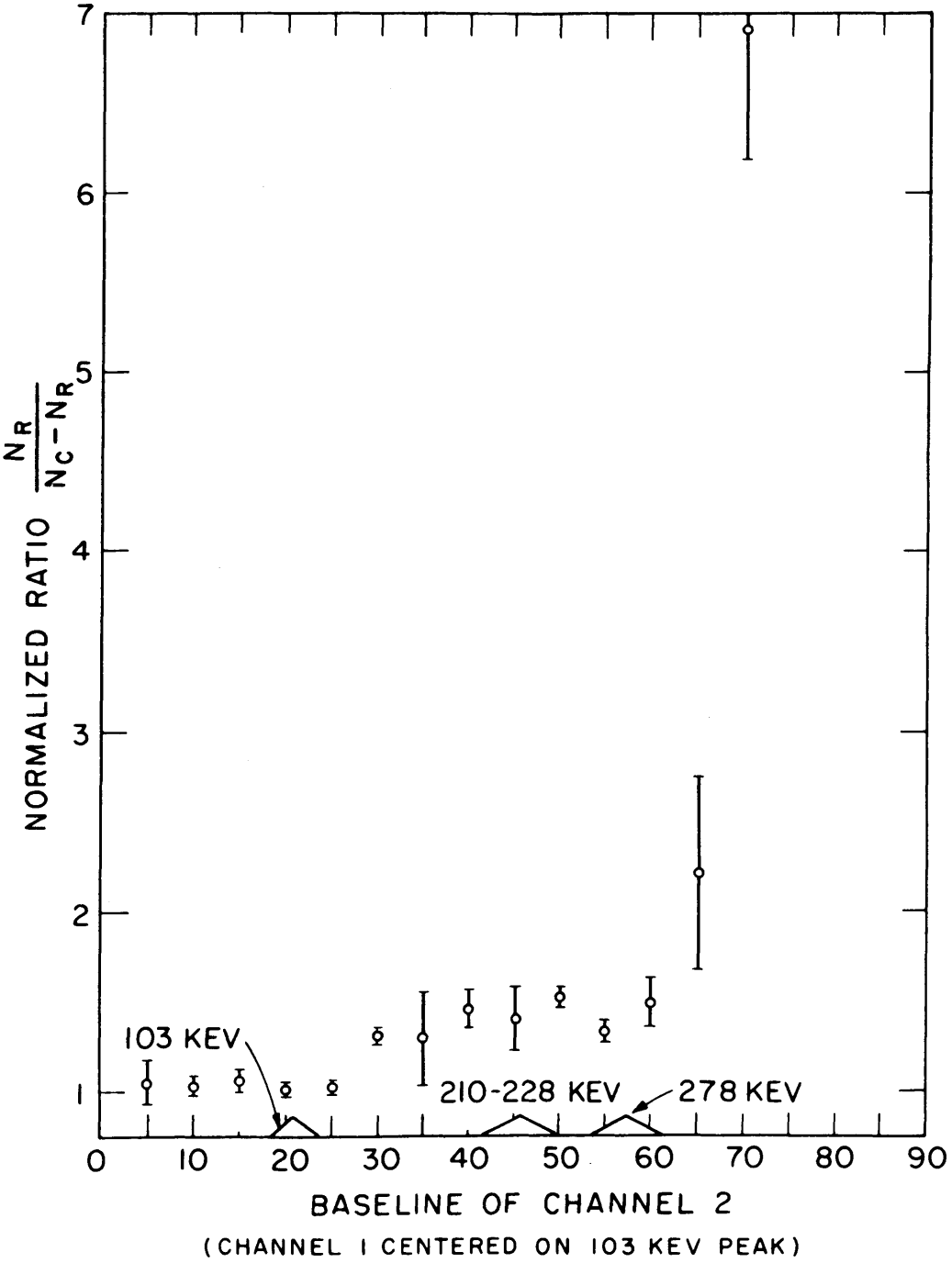

FIG. A-3 ENERGY DEPENDENCE OF RANDOM TO TRUE COINCIDENCE RATIO

level diagram for Np^{239} shows that the 106 kev γ-ray can indeed be coincident with the higher energy γ-rays which, because of a high conversion ratio appear largely as X-rays.

The foil decay measurements were repeated with both channels set to straddle the 103 kev peak with a 60 kev window in each channel. First, bare and Cd covered depleted foils were compared; the results are shown in Table A-1. The measured half lives were obtained by a least squares fit, while the initial activities were obtained by correcting each count for decay, using the accepted half life of 2.33 days, and then averaging. The decay of the singles count rate was included to provide a basis of comparison with the accepted method of γ-counting. Within experimental accuracy, the half lives agree with the accepted value, while the singles and coincidence cadmium ratios are also in agreement.

This demonstrates that the coincidence method yields valid results, as least for depleted foils.

A study of the decay of bare and cadmium covered natural uranium foils (0.005 inches thick) was next undertaken, with the same differential energy settings. The coincidence count rate of the cadmium covered foil decayed with only the Np^{239} half life evident, while after about two weeks the bare foil activity began to

TABLE A-1

Decay of Uranium Foil Depleted to 15 ppm U^{235}

		$T_{1/2}$ (days)[a]	Initial Activity(cpm)
Bare Foil	Channel 1	2.32 ± 0.03	170,400 ± 3,000
	Channel 2	2.29 ± 0.05	161,100 ± 5,300
	Coincidence	2.33 ± 0.04	835 ± 30
Cd Covered Foil	Channel 1	2.36 ± 0.04	51,300 ± 1,100
	Channel 2	2.33 ± 0.03	48,300 ± 1,000
	Coincidence	2.36 ± 0.06	250 ± 11

Cadmium Ratios	Channel 1	3.32 ± 0.09
	Channel 2	3.33 ± 0.13
	Coincidence	3.34 ± 0.19

(a) Accepted half life: 2.33 days.

deviate from the proper half life, eventually exhibiting a decay resembling the $t^{-1.2}$ approximation used to describe the decay of fission products taken as a group.

To verify this result a similar measurement was made for the decay of U^{235} fission products, obtained by irradiating a uranium-aluminum foil fully enriched in U^{235}. These results, combined with those of the previous natural uranium foil measurement, are shown in Figure A-4. Both singles and coincidence decay curves for the bare foil are included. The activities of the natural uranium and U^{235} foils are normalized so that they agree at long times after irradiation. It is evident that the activities of the natural uranium foils can be decomposed into Np^{239} and fission product components. A least squares fit of uncorrected bare natural foil coincidence data taken in the range of 4 to 10 days yields half lives within 5% of the accepted value for Np^{239}. This result appears to be fortuitous, since at these times the fission product coincidence contribution varies from about 8 to 12 per cent of the total. However, the fission products are decaying, during this time range, at rates not too different from the Np^{239} rate and so the contribution goes unnoticed. It will lead to errors in the calculation of initial Np^{239} activities unless corrected for, and at higher enrichments the effect will become increasingly more important.

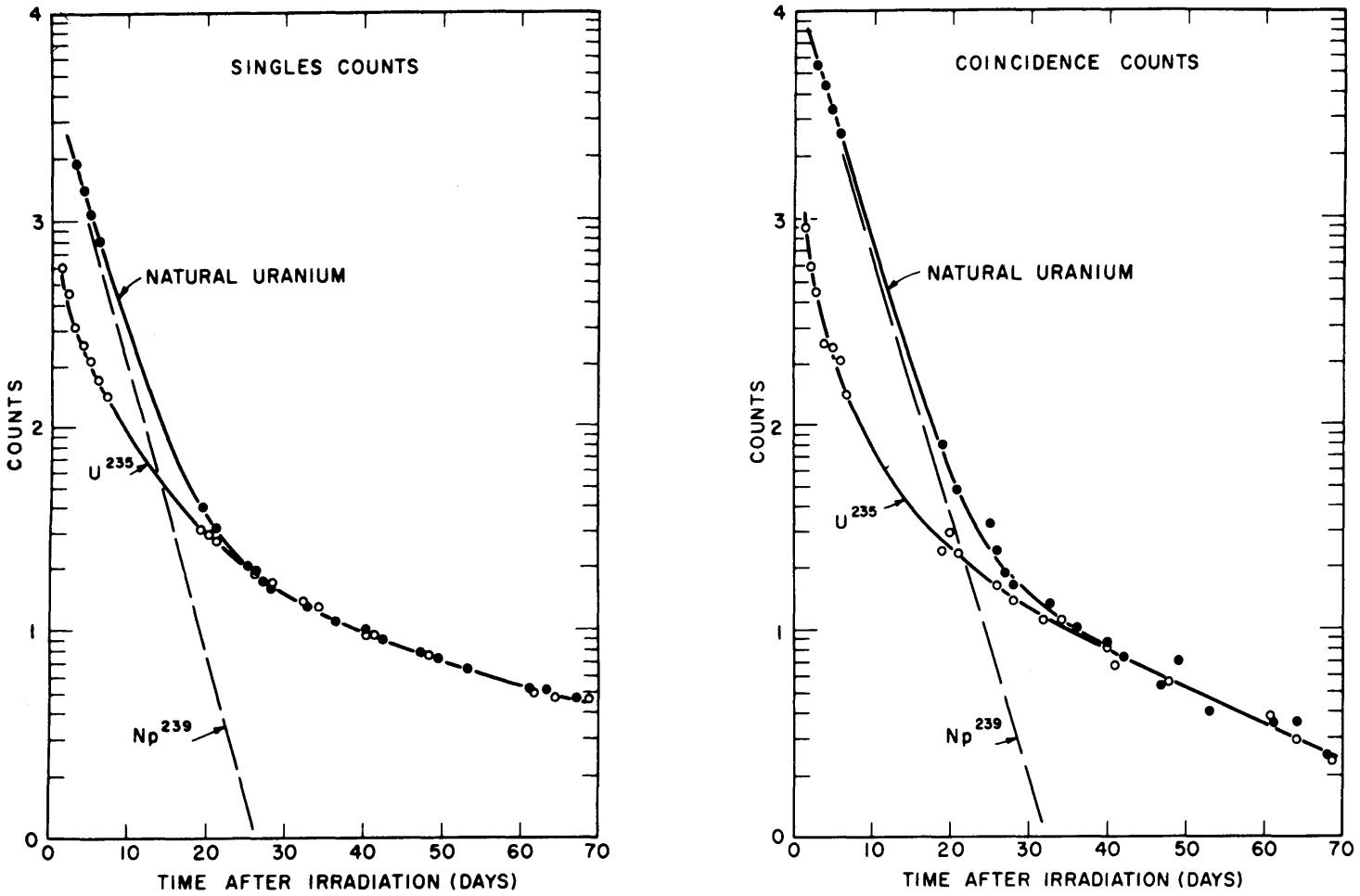

FIG. A-4 DECAY OF NATURAL URANIUM (0.005 INCHES) AND U^{235} FOILS
WINDOW WIDTHS 60 KEV, CENTERED ON 103 KEV PEAK

There are several mechanisms by which the many U^{235} fission products can give rise to actual coincidences in the 103 kev region. These include:

1. actual cascade of two 103 kev γ-rays,
2. degradation by Compton scattering of higher energy cascade γ-rays into the 103 region,
3. coincidence between 103 kev bremsstrahlung and either original or scattered γ-rays of 103 kev,
4. any of the above mechanisms coupled with the photo-electric interaction of higher energy γ-rays with uranium resulting in 97 kev X-rays.

A brief investigation was made to determine the relative importance of the above mechanisms. The singles spectrum of the U^{235}-Al foil was obtained at several times during its decay, using a 256 channel pulse height analyzer. Also a comparison was made between the spectrum obtained by shielding the activated foil with 0.004 inches of depleted uranium during the counting and the spectrum obtained from the unshielded foil. Typical spectra below 200 kev taken 10 days after irradiation are shown in Figure A-5. The unshielded curve shows that the 103 kev Np^{239} peak occurs between two relatively long-lived fission product peaks at 82 and 143 kev. With the 60 kev window settings significant portions of the fission product peaks are included, but the fact that there is

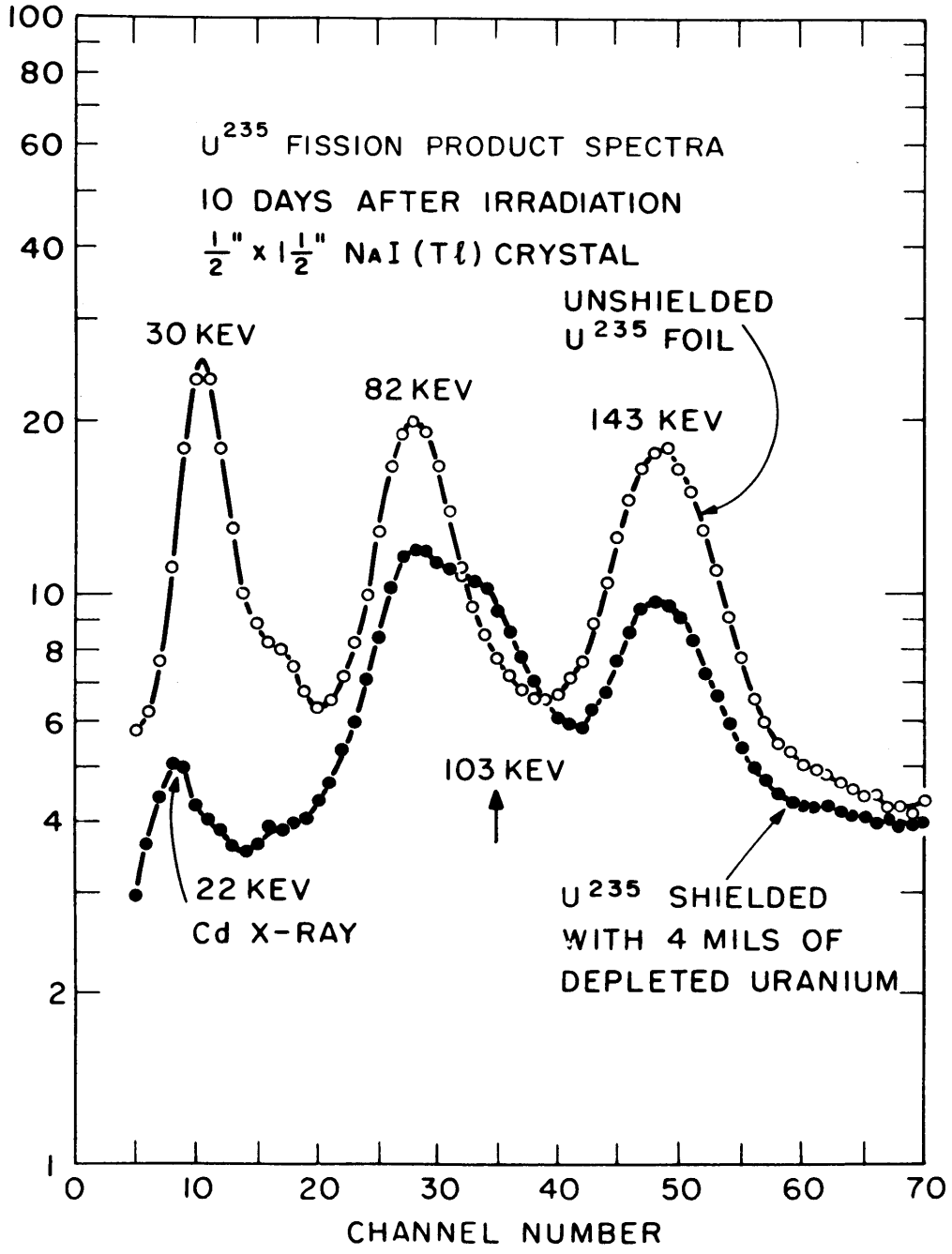

FIG. A-5 U^{235} FISSION PRODUCT SPECTRA BELOW 200 KEV

no particular fission product activity at 103 kev would indicate that mechanism 1 is unimportant. Both mechanism 2 and mechanism 3 would give rise to the characteristic buildup of low energy pulses in the detectors, but this is not particularly evident.

The shielded curve demonstrates the effect of fission product γ-ray interaction with U^{238}, and is representative of the fission product radiation seen from a non-depleted uranium foil several mils thick. It is evident that a considerable number of uranium X-rays are produced which could result in non-Np^{239} coincidence counts. A check showed that for the same U^{235}-Al foil the ratio of coincidence to singles counts was increased by a factor of two in the shielded case. Thus it is concluded that mechanism 4 is the principal cause of the true fission product coincidences in the 103 kev region. Since the resolution of the NaI crystals is not good enough to separate the 97 kev U X-rays from the 103 kev Np^{239} γ and X-rays, one could not expect to reduce the ratio of these fission product coincidences relative to the Np^{239} coincidences to any large degree by changing the spectometer settings.

The effect of uranium foil thickness on the fission product decay rate was studied next. Four U^{235}-Al foils were irradiated simultaneously. One foil was counted

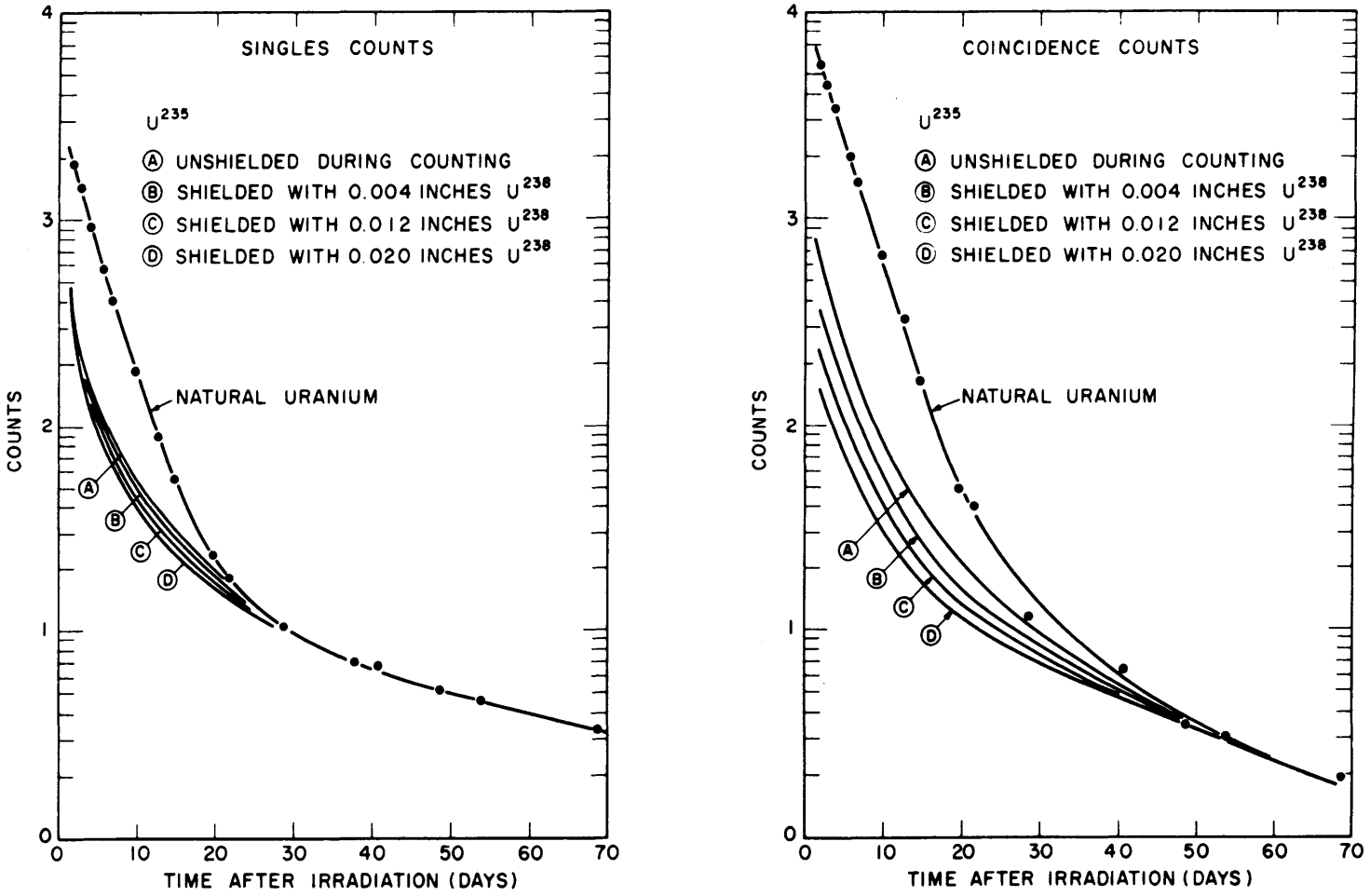

FIG. A-6 DECAY OF 0.020 INCH NATURAL URANIUM FOIL AND U^{235} FOILS SHIELDED DURING COUNTING WITH U^{238}
WINDOW WIDTHS 30 KEV, CENTERED ON 103 KEV PEAK

bare while the others were covered during counting with 0.004, 0.012, and 0.020 inches of U^{238} respectively. Window widths of 60 kev, 30 kev, and 10 kev for both channels were used. It was found that for similar spectrometer settings there were significant differences in the decay rates for the first 30 days after irradiation, but the rates become practically the same after 50 days. Typical results for both singles and coincidence counts, obtained by using the 30 kev spectrometer settings, are shown in Figure A-6, together with the decay curve of a 0.020 inch natural uranium foil. All the curves are normalized to agree at times greater than 50 days after irradiation. From this figure, fission product correction factors, expressed as the ratio of fission product to Np^{239} activity were calculated. They are plotted as a function of time in Figure A-7. The maximum difference in these correction factors amounts to about twenty-five per cent for the singles, and a factor of four for the coincidence counts. This result shows that considerable error is possible when the U^{235} foil used for the extrapolation does not have the same thickness as the non-depleted uranium foil. Even when the thicknesses are the same, the normalization itself introduces some error, especially for the coincidence counts.

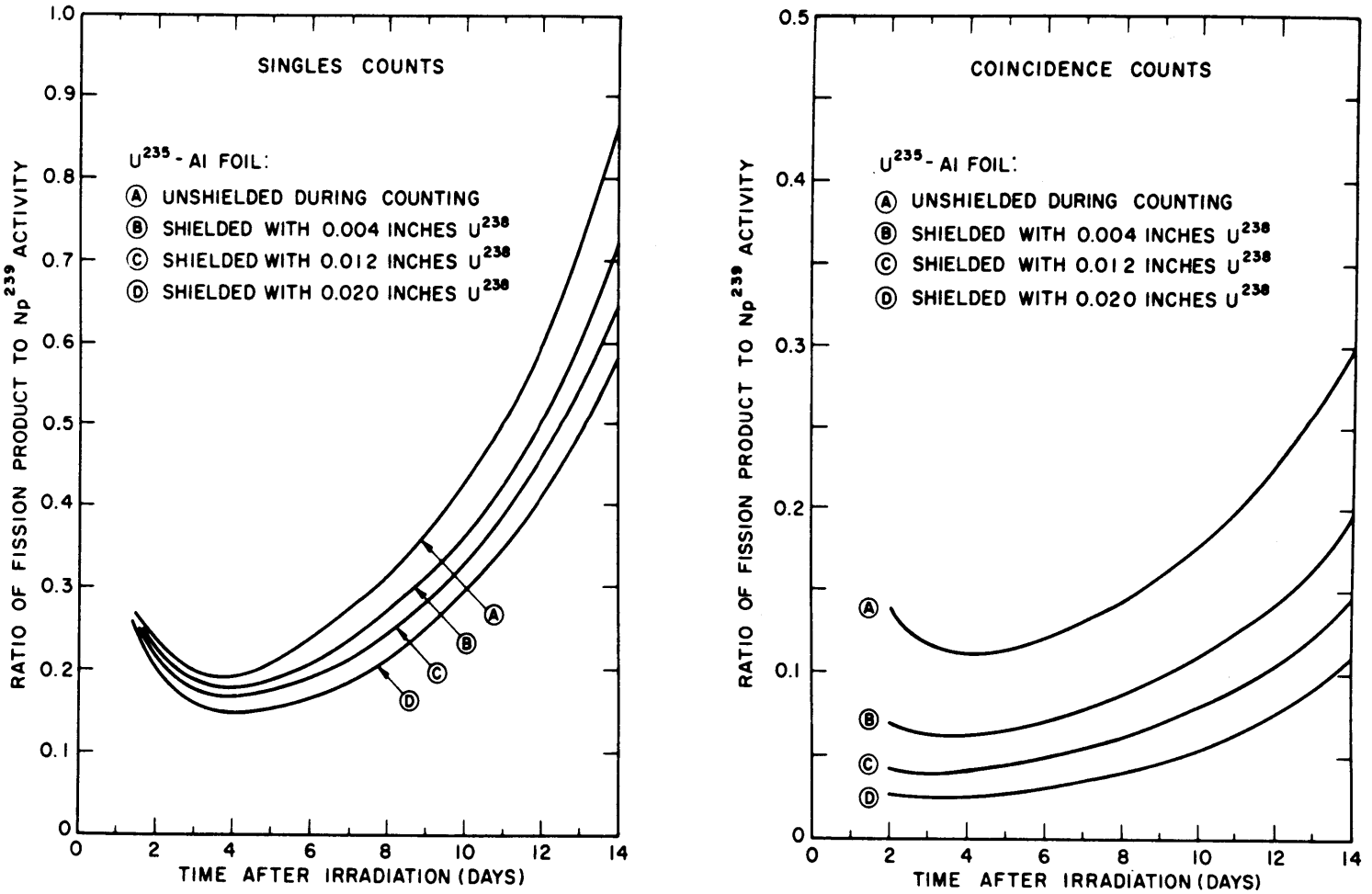

FIG. A-7 COMPARISON OF FISSION PRODUCT CORRECTION FACTORS FOR 0.020 INCH NATURAL URANIUM FOILS
OBTAINED BY EXTRAPOLATION OF FISSION PRODUCT DECAY CURVES OF U^{235} - Al FOILS
WINDOW WIDTHS 30 KEV, CENTERED ON 103 KEV PEAK

To determine these correction factors independently, a study was made of the decay of 0.005 0.010, and 0.020 inch foils of uranium depleted to 15 ppm U^{235}, natural uranium and uranium enriched to 1.15 and 1.30 weight per cents U^{235}. Foils of the same thickness were irradiated under identical conditions and their decay was followed using the 30 kev spectrometer settings. At each point in time, the contribution of the fission products for the non-depleted foils was determined by subtracting the activity of the depleted foils. As would be expected, the fission product contribution was found to be proportional to the U^{235} concentration of the foil. The data for the different concentrations were adjusted to the equivalent natural uranium values by multiplying by the relative U^{235} content, and were then combined to yield an average value for each point. The singles results were reproducible to within five per cent, but the errors in the coincidence counts were much greater. This result was due to the lower coincidence count rates and the smaller differences between the large numbers. Some improvement in the accuracy was obtained for the coincidence counts by combining several data points into an average over an extended time interval.

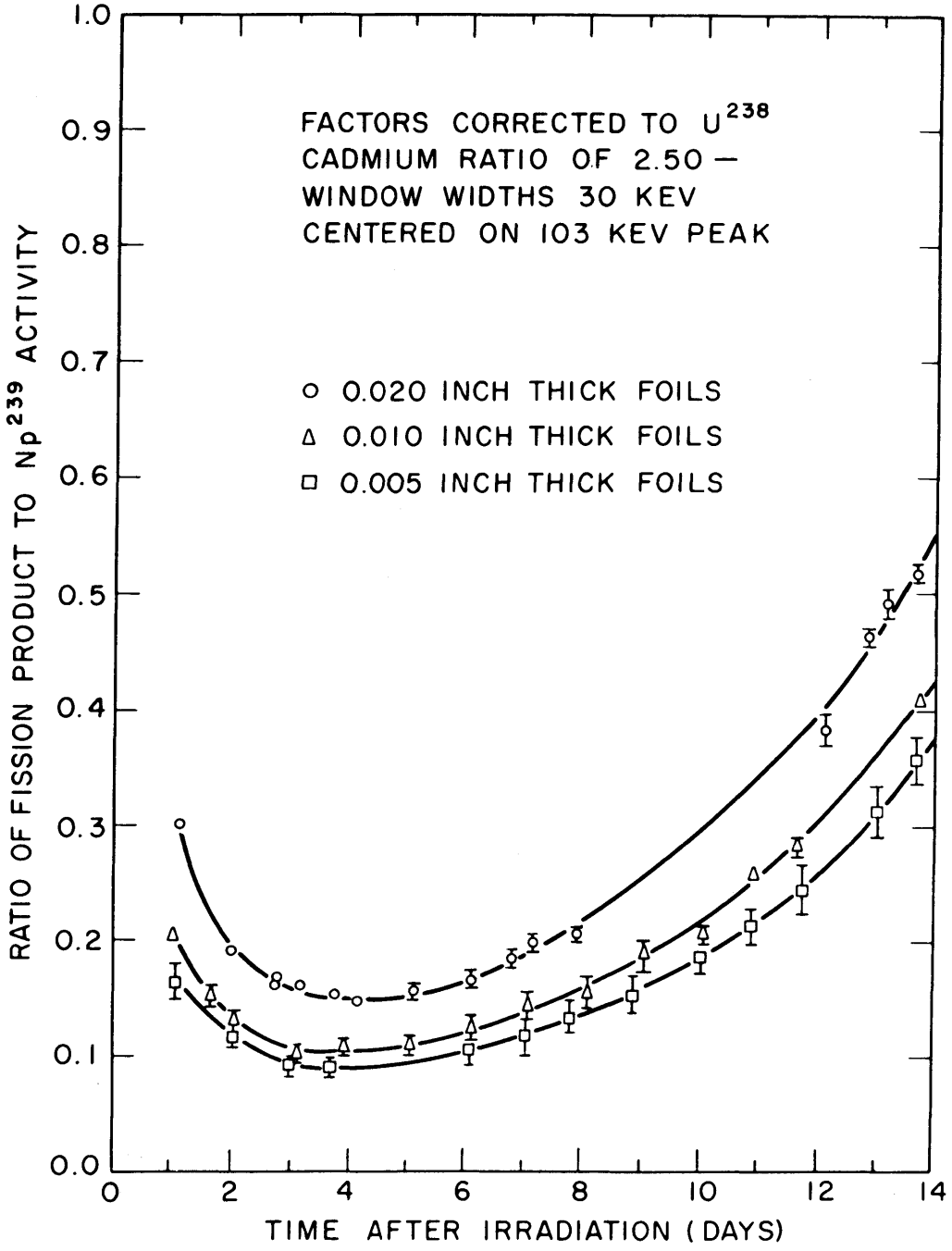

FIG. A-8 FISSION PRODUCT SINGLES CORRECTION FACTORS AS OBTAINED BY THE SUBTRACTION METHOD

To compare the three foil thicknesses on the same basis of U^{238} capture and U^{235} fission rates, it is necessary to know the change in U^{238} activation due to the changing effective resonance integral. The necessary measurements were made and they are described in Appendix B. As will be discussed later, the relative U^{235} fission and U^{238} capture rates can, to a good approximation, be characterized by just the U^{238} cadmium ratio. For convenience, the results for the three foil thicknesses were normalized to the same U^{238} activation which corresponded to a U^{238} cadmium ratio of 2.50. From this point on, all results, whether obtained by the extrapolation method or by the subtraction method, will be adjusted to this value of the cadmium ratio.

The correction factors for the three thicknesses, as obtained by the subtraction technique are shown in Figures A-8 and A-9. The results are averages of two or three separate measurements. The singles correction factors show a monotonic increase with foil thickness, and also show approximately the same time dependence. The trends are not as clear with the coincidence counts owing to the large errors involved.

The results for the subtraction method were next compared with the corresponding results obtained by using the extrapolation method. The results for the singles

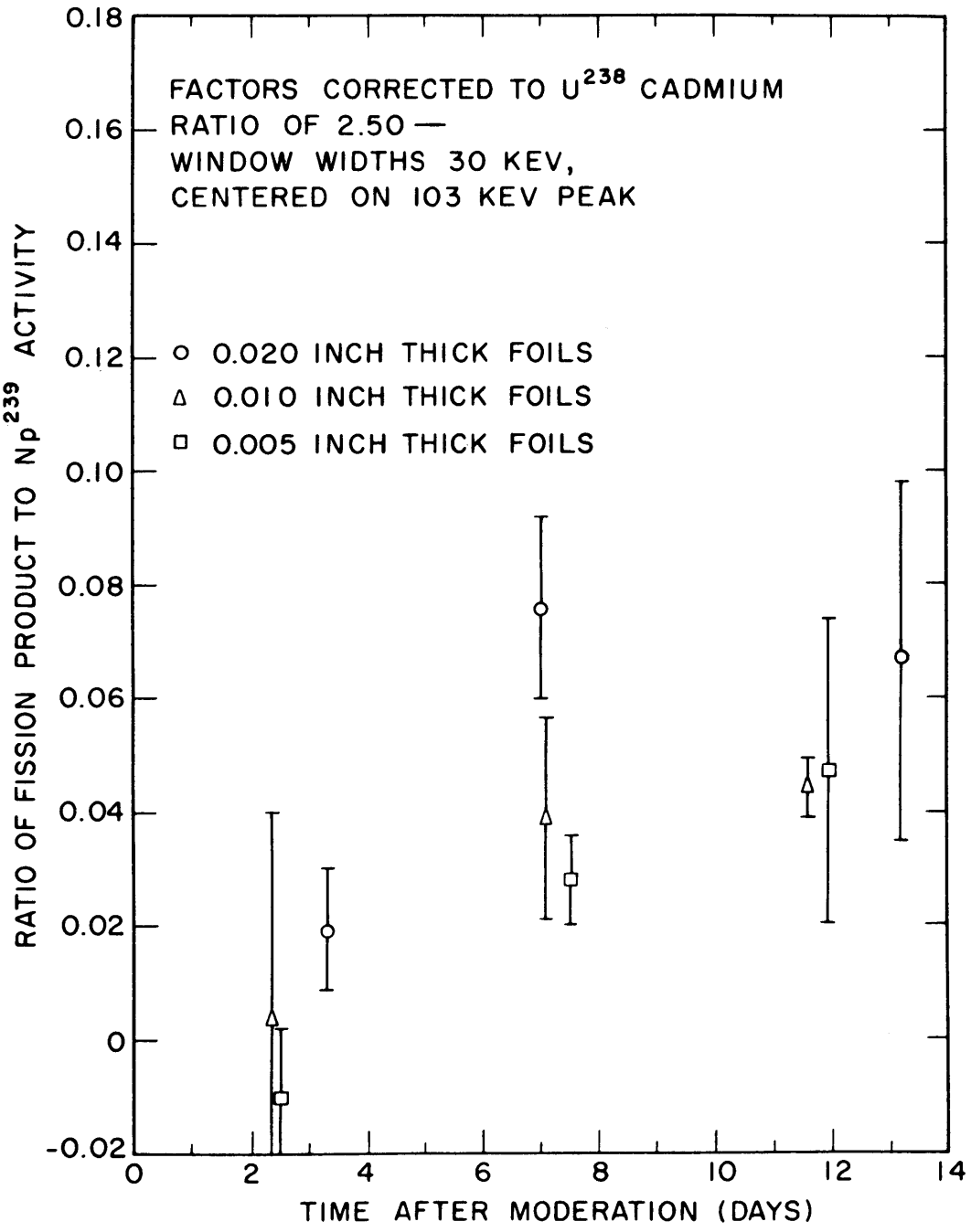

FIG. A-9 FISSION PRODUCT COINCIDENCE CORRECTION FACTORS AS OBTAINED BY THE SUBTRACTION METHOD

counts of the 0.020 inch natural uranium foils are shown in Figure A-10. For the singles counts it is seen that the data points of the subtraction method fall between the curves obtained by shielding the U^{235}-Al foil with 0.012 and 0.020 inches of U^{238}, with the time behavior agreeing nicely. By interpolation it is found that the data points fall in a position roughly equivalent to 0.016 inches of U^{238}. The results for the singles counts of the 0.010 and 0.005 inch foils are quite similar, with the 0.010 inch data points corresponding to about 0.007 inches of U^{238} and the 0.005 inch data points corresponding to about 0.012 inches of U^{238}. Thus, within the experimental error, the agreement between the two techniques is seen to be good for the singles counts. The "best" values for the singles correction factors are now taken to be those obtained by fitting the smooth curves of the extrapolation method to the data points of the subtraction technique, as shown in Figure A-8. The standard deviation of any point on the curves is about five per cent.

The comparison of the correction factors for the coincidence counts, as obtained by the two techniques yields less consistent results. The data for the 0.020 inch natural uranium foils are shown in Figure A-11.

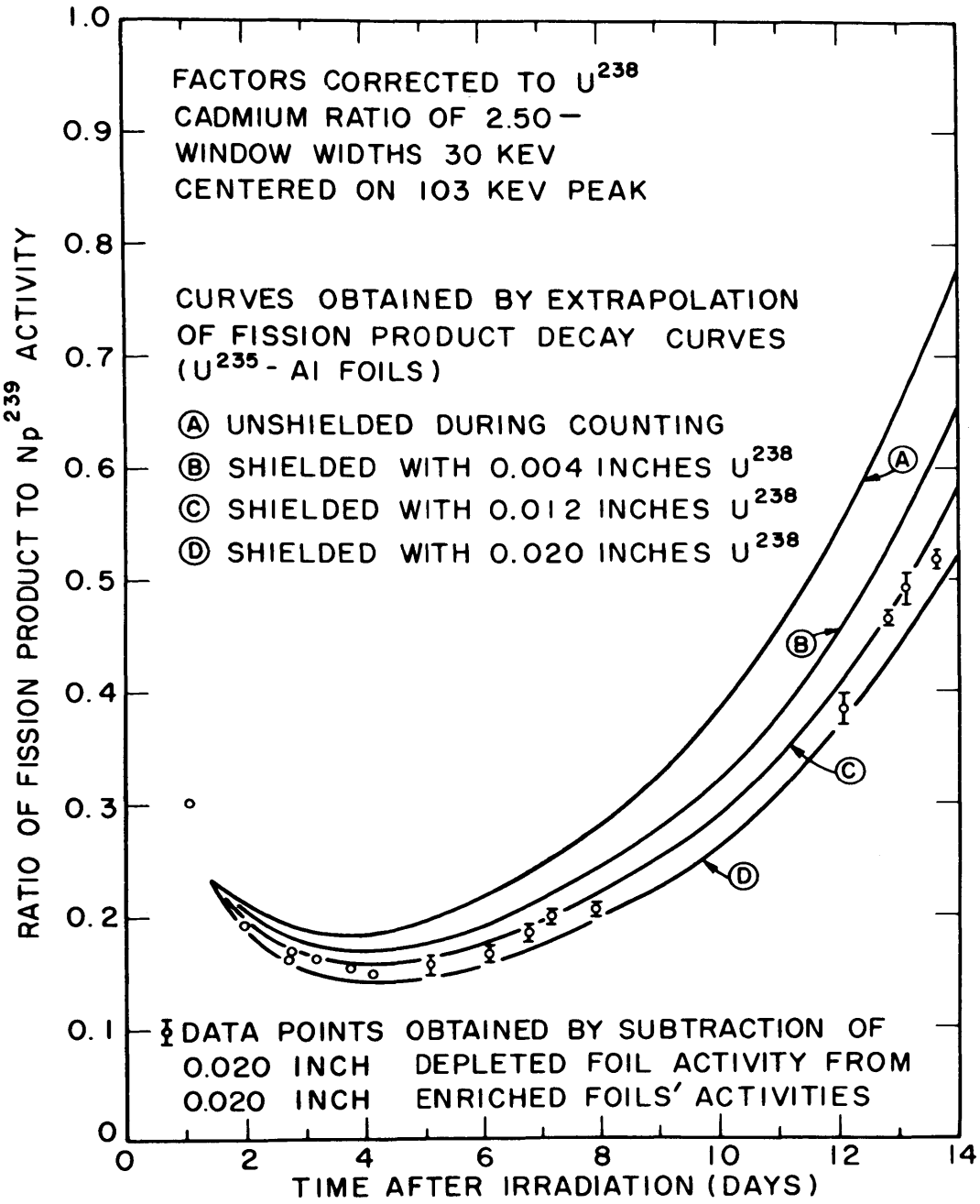

FIG. A-10 FISSION PRODUCT SINGLES CORRECTION FACTORS FOR NATURAL URANIUM FOILS 0.020 INCHES THICK

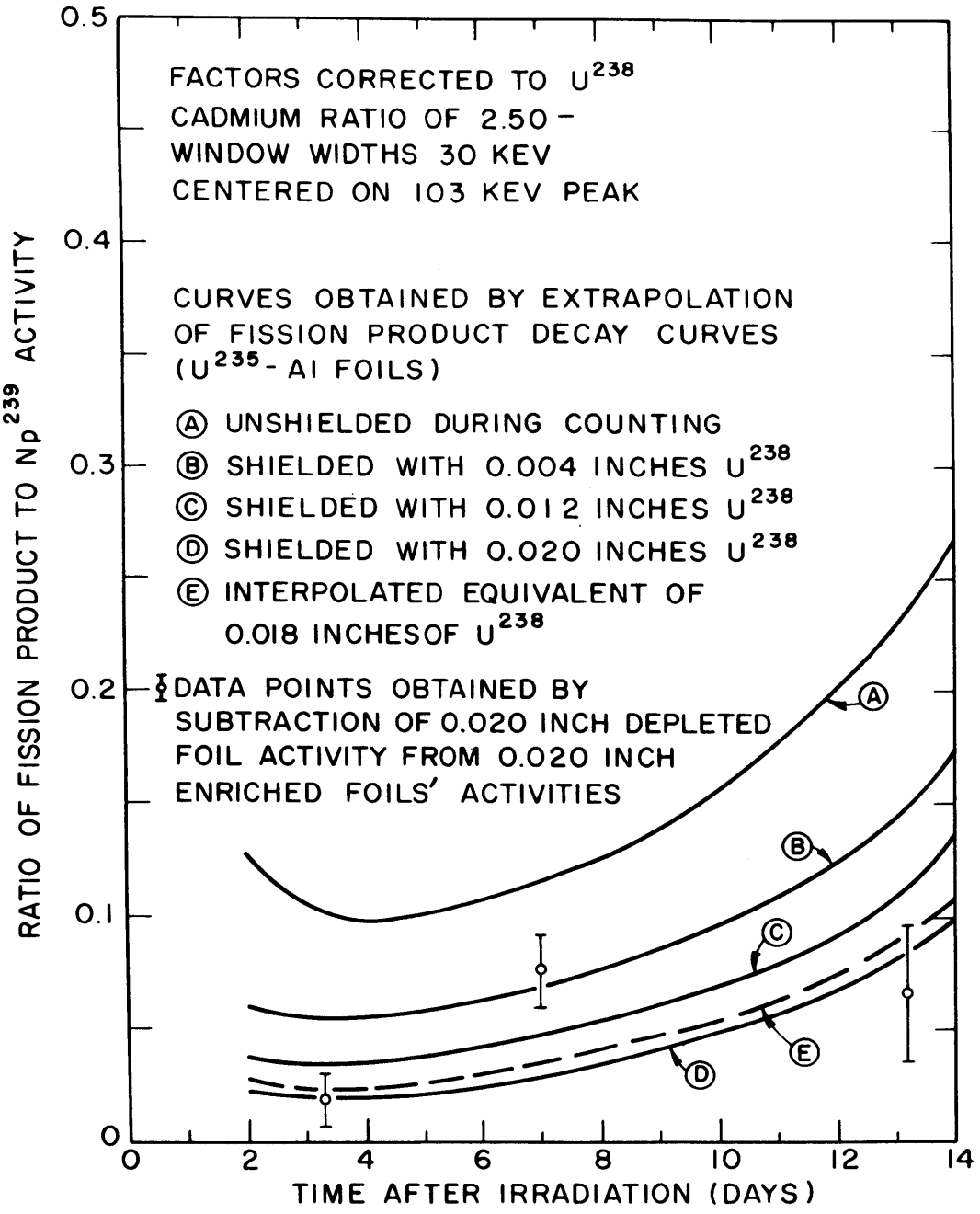

FIG. A-11 FISSION PRODUCT COINCIDENCE CORRECTION FACTORS FOR NATURAL URANIUM FOIL 0.020 INCHES THICK

Considering the large errors in the data points of the subtraction method, it is evident that they could be fitted by a curve whose shape is determined by the extrapolation method. This was done by using the least squares technique, and the resultant curves for the three thicknesses are shown in Figure A-12. The curves fall roughly in the same positions as observed for the singles counts (Figure A-8). However, when these results are compared to those obtained by the extrapolation method, the fit curves are all found to fall at a point roughly equivalent to an interpolated curve obtained with 0.018 inches of U^{238}. This result is consistent with the results for the singles counts of the 0.020 inch natural uranium foils, but does not agree with the results for the 0.010 and 0.005 inch foils. The discrepancy between the two methods apparently is the result of errors in the normalization of the decay curves for the coincidence counts of the U^{235}-Al foils and the non-depleted uranium foils. At times long after irradiation the count rates are necessarily low; the background correction becomes appreciable, and the statistical error in each point is large. For these reasons, the curves obtained by the least squares fit to the data of the subtraction method (Figure A-12) are taken to be the "best" values for the fission product coincidence correction factors. The

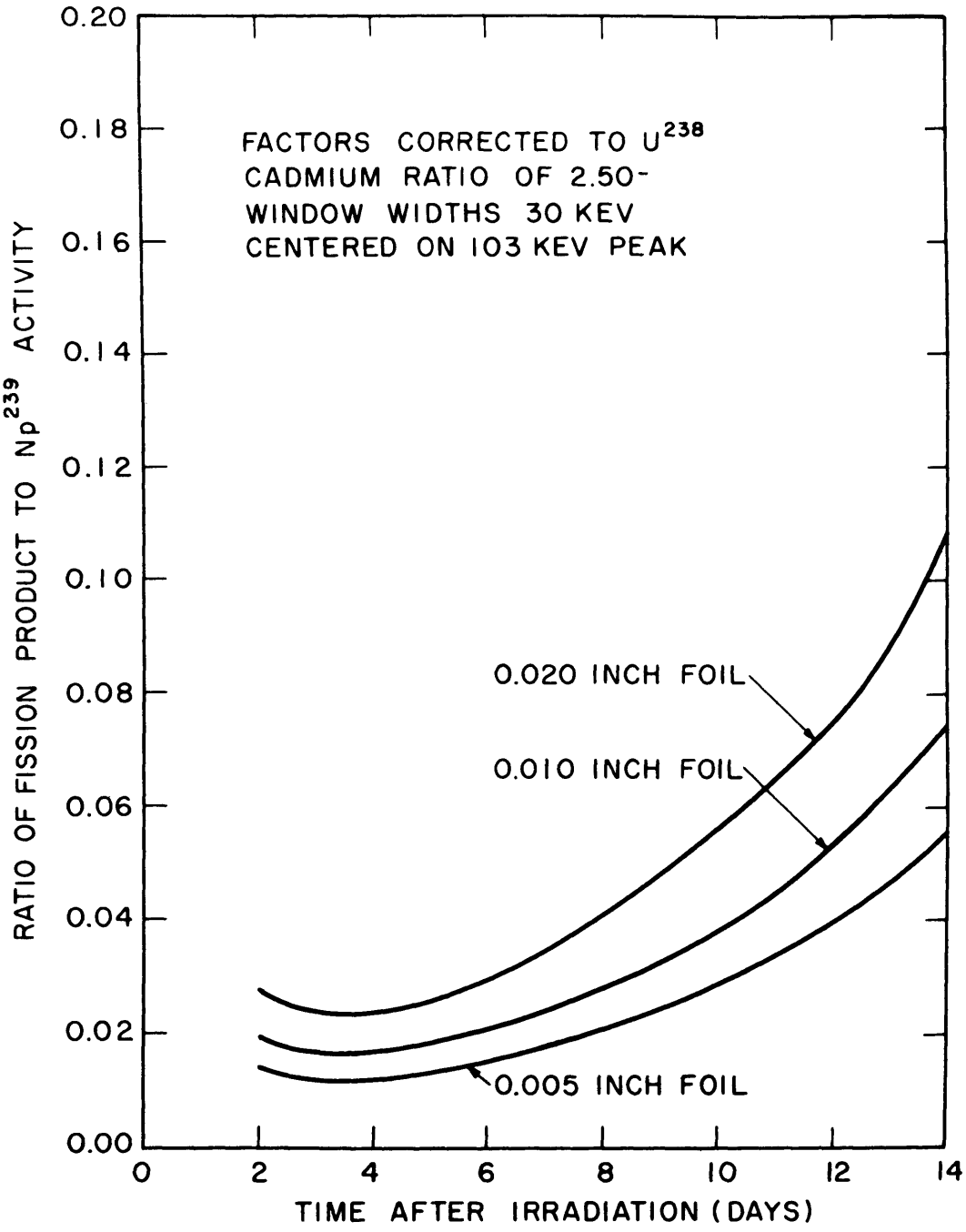

FIG. A-12 FINAL FISSION PRODUCT COINCIDENCE CORRECTION FACTORS FOR NATURAL URANIUM FOILS

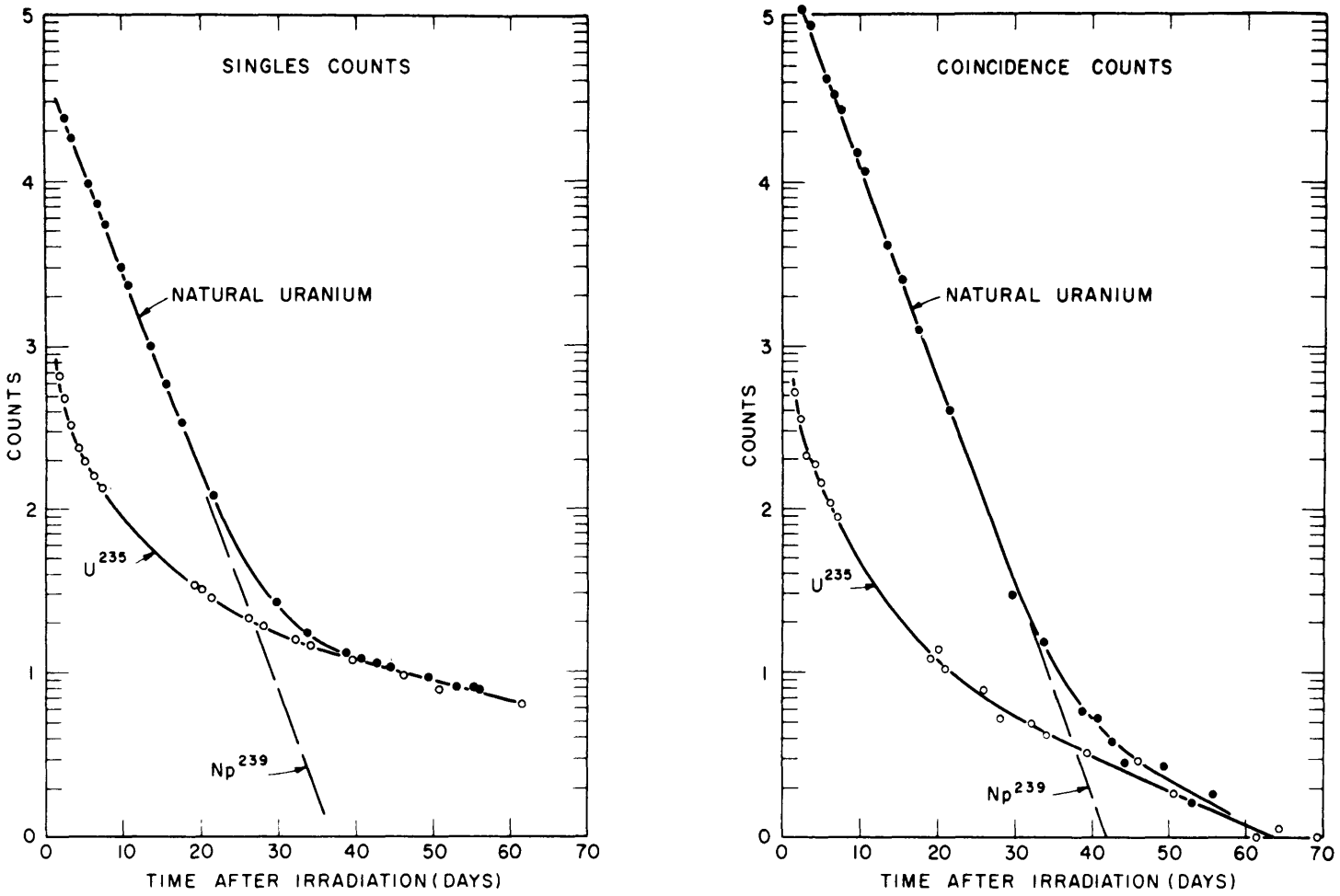

FIG. A-13 DECAY OF DILUTE NATURAL URANIUM AND U^{235} FOILS

WINDOW WIDTHS 30 KEV, CENTERED 103 KEV PEAK

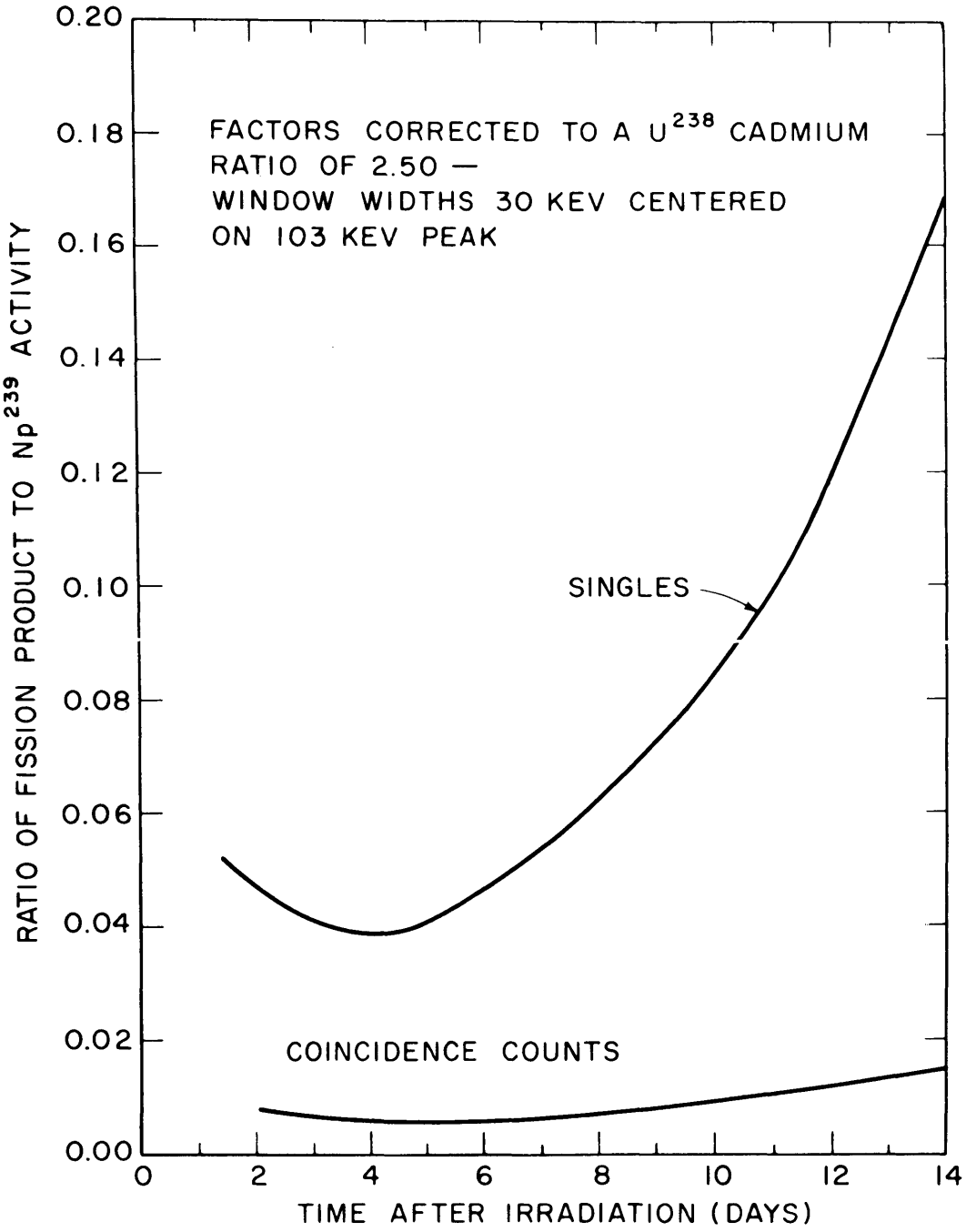

FIG. A-14 FISSION PRODUCT CORRECTION FACTORS FOR INFINITELY DILUTE NATURAL URANIUM FOILS

standard deviation of any point on these curves is approximately 40 per cent.

An additional run was made to determine the correction factors for a foil 0.003 inch thick of an alloy of natural uranium (one per cent by weight) in aluminum. Since the dispersion of the natural uranium is very dilute it was assumed that its fission product radiation would correspond to that of a U^{235}-Al foil which was unshielded during counting, i.e., there is very little interaction of the fission product γ-rays and uranium. The decay curves are shown in Figure A-13, and the resulting correction factors, corrected to a U^{238} cadmium ratio of 2.50, are shown in Figure A-14. For the dilute foils, as well as the uranium metal foils, the correction factors have their minimum value at about four days after irradiation. A comparison of these minimum correction factors is given in Table A-2. It is seen that for each thickness the correction factor for the coincidence counts is a factor of six or seven smaller than that for the singles counts. Even considering the larger standard deviations associated with the coincidence counts, the advantage of coincidence counting is evident.

In an effort to further reduce the relative contribution of the fission products, measurements were made using the channel settings that also showed promise in

TABLE A-2

Minimum[a] Fission Product Correction Factors for Natural Uranium Foil (Corrected to a U^{238} Cadmium Ratio of 2.50)

Foil Thickness (Inches)	Minimum Fission Product Correction Factor[b]	
	Singles	Coincidence
Dilute	3.9 ± 0.3	0.6 ± 0.12
.005	9.0 ± 0.5	1.3 ± 0.5
.010	10.3 ± 0.5	1.7 ± 0.7
.020	15.0 ± 0.8	2.3 ± 0.9

(a) In all cases, minimum occurs 4 days after irradiation.

(b) Ratio of fission product γ-ray activity to Np^{239} γ-ray activity, window widths 30 kev centered on 103 kev peak. Values multiplied by 100.

Figure A-3. With a U^{235}-Al foil and a uranium foil depleted in U^{235}, the ratio of fission product to Np^{239} activity was measured with the window widths of each channel set at 60 kev centered on the 103 kev peak. A second measurement was made with one channel at 103 kev and the other at 278 kev. At the second setting the fission product coincidence contribution was increased by a factor of thirteen. The desirability of the 103 kev settings is again demonstrated. A final measurement of the correction factors for 0.005 inch natural uranium was made with both channels set at 103 kev, and with window widths for both of 60 kev, 30 kev, and 10 kev. Minimum correction factors, at four days after irradiation, were obtained by using the extrapolation technique, with corrections for foil thickness applied as determined by comparison with the subtraction method. These values, adjusted to a U^{238} cadmium ratio of 2.50, are shown in Table A-3.

It is evident that decreasing the window widths significantly reduces the fission product contribution for the singles, but below 30 kev does not materially affect the coincidence counts. This result is consistent with the knowledge of the Np^{239} and fission product spectra in the 103 kev region. Figure A-4 shows that the 103 kev peak of Np^{239} falls in the valley between two fission product peaks and thus, decreasing the channel widths

TABLE A-3

Minimum[a] Fission Product Correction Factors
for 0.005 Inch Natural Uranium Foils
as a Function of Window Widths
Centered on 103 kev Peak
(Corrected to a U^{238} Cadmium Ratio of 2.50)

Ratio of Fission Product to Np^{239} Activity (b)			
	Window Widths of Both Channels		
	60 kev	30 kev	10 kev
Single Counts	16.1 ± 0.8	9.0 ± 0.5	6.6 ± 0.3
Coincidence Counts	3.2 ± 1.2	1.3 ± 0.5	1.0 ± 0.4

(a) Four days after irradiation.

(b) Values multiplied by 100.

would exclude the fission product radiation preferentially. As was demonstrated previously, the principle cause of fission product coincidences is photoelectric interaction with the uranium giving rise to 97 kev X-rays. The NaI detectors are unable to resolve the 97 and 103 kev peaks, and so there is little reduction in the fission product coincidence contribution when the narrower widths are employed.

It is now apparent that for the method of counting the Np^{239} gamma radiation, the fission product contributions as presented in Figures A-8, A-12, and A-14, and summarized in Table A-3, are close to the lowest possible values. Although the singles contribution may be reduced slightly, the coincidence method still gives a considerably lower fission product background.

4. Summary

The superiority of the gamma-gamma coincidence technique over the simpler method of singles counting has been demonstrated. With the optimum gamma spectrometer, 103 kev for both singles' channels, the coincidence technique gives a lower fission product background by a factor of six or seven. It must be noted, however, that these results depend strongly on the size of the NaI detector used. This series of measurements was made

with 1/2 inch thick, 1 1/2 inch diameter crystals.

Fission product correction factors, expressed as the ratio of fission product to Np^{239} activity, have been given for both the singles and coincidence counts. Table A-2 summarizes these results for infinitely dilute, 0.020, 0.010, and 0.005 inch natural uranium foils that were irradiated bare, and with relative U^{235} fission and U^{238} capture rates equivalent to a U^{238} cadmium ratio of 2.50. Similar measurements for cadmium covered natural uranium foils, give correction factors about seven per cent of those for the bare foils. Since the ratio of epi-cadmium U^{238} captures to total U^{238} captures is 0.4, the value of seven per cent is equivalent to an epi-cadmium U^{235} fission fraction of about 0.03. Examination of the data presented in Tables 7 and 10 of Reference 18 shows that for lattices with a U^{238} cadmium ratio of about 2.50, the epi-cadmium U^{235} fission factor is about 0.03. Thus we see the correction factors are proportional to the ratio of the U^{235} fission rate to the U^{238} capture rate. By applying simple correction factors the results obtained can be generalized to any thermal reactor neutron spectrum and to any value of the effective resonance integral of U^{238}.

If the reasonable assumption is made that the U^{235} fission product activity is proportional to the U^{238} thermal activation, then only the U^{238} cadmium ratio is needed to characterize the system. This ratio gives the relative thermal and epi-thermal U^{238} activation regardless of the flux spectrum and the effective cross-sections and, for well-thermalized systems, most of the U^{235} fissions are caused by neutrons having energies below the cadmium cutoff. If the U^{235} epi-cadmium fission factor is known then this correction may also be applied to improve the approximation.

If R_{28} is the U^{238} cadmium ratio, then:

$$R_{28} = \frac{\text{Total } U^{238} \text{ activation}}{\text{Resonance } U^{238} \text{ activation}}, \quad \text{(A-1)}$$

$$R_{28}\text{-}1 = \frac{\text{Thermal } U^{238} \text{ activation}}{\text{Resonance } U^{238} \text{ activation}} \propto \frac{U^{235} \text{ fission products}}{\text{Resonance } U^{238} \text{ activation}}, \quad \text{(A-2)}$$

and therefore,

$$\frac{R_{28}\text{-}1}{R_{28}} \propto \frac{U^{235} \text{ fission products}}{\text{Total } U^{238} \text{ activation}} . \quad \text{(A-3)}$$

On denoting the known fission product correction factor by $F_{2.50}$, which is a function of time after irradiation, the generalized factor $F_{R_{28}}$ can be expressed as:

$$F_{R_{28}} = 1.67\ F_{2.50}\ \frac{R_{28}-1}{R_{28}} \quad . \qquad \text{(A-4)}$$

As would be expected the fission product correction factors were also found to be proportional to the U^{235} concentration of the foil. If c is the concentration, in atom fraction of U^{235}, then multiplying these natural uranium correction factors by $\frac{c}{1-c} \times \frac{0.9928}{0.0072}$ will give the value for the new enrichment. With the corrections made for foil enrichment and relative U^{235} and U^{238} reaction rates, the only remaining parameter is the foil thickness. With the correction factors given for foils of infinite dilution and of thicknesses 0.005, 0.010, and 0.020 inches it is easy to interpolate in this range.

With the results presented here it is possible to estimate the undesirable fission product contribution to the Np^{239} activity for a wide range of situations. Use of the coincidence technique will reduce this contribution considerably, but the greater degree of accuracy obtained for the singles correction factors makes this method almost as desirable.

APPENDIX B.

Effective Resonance Integrals for U^{238} in Thin Foils

To determine the effective resonance integral (ERI) of U^{238} in thin foils, the U^{238} cadmium ratio was measured for foils of different thickness, and also for a foil of infinitely dilute U^{238} concentration. For each thickness, the resonance activity was normalized to the thermal activity and compared directly to the infinitely dilute foil for which the resonance integral is known. This approach is essentially that used by Macklin and Pomerance (20).

All foils were irradiated in the same position in the MIT Reactor, and so were exposed to the same flux. The resonance neutron spectrum at this position was assumed to vary as 1/E and measurements by C. Anderson (2) showed that this assumption was valid. The dilute foils, 0.003 inches thick, were an alloy of natural uranium, one per cent by weight, in aluminum, with an effective U^{238} thickness of 0.2 mg/cm^2. The resonance self-shielding of these foils was proven to be negligible by measuring the same specific activation for thicknesses up to 0.015 inches, when cadmium covered foils were irradiated. The thin foils were of uranium depleted to fifteen parts per million U^{235}, and were laminated in nominal thicknesses of 0.004, 0.010, 0.015, 0.025 inches.

After irradiation, the foils were counted in the gamma spectrometer system described in Section 2 of Appendix A, with the pulse height analyzers set to straddle the 103 kev Np^{239} γ-ray peak with a window width of 30 kev. Both single channels were used and the counts in each summed. For the depleted uranium foils, no correction for non-Np^{239} activity was necessary, but for the bare dilute uranium foil a correction of about two per cent was required to account for the presence of U^{235} fission products. It was not necessary to correct for the self-attenuation of the γ-rays in the depleted foils since each pair of foils was matched in weight to within 0.1 per cent, but it was necessary to correct for the different effects of self-shielding of the thermal neutrons for each thickness. For this correction, Wilkins' (27) equation for the fractional activation f of a foil of thickness t when irradiated in a thermal flux was used:

$$f = 1 + \pi^{-1/2} y \ln y \left(1 + \frac{y^2}{12}\right) + 0.131y - y^{2/3} - 0.007y^3, \quad \text{(B-1)}$$

where $y = t/\lambda$; in the depleted uranium the absorption mean free path λ, is 3.0 inches.

If R_{28} is the measured U^{238} cadmium ratio, and the infinitely dilute foil and the thin foil are denoted by the subscripts ∞ and x respectively, then:

$$(R_{28} - 1)^{-1} = \frac{U^{238} \text{ resonance activity}}{U^{238} \text{ thermal activity}}, \qquad \text{(B-2)}$$

and

$$ERI_x = \frac{(R_{28}-1)_\infty}{(R_{28}-1)_x} \times 282 \text{ barns}, \qquad \text{(B-3)}$$

where 282 barns is the U^{238} infinite resonance integral. The epicadmium 1/v capture in the ERI is included in equation (B-3) but it may be removed simply by considering the ERI to be made up of two portions, one the true ERI, and the other the integral of the 1/v contribution from cadmium cutoff to infinity. Thus

$$ERI_x + 1.4 \text{ barns} = \frac{(R_{28} - 1)_\infty}{(R_{28}-1)_x}(282 + 1.4) \text{ barns}, \qquad \text{(B-4)}$$

where 1.4 barns is the epicadmium 1/v contribution, with the cadmium cutoff energy taken to be 0.40 ev for cadmium 0.020 inches thick.

The experimental data, the f-factors calculated with equation (B-1), and the values of the effective resonance integral calculated with equation (B-4) are summarized in Table B-1. The resonance integrals are also shown in Figure B-1, plotted against the square root of the ratio of surface to mass $(S/M \text{ cm}^2/\text{gram})^{1/2}$. Included in the figure is the straight line obtained from the ERI of uranium rods by Hellstrand (16):

TABLE B-1

Summary of Data and Results of the Measurements of the U^{238} Effective Resonance Integral[a] for Thin Foils

Depleted Uranium Foil Thickness (inches)	$(\frac{S}{M}\frac{cm^2}{gram})^{1/2}$	Measured U^{238} Cadmium Ratio	Calculated f-factor	$(R_{28}-1)^{-1}xf$ (corrected)	U^{238} ERI (barns)
0.00431	3.18	2.251 ± 0.006	0.995	0.795 ± 0.004	73.9 ± 8.0[b]
0.0102	2.12	2.717 ± 0.011	0.989	0.576 ± 0.004	53.2 ± 6.4
0.0144	1.81	3.075 ± 0.003	0.986	0.475 ± 0.001	43.6 ± 5.2
0.0195	1.58	3.447 ± 0.021	0.981	0.401 ± 0.003	36.6 ± 4.4
0.0253	1.41	3.740 ± 0.016	0.977	0.357 ± 0.002	32.4 ± 3.9
Infinitely Dilute Uranium Foil		1.334 ± 0.040	1	2.99 ± 0.22	assumed value 282

(a) Epicadmium 1/v capture excluded.

(b) Errors do not include uncertainty in assumed value for the dilute resonance integral of U^{238}.

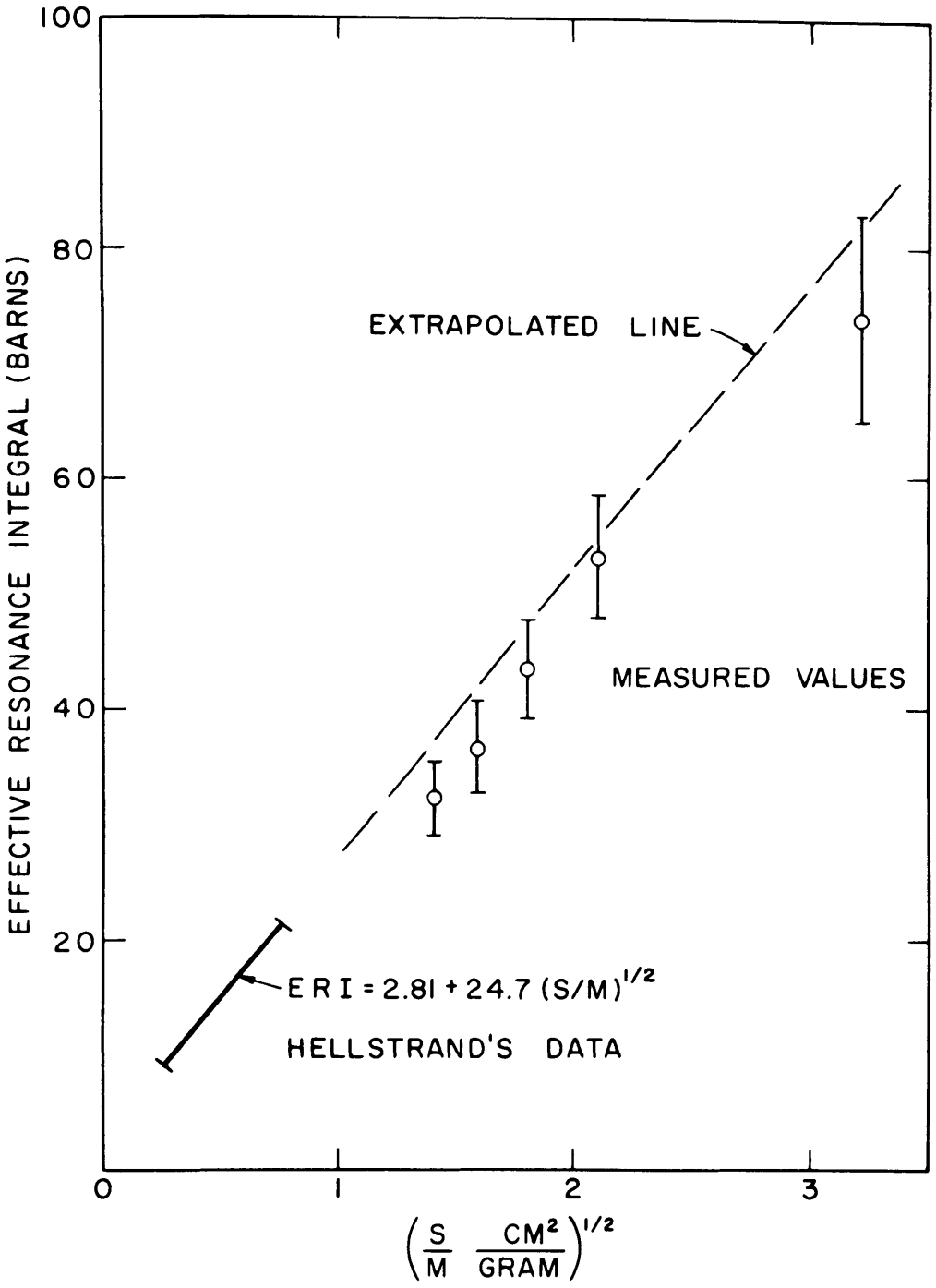

FIG. B-1 U^{238} EFFECTIVE RESONANCE INTEGRALS FOR THIN FOILS

$$ERI = 2.81 \pm 24.7 \left(\frac{S}{M}\right)^{1/2} \text{ barns}, \qquad (B\text{-}5)$$

which fits data in the range of $\left(\frac{S}{M}\right)^{1/2}$ from 0.26 to 0.74 $(cm^2/gram)^{1/2}$. If equation (B-5) is extrapolated to higher values of $\left(\frac{S}{M}\right)^{1/2}$, it is seen that the measured thin foil resonance integrals are consistently smaller. It is possible that the difference is significant but, owing to the large experimental uncertainties, the results are inconclusive. The large uncertainties result almost entirely from the uncertainty in the dilute foil cadmium ratio, which is very close to unity. A three per cent error in the dilute cadmium ratio, which is not an unreasonable error, results in a twelve per cent error in the thin foil resonance integrals. Without considerable additional experimentation, this is the limit of the measurement. However, for the purpose of comparison of the thin foil resonance integrals, without the absolute calibration, the present measurements are satisfactory.

APPENDIX C.

Self-Attenuation of 103 Kev Gamma Rays in Thin U^{238} Foils

To estimate the effect of self-attenuation of 103 kev Np^{239} gamma rays in thin U^{238} foils, the simple model illustrated in Figure C-1 was used. In the actual counting arrangement of the gamma spectrometer system used for most of the measurements described in this report, the distance, d, from the foil to the detector was sufficiently large so that only the path through the foil normal to the surface need be considered. The probability of transmission, T_x, of a gamma ray originating in an element dx at position x is:

$$T_x = e^{-\sigma(t-x)}, \qquad (C-1)$$

where σ is the attenuation cross section and t is the foil thickness. For the thin foils in question, it was also assumed that the source of the gamma rays was flat throughout the foil, i.e., the flux depression within the foil was negligible. Thus, the average value of T is simply:

$$T = \frac{1}{t}\int_0^t T_x dx = \frac{1}{\sigma t}\left(1-e^{-\sigma t}\right). \qquad (C-2)$$

The value of σ to be used with equation C-2 was obtained from a simple transmission experiment. A uranium foil depleted to fifteen parts per million U^{235}, 0.005 inches thick and 0.25 inches in diameter was irradiated in the MIT Reactor and served as the source of 103 kev Np^{239} gamma rays. It was placed in the gamma spectrometer system described in Section 2 of Appendix A and its activity measured with the pulse height analyzer set to straddle the 103 kev peak with a window width of 30 kev. To increase the amount of data taken both single channels were used and the counts in each summed. The foil was then counted successively with unirradiated shields of the same material with thicknesses varying from 0.005 to 0.025 inches. The measured activities plotted against shield thickness are shown in Figure C-2. For shield thickness up to 0.015 inches, the activities follow the expected exponential attenuation, but beyond that, the effect of buildup becomes evident. The buildup appears to be due to photoelectric interaction of the higher energy (210, 228, 276 kev) Np^{239} gamma rays with the uranium which results in 97 kev uranium x-rays. These cannot be resolved from the original 103 kev Np^{239} gamma rays. The value of σ obtained by taking the slope of the tangent to the curve at zero shield thickness is 73.5 inches^{-1}.

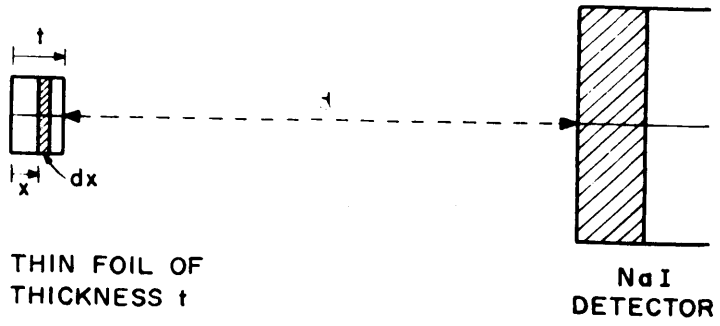

FIG. C-1 MODEL USED TO CALCULATE THE SELF-ATTENUATION OF γ-RAYS IN THIN FOILS

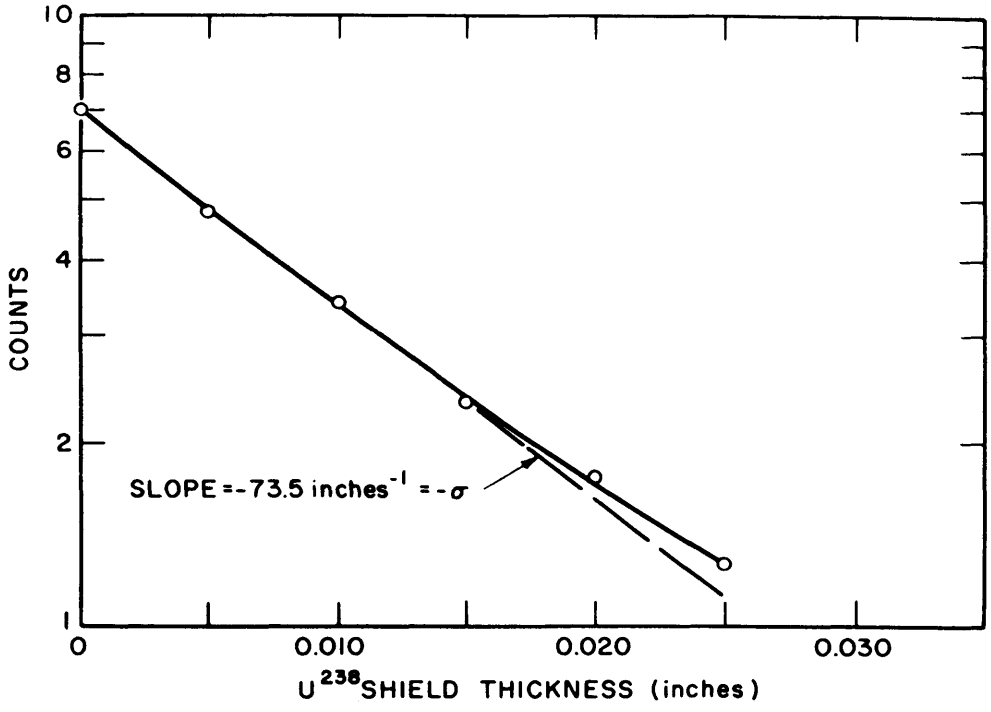

FIG. C-2 ATTENUATION OF 103 KEV Np^{239} γ-RAYS IN THIN U^{238} FOILS.

Evaluating equation C-2 for foils 0.010 and 0.011 inches thick with σ = 73.5 inches^{-1} gives T (0.010 inches) = 0.708 and T(0.011 inches) = 0.686--a difference of only 3 per cent for a 10 per cent difference in foil thickness. For a similar 10 per cent difference in thickness of 0.005 inch foils, the difference in T is only 2 per cent. Thus, the effect of self-attenuation of the 103 kev gamma rays is seen to be small. Since the purpose of these calculations is to permit corrections to be made for attenuation in foils of slightly different thicknesses, rather than an absolute determination of the attenuation factor, and since the magnitude of the correction is small, it was considered that the approximations made in the calculations are adequate.

APPENDIX D

Flux Depression in Composite Foils

The fractional activation f of a single foil is defined as the ratio of its specific activation to that of a foil of infinite dilution. For thin foils ($1-f \ll 1$) it may be assumed that the flux incident upon the foil is separated into two equal directional fluxes $\phi^+ = \phi^- = \frac{\phi}{2}$, each of which is depressed linearly while traversing the foil. If the average fluxes within the foil are f times the incident fluxes, then the emergent fluxes are 2f - 1 times the incident fluxes. This is illustrated for the positive flux ϕ^+ in Figure (D-1-a). The average activation for the foil is:

$$(\phi^+)_{avg} + (\phi^-)_{avg} = f\phi. \qquad \text{(D-1)}$$

For two adjacent foils, the flux emerging from one is incident upon the second, as shown in Figure (D-1-b) for the positive flux component. Here:

$$(\phi_1^+)_{avg} = f_1\phi^+ \text{ and } (\phi_2^+)_{avg} = f_2(2f_1-1)\phi^+. \qquad \text{(D-2)}$$

The analogous relations hold for the negative component;

$$(\phi_2^-)_{avg} = f_2\phi^- \text{ and } (\phi_2^-)_{avg} = f_1(2f_2-1)\phi^-. \qquad \text{(D-3)}$$

(a) POSITIVE FLUX INCIDENT UPON SINGLE FOIL

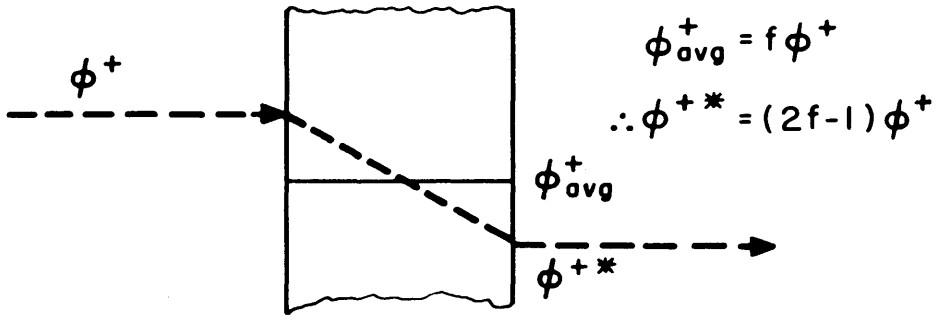

FRACTIONAL ACTIVATION = f

(b) POSITIVE CURRENT INCIDENT UPON TWO FOILS OF DIFFERENT MATERIALS

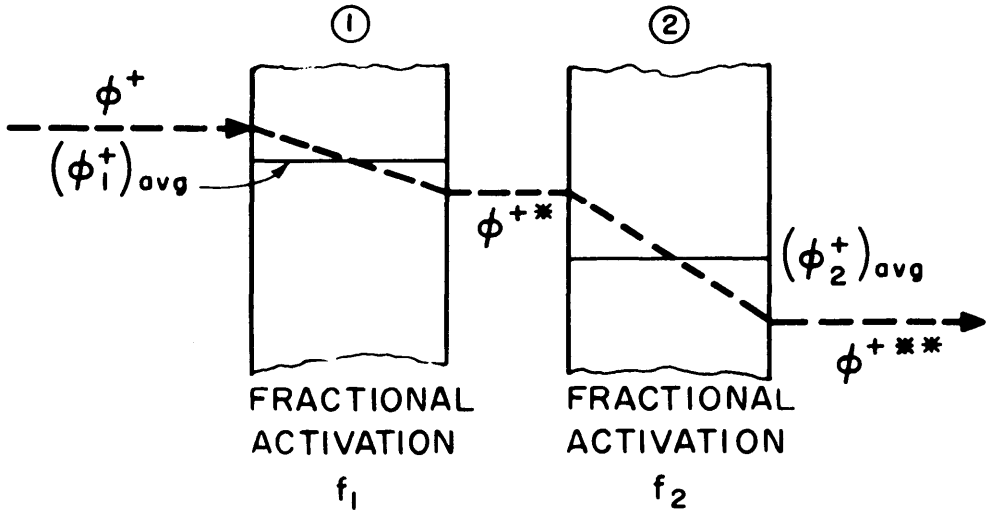

$(\phi^+_1)_{avg} = f_1\phi_+$, $\therefore \phi^{+*} = (2f_1 - 1)\phi^+$ and

$(\phi^+_2)_{avg} = f_2(2f_1 - 1)\phi^+$

FIG. D-1 FLUX DEPRESSION IN COMPOSITE FOILS

To obtain the average flux in each foil, $(\phi^-)_{avg}$ and $(\phi^+)_{avg}$ are added:

$$(\phi_1)_{avg} = f_1\phi^+ + f_2(2f_2-1)\phi^- = (f_1 + 2f_1f_2 - f_1)\frac{\phi}{2}$$

$$= f_1f_2\phi,$$

and similarly;

$$(\phi_2)_{avg} = f_1f_2\phi. \qquad \text{(D-4)}$$

Thus, it is shown that the flux depression and hence the fractional activation of two foils in adjacent positions is the same. This is equally true for any number of foils i, j, k ..., providing that $(1-f_i) \ll 1$ and also $(1-f_if_jf_k\ldots) \ll 1$. When these conditions are fulfilled, the original assumption of linear flux depression is valid.

APPENDIX E

References

1. Adler, F. T., et al, A/Conf.15/P/1988 (1958).
2. Anderson, C. A., "Measurement of Neutron Energy Spectra with the M.I.T.R. Fast Chopper," (doctoral dissertation) M.I.T. (1961).
3. Baer, W., et al, Nucl. Sci. Eng. 3,133 (1958).
4. Brown, P. S., private communication.
5. Campbell, C. G. and M. D. Carter, BNL-433, p. 26 (1957).
6. Creutz, E., et al, Jour. Appl. Phys. 26, 271 (1955).
7. Curtis, C. D., et al, ANL-5222 (1954).
8. Dancoff, S. M. and M. Ginsburg, CP-2157 (1944).
9. Davis, M. V., Jour. Appl. Phys. 28, 250 (1957).
10. Dayton, I. E. and W. G. Pettus, Nucl. Sci. Eng. 3, 286 (1958).
11. Dressner, L., Nucl. Sci. Eng. 1, 501-510 (1956).
12. Goldstein, N. and D. J. Hughes, CP-3580 (1946).
13. Cristy, R. F., A. M. Weinberg, and E. P. Wigner, CP-2062 (1944).
14. Gurevich, I. I., and I. Y. Pomeranchouck, PICG 5, 466 (1955).
15. Heavy Water Lattice Research Project Annual Report, NYO-9658, p. 5-18, (Sept. 30, 1961).
16. Hellstrand, E., Jour. Appl. Phys. 28, 1493 (1957).
17. Honeck, H. C., "A Method for Computing Thermal Neutron Distributions in Reactor Lattices as Functions of Space and Energy," (doctoral dissertation), MIT (1959).

18. Kouts, H. and R. Sher, BNL-486 (T-111), (1957).

19. Kranz, A. Z. and G. G. Smith, WAPD-151 (May 1956).

20. Macklin, R. L. and H. S. Pomerance, PICG 5, p.96 (1955).

21. Muelhause, C. O., et al, ANL-4323 (1949) p. 26.

22. Palmedo, P. F., "Measurements of the Material Bucklings of Lattices of Natural Uranium Rods in D_2O," (doctoral dissertation) M.I.T. (1962).

23. Risser, J. R., et al, ORNL-958 (1951).

24. Sher, R., Nucl. Sci. Eng. 7, 479 (1960).

25. Weinberg, A. M. and E. P. Wigner, "The Physical Theory of Neutron Chain Reactors," Chicago, the University of Chicago Press, p. 170.

26. Westcott, C. H., AECL-1101 (CRRP-960), (1960).

27. Wilkins, J. E., CP-3581 (1946).

28. Wolberg, J. R., "A Study of the Fast Fission Effect in Lattices of Uranium Rods in Heavy Water," (doctoral dissertation) M.I.T. (1962).

APPENDIX F

Supplementary Literature Survey

In this Appendix, a number of papers on the general subject of resonance capture of neutrons in reactors are listed to serve as a guide to future workers in this area. The papers are divided among several subheadings and, in each group, are listed in chronological order. The list is not complete, but contains most of the more important papers. Occasional cross references are included and these refer to other references in this section.

Contents

		Page
F.1	General Summaries	122
F.2	Experiments	
	a. Cadmium Ratio Measurements	123
	b. Conversion Ratio Measurements.	126
	c. Effective Resonance Integral Measurements.	127
	d. Miscellaneous Experiments.	129
F.3	Methods of Calculating Lattice Parameters	
	a. Analytical and Semi-Empirical Methods. . .	131
	b. Machine Calculations	134
F.4	Theory of Resonance Capture.	136
F.5	Doppler Temperature Coefficient Measurement and Calculation.	140
F.6	Dancoff Factor Measurement and Calculation . .	142
F.7	Nuclear Data	144
F.8	Miscellaneous.	145

F.1 General Summaries

1. "Proceedings of the Brookhaven Conference on Resonance Absorption of Neutrons in Nuclear Reactors," BNL-433 (C-24), (Sept. 1956).

2. Sampson, J. B., and J. Chernick, "Resonance Escape Probability in Thermal Reactors," KAPL-1754 (1957); also Progress in Nuclear Energy, Physics and Mathematics, 2, 233 (London, Pergamon Press, 1958).

3. Kouts, H., et al, "Physics of Slightly Enriched, Normal Water Lattices (Theory and Experiment)," PICG 12, 446 (1958).

4. Spinrad, B. I., et al, "Resonance Capture in Uranium and Thorium Lumps," A/Conf. 15/P/1847 (1958).

5. Edlund, M. C., et al, "Physics of Water Moderated Thorium Reactors," A/Conf. 15/P/2405 (1958).

6. Weinberg, A. M., and E. P. Wigner, "The Physical Theory of Neutron Chain Reactors," Chicago, The University of Chicago Press, Chapter 19 (1958).

F.2 Experiments

F.2.a Cadmium Ratio Measurements

1. Kouts, H., "Resonance Escape Probability Measurement," BNL-2077 (October (1953).

   Presents technique for measurement of p, with discussion of sources of error and possible methods of improvement of the technique.

2. Kouts, H., "Analysis of p Measurement," BNL-2095 (April 1954).

   Derives equation relating to p to measured U^{238} cadmium ratio, including effects of fast capture and leakage of fast, resonance and thermal neutrons.

3. Krasik, S. and A. Radkowsky, Pressurized Water Reactor Critical Experiments," PICG 5, 203 (1955).

   Reports results of measurements of ρ_{28} in H_2O lattices.

4. Kranz, A. Z., "Measurements of Thermal Utilization, Resonance Escape Probability, and Fast Fission Factor of Water Moderated Slightly Enriched Uranium Lattices," WAPD-134 (September 1955).

   Measures ρ_{28} using γ-counting technique.

5. Klein, D., et al, "Measurements of f, p, and ϵ in Slightly Enriched Low Density UO_2 Fueled Lattices," WAPD-P-721 (1956).

   Measures ρ_{28} using γ-counting technique.

6. Kranz, A. Z. and G. G. Smith, "f, p and ϵ Measurements on 0.6" Diameter 1.3% Enriched Low Density UO_2 Fueled TRX Lattices," WAPD-PWR-Ph-105 (May 1956).

   A brief summary of these UO_2-H_2O lattice measurements are presented.

7. Kranz, A. Z. and G. G. Smith, "A Second Report of Measurements of f, p and ϵ of Water Moderated Slightly Enriched Uranium Lattices," WAPD-151 (May 1956).

A continuation of Ref. F.2.a.2 with some changes in the experimental techniques.

8. Egiazarov, V. B., et al, "Measuring the Resonance Absorption of Neutrons in a Uranium-Graphite Lattice," CASU 1, 59 (1956).

   Measure U^{238} cadmium ratio using chemical separation technique.

9. Niemuth, W. E., "Measurements of Resonance Escape Probability in Hanford Lattices," BNL-433, p.5 (1957).

   Measures distribution of U^{238} and U^{235} resonance absorptions using pin detectors as well as foils.

10. Klein, D., et al, "Measurements of Resonance Escape Probability in 1.3 Per Cent Enriched Uranium and Uranium Oxide Fueled Lattices," BNL-433, p. 43 (1957).

    Measures ρ_{28} using γ-counting technique.

11. Anthony, J. P., et al, "Mesure de l'absorption resonnants," CEA-670 (I), (1957).

    Measures cadmium ratio for uranium and thorium in the G1 reactor using a chemical separation technique.

12. Kouts, H. and R. Sher, "Exponential Studies of Slightly Enriched Uranium Water Moderated Lattices, Part 1. 0.600 Inch Diameter Rods," BNL-486 (T-111), (1957).

    Reports the results of extensive study of the above lattices. Measures ρ_{28} using chemical separation technique.

13. Phelps, J. P. and R. Sher, "Resonance Escape Probability Measurements in TH-2% U^{235} Light Water Moderated Lattices," Nucl. Sci. Eng. 2, 676 (1957).

    Uses technique analogous to that of Ref. F.2.a.12.

14. Klein, D., et al, "Measurements of Thermal Utilization, Resonance Escape Probability and Fast Effects in Water Moderated Slightly Enriched Uranium and Uranium Oxide Lattices," Nucl. Sci. Eng. 3, 403 (1958).

    Summarizes the work reported in Refs. F.2.a.4, 5 and 7, with some additional work included.

15. Redman, W. C. and J. A. Thie, "Properties of Exponential and Critical Systems of Thoria-Urania and Heavy Water and Their Application to Reactor Design," PICG 12, 402 (1958).

Measures Th^{232} cadmium ratio by γ-counting technique and also measures p by the fuel substitution method.

16. Niemuth, W. E. and R. Nilson, "Lattice Parameters Derived from Neutron Distributions," PICG 12, 643 (1958).

Measures U^{238} cadmium ratio for small pins imbedded in fuel rods and integrates results over rod to obtain p.

17. Skeen, C. H. and W. W. Brown, "Resonance Escape Probability of a Lattice of Multirod Fuel Elements," NAA-SR-3211 (1959).

Reports the results of ρ_{28} measurements for rod clusters in graphite moderator.

18. Babcock, D. F., et al, "Heavy Water Moderated Power Reactors Progress Report - April 1960," DP-495 (May 1960).

Reports measurements for ρ_{28} and gives method of measuring the Dancoff correction factor.

19. Grob, V. E., et al, "Multiregion Lattice Studies. Results of Critical Experiments in Loose Lattices of UO_2 Rods in H_2O," WCAP-1412 (March 1960).

Reports results of several ρ_{28} measurements.

F.2.b Conversion Ratio Measurements

1. Levenson, M., "Determination of the Conversion Ratio of the EBR by Radiochemical Methods," ANL-5095 (1953).

   Measures conversion ratio by mass spectroscopic and radiochemical methods to provide a check for physical measurements.

2. Curtis, C. D., et al, "A Physical Determination of the Conversion Ratio of the Experimental Breeder Reactor," ANL-5222 (1954).

   Describes in detail an experimental technique for the conversion ratio determination.

3. Campbell, C. G. and M. D. Carter, "The Experimental Determination of Conversion Factors," BNL-433, p. 26 (1957).

   Describes experimental technique for conversion ratio measurements.

4. Baer, W., et al, "Measurements of the Conversion Ratio of the PWR Critical Facility Blanket," Nucl. Sci. Eng. 3, 113 (1958).

   Presents an experimental technique for conversion ratio measurements.

F.2.c Effective Resonance Integral Measurements

1. Mitchell, A. C. G., et al, "Resonance Absorption of Uranium in Mixtures," CP-1676 (1944).

   Measures resonance integrals for uranium in mixtures by comparing produced U^{239} activity with iodine, gallium and indium monitors.

2. Goldstein, N. and D. J. Hughes, "Resonance Absorption of Uranium," CP-3580 (1946).

   Measures ERI for U metal and UO_2-C mixtures by comparing with indium standards.

3. Untermeyer, S., "Experimental Nuclear Physics Division and Theoretical Nuclear Physics Division Quarterly Report, July-September 1949," ANL-4350, p. 53 (1949).

   Resonance integrals measured for uranium rods by danger coefficient technique. Use gold for absolute standardization.

4. Untermeyer, S. and C. Eggler, "Reactor Engineering and Services Division Quarterly Report for December 1, 1950 to February 28, 1951," ANL-4596, p. 23 (1951).

   Resonance integrals for thorium rods measured by reactivity technique.

5. Risser, J. R., et al, "Surface to Mass Dependence of Effective Resonance Integrals for U^{238} Cylinders," ORNL-958 (1951).

   Measured the ERI for various U^{238} rods by comparing with the published ERI for a rod with infinite shielding. Used an activation technique for the measurements.

6. Creutz, E., et al, "Effect of Geometry on Resonance Absorption of Neutrons by Uranium," Jour. Appl. Phys. 26, 271 (1955).

   Measures ratio of thin sample U^{238} activation to that of bulk U^{238} in spheres of metal and oxide.

7. Eriksen, V. O., et al, "Measurements of the Effective Resonance Integral of Uranium with the Pile Oscillator," PICG 5, 105 (1955).

8. Hellstrand, E., "Measurements of Effective Resonance Integral in Uranium Metal and Oxide in Different Geometries," Jour. Appl. Phys. 28, 1493 (1957).

Measures ERI for single rods by comparing to a dilute U^{238} sample of known resonance integral. Also measures spatial distribution of resonance captures.

9. Davis, M. V., "Resonance Absorption of Neutrons by Uranium Cylinders," Jour. Appl. Phys. 28, 250 (1957).

Measures the ERI and Doppler coefficient by danger coefficient technique.

10. Davis, M. V., "Resonance Absorption of Neutrons by Thorium Cylinders," Jour. Appl. Phys. 28, 714 (1957).

Measures the ERI and Doppler coefficient by danger coefficient techniques.

11. Davis, M. V., "Resonance Absorption of Neutrons in Metal and Oxide Cylinders, "Nucl. Sci. Eng. 2, 488 (1957).

Reports results of danger coefficient measurements of the ERI of 1.73 cm radius cylinders of U, UO_2, Th and ThO_2.

12. Dayton, I. E. and W. G. Pettus, "The Effective Resonance Integral of Thorium and Thorium Oxide," Nucl. Sci. Eng. 3, 286 (1958).

Uses danger coefficient techniques to measure ERI for plates and rods.

13. Skeen, C. H., et al, "Exponential Experiment with a Thorium-Uranium Fuel in Graphite," NAA-SR-4238 (March 1960).

Reports ERI for thorium as measured by activation technique (Ref. F.2.a.17).

F.2.d Miscellaneous Experiments

1. Mummery, P. W., "The Experimental Basis of Lattice Calculations," PICG 5, 282 (1955).

   Derives S/M dependence of ERI from measurements of other lattice parameters.

2. Cohen, E. R., "Exponential Experiments on D_2O-Uranium Lattices," PICG 5, 268 (1955).

   Presents results of lattice bucklings and thermal disadvantage factors from which resonance escape probabilities can be calculated.

3. Baer, W., et al, "A Method for Determination of Plutonium Production in Reactors," WAPD-P-699 (1956).

   A radiochemical separation technique for neptunium is presented.

4. Kouts, H., and R. Sher, "Effective Resonance Integrals from Exponential Experiments," BNL-433, p. 5 (1957).

   Derives ERI from other lattice measurements.

5. Persson, R., et al, "Exponential Pile Measurements with Natural Uranium and Heavy Water," Jour. Nucl. Eng. 3, 188 (1956).

   Derives ERI from other lattice measurements.

6. Burgov, N. A., "Resonance Absorption of Neutrons in Heterogeneous Systems," CASU 1, 69 (1956).

   Measures p directly by a substitution of Bi slugs for U slugs in cadmium covered tubes in a D_2O moderator.

7. Richey, C. R., "Lattice Calculations Based on Exponential Pile Results," HW-56646 (1958).

   Derives ERI from other lattice measurements.

8. Persson, R., et al, "Exponential Experiments on Heavy Water Natural Uranium Metal and Oxide Lattices," PICG 12,364 (1958).

   Derives ERI from other lattice measurements and includes a correction for the fine structure of the resonance flux.

9. Klein, D., et al, "Spatial Distribution of U^{238} Resonance Neutron Capture in Uranium Metal Rods," Nucl. Sci. Eng. 3, 698 (1958).

Measures the spatial distribution of U^{238} resonance neutron captures in 0.387 inch rods by two techniques.

10. Hone, D. W., et al, "Natural Uranium D_2O Lattices - Experiment and Theory," PICG 12, 351 (1958).

Reports the results of measurements of bucklings and disadvantage factors. Derives a semi-empirical expression for the resonance integral using Hellstrand's (Ref. F.2.c.8) experimental data.

11. Girard, Y., et al, "Natural Uranium - Heavy Water Lattices," PICG 12, 281 (1958).

Derives ERI from other lattice measurements.

12. Anderson, R. C., et al, "Thorium Uranium Physics Experiments (TUPE) Monthly Report," BAW-1179 (October 1959).

The thorium resonance integral and resulting cadmium ratios were calculated and compared with measured cadmium ratios.

13. Zink, J. W., and G. W. Rodeback, "The Determination of Lattice Parameters by Means of Measurements on a Single Fuel Element," NAA-SR-5392 (1959).

Determines p from slowing down equations with experimental data from cadmium covered indium foil measurements used to give parameters characteristic of rods in question.

14. Smith, G., et al, "Comparison of Measurements with a Monte Carlo Calculated Spatial Distribution of Resonance Neutron Capture In a Uranium Rod," Nucl. Sci. Eng. 8, 449-51 (November 1960).

15. Cohen, Ira H., "Multiregion Reactor Lattice Studies Quarterly Progress Report, January 1 to March 31, 1961," WCAP-1432 (1961).

General report on parameter studies of multiregion cores, including results of ρ_{28} measurements and their use to calculate conversion ratios. Describes ρ_{28} measurements by a monitor foil technique.

F.3 Methods of Calculating Lattice Parameters

F.3.a Analytical and Semi-empirical Methods

1. Dancoff, S. M., and M. Ginsburg, "Resonance Absorption in Lumps and Mixtures," CP-1589 (1944)

   Resonance absorption calculations are made using Wigner's original model.

2. Davey, W. G., "The Experimental Basis of Lattice Calculations for Natural Water Moderated Assemblies," AERE-RP/R-1842 (1955).

   Obtains the ERI from other lattice parameters.

3. Carlvik, I., and B. Pershagen, "Calculation of Effective Surfaces for Resonance Absorption in Tubes and Parallel Plates," AEF-49 (1955).

4. Critoph, E., "Comparison of Theory and Experiment for (a) Lattice Parameters of D_2O-U Reactors, (b) Central Rod Experiments, and (c) Foreign Rod Experiments;" (AECL-350) CRRP-655 (July 1956).

   Suggests modification to original diffusion theory approach to p calculations to allow for non-uniformity of resonance flux across cell.

5. Stein, S., "Resonance Capture in Heterogeneous Systems," WAPD-139 (1955).

   Presents a simple analytical technique for calculating the resonance escape probability for water moderated lattices.

6. Neumann, H., "Resonance Escape Probability in Reactor Lattices," BNL-433, p. 110 (1957).

   Presents a method of calculating p by using blackness theory.

7. Pershagen, B., and I. Carlvik, "The Resonance Escape Probability in a Lattice," AEC-tr-3316 (AEF-71), (1957).

   Calculational method for p considering the slowing down distribution in cell as determined by Fermi Age treatment.

8. Pershagen, B., et al, "Calculation of Lattice Parameters of Uranium Rod Clusters in Heavy Water and Correlation with Experiments," PICG 12, 341 (1958).

p is calculated by method of F.3.a.7. The problem of calculating an effective surface for rod clusters is also considered.

9. Lehmann, P., et al, "The Physical Properties of Some Composite Fuel Elements in U-D_2O Type Reactors," PICG 12, 395 (1958).

Presents a new method for calculating p for complex fuel shapes.

10. Dessuer, G., "Physics of Natural Uranium Lattices in Heavy Water," PICG 12, 320 (1958).

Presents results of theory and experiments for D_2O and mixed D_2O-H_2O lattices. p is inferred from other lattice data and is calculated by the method of F.3.a.4.

11. Barden, S. E., et al, "Some Methods of Calculating Nuclear Parameters for Heterogeneous Systems," A/Conf. 15/P/272 (1958).

Reactor lattice parameters are calculated by two general methods: Wigner-Seitz, and individual source-sink method. p is calculated by Stuart's method of successive generations (Ref. F.4.6).

12. Vaughn, E. U., "Spatial Distribution of Resonance Neutrons in the Moderator of Reactor Lattices and its Effects on Resonance Escape Probability," NAA-SR-Memo-3852 (May 13, 1959).

Calculates the resonance escape probability for a lattice cell by solving the age equation in the cell and assuming that the central rod is a sink of known ERI.

13. "Study of Slightly Enriched Uranium-Water Lattices with High Conversion Ratio, Quarterly Progress Report May 1 to July 31, 1959," NYO-2701 (1959).

A general survey of experimental and calculational methods pertaining to these lattices.

14. Baumann, N. P., "Process Development Pile Measurements of Lattice Parameters of Natural Uranium in Heavy Water," DP-407 (July 1959).

Derives ERI from PDP buckling measurements using method of Ref. F.3.a.4.

15. "Study of Slightly Enriched Uranium-Water Lattices with High Conversion Ratio, Quarterly Progress Report for August 1, 1959 to October 31, 1959," NYO-2702 (1959).

Presents calculational methods for analyzing above lattices.

16. Arnold, W. H., "Critical Masses and Lattice Parameters of H_2O-UO_2 Critical Experiments: A Comparison of Theory and Experiment," YAEC-152 (Nov. 1959).

Presents semi-empirical methods of calculation of lattice parameters and compares results with experiments.

17. Brooks, W. L., and H. Soodak, "Resonance Absorption in D_2O Lattice Reactors," NDA-2131-19 (1960).

Nine group calculation of resonance absorption based on microscopic cross-section data and the experimental results of Hellstrand (Ref. F.2.c.8). Flux disadvantage factors are calculated for each of the nine groups of resonance neutrons.

18. Chernick, J., "Calculation Methods for Heterogeneous Systems", BNL-622 (T-189)(August 1960).

19. Agresta, J., et al, "A Method for Calculating the Reactivity of Simple D_2O Moderated Natural Uranium Lattices," NDA-2131-20 (September 1960).

Calculates p by method of Ref. F.3.a.16.

20. Joanou, G. D., "Notes on Lattice Parameter Calculations," HW-60422 (Revised by R. E. Tiller, October 1960).

Discussion of methods of calculation of p including consideration of non-solid fuel lumps and Doppler coefficient.

F.3.b Machine Calculations

1. Richtmeyer, R. D., "Resonance Capture Calculations for Lattices by the Monte Carlo Method," BNL-433, p. 82 (1957).

   A general discussion of a Monte Carlo code for calculation of resonance capture.

2. Richtmeyer, R. D., et al, "The Monte Carlo Calculation of Resonance Capture in Reactor Lattices," A/Conf. 15/P/2489 (1958).

   Description of the NYU REP 704 code for calculating resonance escape probabilities.

3. Morton, K. W., "A Calculation of Resonance Escape Probability by Monte Carlo Methods," A/Conf. 15/P/19 (1958).

   Describes Monte Carlo program for the IBM 704 to calculate p and especially $\partial p/\partial T$, the variation of p with temperature.

4. Adler, F. T., and L. W. Nordheim, "The Effective Resonance Integrals," GA-282 (1958).

   Discussion of the calculation of the effective resonance integrals.

5. Adler, F. T., et al, "The Quantitative Evaluation of Resonance Integrals," GA-350 or A/Conf. 15/P/1988 (1958).

   Calculational method for obtaining the ERI for rods is described. Uses computer to integrate Doppler-broadened Breit-Wigner line shapes over each resonance; uses original Wigner model of the surface and volume resonance absorption.

6. Adler, F. D., et al, "Tables for the Computation of Resonance Integrals," GA-377 (1958).

   Tables are presented from which the effective resonance integral may be calculated from individual resonance parameters by the method of Ref. F.3.b.5.

7. Roos, B., "Resonance Escape Probabilities for the Graphite Moderated MGCR," AECU-4490 (1958).

Calculates ERI using methods of Adler, et al (Refs. F.3.b.4, 5, 6).

8. Taylor, A. J., "A Programme for the Evaluation of Resonance Escape Probabilities and Self Shielding Factors in Hydrogen Moderated Lattices," AERE-R-3364 (June 1960).

An approximate computer calculation based on the work of Rothenstein (Ref. F.4.17) and Chernick (Ref. F.4.15).

9. Klahr, C. N., and L. B. Mendelsohn, "Heterogeneous Reactor Calculation Methods, Quarterly Progress Report No. 4 for January 1 to March 31, 1960," NYO-2676 (1960).

Description of machine code for analysis of reactor lattices. A set of heterogeneous equations is set up and solved by an iterative procedure.

10. Crafton, C., and J. D. Garrison, "Program for the Estimates of Resonance Integrals," GAMD-1347 (1960).

IBM-650 program for estimating infinite resonance integrals from resonance level data.

11. Joanou, G. D., "A Proposed Monte Carlo Method for Computing the Lattice Parameters and the Space Dependent Neutron Spectre," NAA-SR-Memo-4805 (December 7, 1959).

Treatment of resonance captures is essentially that of Richtmeyer (Refs. F.3.b.1 and 2) with improvements to reduce computer time.

12. Memmert, G., "Resonance Absorption in Heterogeneous Systems," Nukleonik 1, No. 2, 48-57 (1958), translated by E. L. Poole, AERE (Trans. 853), (1960).

A calculational method for obtaining ERI's for rods, empty tubes and filled tubes.

13. Wick, R. S., "Resonance Escape Probability Calculations in Non-Uniform Lattice Arrays," WAPD-BT-17, p. 1 (Feb. 1960).

Computer oriented study to extend older work on uniform arrays to the non-uniform situation.

F.4 Theory of Resonance Capture

1. Cristy, R. F., A. M. Weinberg, and E. P. Wigner, "Resonance Escape Probability in Lattices," CP-2062 (1944).

   Early method of calculating p using one group diffusion theory to get resonance disadvantage factor. Also presents the original formulation of the surface and mass resonance absorption.

2. Gurevich, I. I., and I. Y. Pomeranchouck, "Resonance Absorption in Heterogeneous Systems," PICG 5, 466 (1955).

   Original presentation of "optical model" for calculation of resonance absorption.

3. Dressner, L., "The Effective Resonance Integrals of U-238 and Th-232," Nucl. Sci. Eng. 1, 68 (1956).

   Method for calculating ERI for homogeneous mixtures with exact inclusion of Doppler broadening of resonance lines.

4. Fillmore, F. L., "Calculation of ln E_1/E_2 for Resonance Neutrons in Uranium Lattices," Nucl. Sci. Eng. 1, 355 (1956).

   Using a diffusion theory model, ln E_1/E_2 is obtained from an experimental value of the ERI.

5. Dressner, L., "Effect of Geometry on Resonance Neutron Absorption in Uranium," Nucl. Sci. Eng. 1, 501 (1956).

   Discussion of the geometrical dependence of the ERI with comparison to experimental values.

6. Stuart, G. W., "Multiple Scattering of Neutrons," Nucl. Sci. Eng. 2, 617 (1957).

   Derives a variational form for the probability that a neutron incident upon a body and suffering multiple collisions within it, will be absorbed. Using the successive generation technique, exact results are calculated.

7. Corngold, N., "Resonance Escape Probability in Lattices," J. Nucl. Energy 4, 293 (1957) or BNL-445 (T-93), (1957).

One-dimensional, coupled integral equations are set up and solved for the case of hydrogen moderator.

8. Spinney, K., "Resonance Absorption in Homogeneous Mixtures," J. Nucl. Energy 6, 53 (1957).

Examines the narrow resonance vs. the infinite absorber approximations for homogeneous mixtures.

9. Corngold, N., "Slowing Down of Neutrons in Infinite Homogeneous Media," Proc. Phys. Soc. A, 70, 793 (1957).

Uses variational technique to solve integral equation.

10. Dressner, L., "The Effect of Geometry on Resonance Neutron Absorption in Uranium," BNL-433, p. 95 (1957).

By comparison with experiment, it is shown that an additional geometrical factor must be included in the usual S/M form of the ERI.

11. Stuart, G. W., and R. W. Woodruff, "Method of Successive Generations," Nucl. Sci. Eng. 3, 339 (1958).

Continuation of method described in F.4.6. Develops an equation relating rod blackness, β, as calculated by successive generations technique to p.

12. Stippel, H., "Generalization of Source-Sink Methods in Heterogeneous Reactor Calculations," A/Conf. 15/P/1440 (1958).

13. Petrov, G. V., "Resonance Absorption in a Close-Packed Lattice," J. Nucl. Energy 6, 251-4 (1958).

Applies method of Gurevich and Pomeranchonck (Ref. F.4.2) specifically to the problem of resonance absorption in tight lattices.

14. Stein, J. M., "Effect of Reflectors on Resonance Escape Probability," AECU-4482 (GAMD-610), (1958).

Discussion of this problem.

15. Chernick, J., and R. Vernon, "Some Refinements on the Calculation of Resonance Integrals," Nucl. Sci. Eng. 4, 649 (1958).

16. Bell, G. I., "A Simple Treatment for Effective Resonance Absorption Cross-Sections in Dense Lattices," Nucl. Sci. Eng. 5, 138 (1959).

Suggests replacing $S_0 = \frac{S}{4V_0}$ in the Wigner rational approximation for the collision probability in isolated fuel lumps with $\tau_0 = \frac{S_0 \Sigma_1}{\Sigma_1 + S_0 \frac{V_0}{V_1}}$ for clustered fuel lumps. Here S is lump area, V_0 is lump volume, V_1 is moderator volume and Σ_1 is the moderator cross-section.

17. Rothenstein, W., "Collision Probabilities and Resonance Integrals for Lattices," BNL-563 (T-151), (1959); also Nucl. Sci. Eng. 7, 162-71 (Feb. 1960).

Coupled integral equations for the collision densities in a lattice are solved by means of escape probabilities. Corrections to the zero order solution are made.

18. Keane, A., et al, "A Derivation of the Effective Resonance Integral in Heterogeneous Systems," AAEC/E-43 (1959).

Derives ERI for both close-packed heterogeneous and also homogeneous systems using the method of Gurevich and Pomeranchonck (Ref. F.4.2).

19. Bakshi, P. M., "Equivalence Principles and Resonance Integrals," BNL-4381 (Sept. 1959).

Derives equivalence relationships between resonance capture in heterogeneous and homogeneous systems and compares ERI for single rod to that for a lattice.

20. Nordheim, L., "The Theory of Resonance Absorption," GA-638 (Rev.), (1959).

A comprehensive study of several different methods of calculating effective resonance integrals.

21. Rothenstein, W., "Resonance Capture in Lattices," Nucl. Sci. Eng. 8, 122-7 (Aug. 1960).

Compares results of calculational method of Ref. F.4.17 with that of Monte Carlo calculations.

22. Takahashi, H., "First Flight Collision Probability in Lattice Systems," J. Nuc. En. Part A: Reactor Science 12, 1-5 (1960).

Calculates collision probabilities for multiregion cylindrical cell which is approximation to actual rod and slab lattices.

23. Takahashi, H., "Resonance Escape Probabilities in Circular Cylindrical Systems," J. Nuc. En. Part A: Reactor Science 12, 26-31 (May 1960).

Uses a circular cell system as approximation to actual rod lattice and integral form of Boltzmann transport equation. Results compared with those of Corngold (Ref. F.4.7).

F.5 Doppler Temperature Coefficient Measurement and Calculation

1. Mitchell, A. C. G., et al, "Effect of Temperature on the Resonance Absorption of Neutrons by Uranium," CP-597 (1943).

   Measures Doppler coefficient for U and UO_2 by an activation technique.

2. Creutz, E., et al, "Effect of Temperature on the Total Resonance Absorption of Neutrons by Spheres of Uranium Oxide," Jour. Appl. Phys. 26, 276 (1955).

   Measures the temperature coefficient for UO_2 spheres.

3. Lane, A. M., et al, "An Estimation of the Doppler Effect in Fast Neutron Reactors," AERE-T/M-137 (1956).

   Theoretical discussion of the Doppler effect with specific reference to fast reactors.

4. Rodeback, G. W., "Temperature Coefficients of Uranium and Thorium Resonance Integrals," NAA-SR-1641 (1956).

   Measures temperature coefficients by an activation technique.

5. Goertzel, G. and C. Klahr, "Interpretation of an Experiment to Measure the Doppler Effect," NDA-14-127 (1956).

   Theoretical discussion of Doppler effect measurements.

6. Frost, R. T., et al, "Measurement of Doppler Temperature Coefficient in Intermediate and Fast Assemblies," PICG 12, 79 (1958).

   Doppler coefficient measured by modulating the temperature of a sample in a reactor together with a mechanical oscillation.

7. Keane, A., et al, "The Doppler Coefficient for Reactors Containing Thorium," AAEC/E-49 (1959).

   Calculation of the Doppler coefficient and comparison of results with other calculational methods and experiments.

8. Engesser, F. C. and T. J. Oakes, "The Fuel Temperature Coefficient for 7 Rod Clusters of Uranium Oxide with Air Coolant," HW-63576, p. 36 (1960).

Measured Doppler coefficient using reactivity technique in test region of PCTR.

9. Rosen, J., "The Dependence of the Resonance Integral on the Doppler Effect," AE-39 (December 1960).

Calculation of the Doppler effect using the method of Adler, Hinman and Nordheim (Ref. F.3.b.6).

10. Solbrig, A. W., "Doppler Broadening of Low Energy Neutron Resonances," Nucl. Sci. Eng. 10, 167-168 (1961).

Theoretical discussion of Doppler-broadened neutron resonances with approximate forms developed for the equation of the line shape.

F.6 Dancoff Factor Measurement and Calculation

1. Dancoff, S. M. and M. Ginsburg, "Surface Resonance Absorption in a Close Packed Lattice," CP-2157 (1944).

   Original paper on the mutual shielding effect of lattice rods on the surface portion of the resonance absorption.

2. Pettus, W. G. and I. E. Dayton, "Mutual Shielding of Lattice Pins in the Resonance Escape Region," Nucl. Sci. Eng. 4, 522 (1958).

   Experimentally verifies theory of Dancoff and Ginsburg using danger coefficient technique.

3. Thie, J. A., "A Simple Analytical Formulation of the Dancoff Correction," Nucl. Sci. Eng. 5, 75-77 (1959).

   Simplifies the calculation of the Dancoff factor for parallel cylinders and also includes a derivation of the factor for the interior surface of a hollow rod.

4. Carlvik, I. and B. Pershagen, "The Dancoff Correction in Various Geometries," AE-16 (1959).

   Calculates Dancoff factor for square or circular tubes, parallel plates and parallel circular cylinders.

5. Pettus, W. G., "Measurement of the Dancoff Effect in H_2O-D_2O Moderated Lattices," BAW-177 (February 1960).

6. Babcock, D. F. et al, DP-535, (November 1960).

   Measurements of Dancoff effect in 3, 7, and 19 rod 1.0 inch diameter clusters of uranium rods in D_2O. Experimental technique described in DP-495 (Ref. F.2.a.18).

7. Pettus, W. G., "The Dancoff Effect in H_2O-D_2O Moderated Lattices," Nucl. Sci. Eng. 8, 361-2 (October 1960).

   Experimentally investigates the validity of Bell's formula for the Dancoff factor (Ref. F.4.16).

8. French, R. J., "The Dancoff Correction to the Resonance Absorption in Close Packed Cylindrical Fuel Rod Lattices," YAEC-149 (December 1960).

General discussion of the topic. Computer code is described that calculates the Dancoff factor for infinite parallel right circular cylinders.

9. Fukai, Y., "New Analytical Formula for the Dancoff Correction for Cylindrical Fuel Lattices," Nucl. Sci. Eng. 9, 370-6 (March 1961).

Presents new calculational technique and compares with older methods.

F.7 Nuclear Data

1. Anderson, H. L., "Resonance Capture of Neutrons by Uranium," Phys. Rev. 80, 499 (1950).

   Early measurement of uranium absorption by transmission technique with spectra of varying degrees of hardness.

2. Macklin, R. L., and H. S. Pomerance, "Resonance Capture Integrals," PICG 5, 96 (1955).

   Basic measurements of dilute resonance integrals for many nuclides.

3. Crocker, V. S., "Studies on the Neutron Resonance Absorption of U^{238}," PICG 5, 102 (1955).

   Investigates U^{238} resonance capture by transmission experiments.

4. Hollander, J. M., et al, "Beta Radioactivity and Energy Levels of Heavy Nuclei: Decay Schemes of Np^{239}, U^{237}, and Np^{238}," A/Conf. 15/P/650.

5. Desjardins, J. S., et al, "Neutron Physics Progress Report for January - March 1958," CU-174, p. 5 (1958).

   Reports the results of measurements of U^{238} neutron resonance parameters up to 1000 ev.

6. Ewan, G. T., et al, "Conversion Electron Spectrum of Np^{239} and Level Scheme of Pu^{239}," Phys. Rev., Ser. 2, 116, 950 (November 1959).

   Latest data on Np^{239}-Pu^{239} level scheme.

7. Cooper, J. R., and W. B. Henderson, "A Program for the Preparation of a Nuclear Data Tape with Fine Energy Detail," TID-6647 (May 13, 1960).

8. Westcott, C. H., "Effective Cross Section Values for Well-Moderated Thermal Reactor Spectra," AECL-1101 (CRRP-960), (1960).

   Presents tables of g and s factors to calculate effective cross sections: $\hat{\sigma} = g + rs$.

F.8 Miscellaneous

1. Wilkins, J. E., "The Activation of Thin Foils," CP-3581 (1945).

   Factors are calculated for correcting for self-shielding of foils of finite thickness.

2. Roe, G. M., "Curves for Calculating the Effect of Self-Absorption and Doppler Broadening on Resonance Absorption Lines," AECD-3782 (1948).

3. Axtmann, R. C., and J. S. Stutheit, "Scintillation Counting of Natural Uranium Foils," AECD-3513 (ANL-HDY-715), (Decl. 1953).

4. Sailor, V. L., "A Table of the Integral:

$$\psi(x,t) = \frac{1}{2\sqrt{\pi t}} \int_{-\infty}^{\infty} \frac{\exp - \frac{(x-y)^2}{4t}}{1 + y^2} \, dy."$$

BNL-257 (1953).

5. Rose, M. E., et al, "A Table of the Integral:

$$\psi(x,t) = \frac{1}{2\sqrt{\pi t}} \int_{-\infty}^{\infty} \frac{\exp - \frac{(x-y)^2}{4t}}{1 + y^2} \, dy."$$

   WAPD -SR-506, Vols. 1 and 2 (1954).

6. Harvey, J. A., et al, "Spacings and Neutron Widths of Nuclear Energy Levels," Phys. Rev. 99, 10 (1955).

7. Porter, C. E., and R. G. Thomas, "Fluctuations of Nuclear Reaction Widths," Phys. Rev. 104, 483 (1956).